Generation of Antibody-based Therapeutics for Treatment of Acute Leukemia

Dissertation an der Fakultät für Biologie zur Erlangung des Doktorgrades
der Naturwissenschaften Doctor rerum naturalium
der Ludwig-Maximilians-Universität München

Jonathan Meinrad Schwach

17.10.2024

Diese Dissertation wurde angefertigt unter der Leitung von

Herrn Prof. Dr. Heinrich Leonhardt

im Bereich Humanbiologie und Bioimaging an der Biologischen Fakultät
der Ludwig-Maximilians-Universität München

Erstgutachter: Prof. Dr. Heinrich Leonhardt

Zweitgutachterin: PD Dr. Anna Friedl

Dissertation eingereicht am: 17.10.2024

Tag der mündlichen Prüfung: 04.02.2025

Eidesstattliche Versicherung

Hiermit versichere ich an Eides statt, dass die vorliegende Dissertation von mir selbstständig verfasst wurde und dass keine anderen als die angegebenen Quellen und Hilfsmittel benutzt wurden. Die Stellen der Arbeit, die anderen Werken dem Wortlaut oder dem Sinne nach entnommen sind, wurden in jedem Fall unter Angabe der Quellen (einschließlich des World Wide Web und anderer elektronischer Text- und Datensammlungen) kenntlich gemacht. Zur Erstellung dieser Arbeit wurde keine künstliche Intelligenz verwendet. Diese Erklärung gilt für alle in der Arbeit enthaltenen Texte, Grafiken, Zeichnungen und bildlichen Darstellungen.

München, den 17.10.2024 _____

Jonathan Schwach

Erklärung

Die vorliegende Dissertation wurde weder ganz noch in Teilen bei einer anderen Prüfungskommission vorgelegt. Ich habe noch zu keinem früheren Zeitpunkt versucht, eine Dissertation einzureichen oder an einer Doktorprüfung teilzunehmen.

München, den 17.10.2024 _____

Jonathan Schwach

Parts of this thesis have been published or submitted for publication elsewhere:

Jonathan Schwach, Ksenia Kolobynina, Katharina Brandstetter, Dr. Marcus Gerlach, Philipp Ochtrop, Dr. Jonas Helma, Prof. Dr. Christian P. R. Hackenberger, Dr. Hartmann Harz, Prof. Dr. M. Cristina Cardoso, Prof. Dr. Heinrich Leonhardt, Dr. Andreas Stengl. Site-Specific Antibody Fragment Conjugates for Reversible Staining in Fluorescence Microscopy. ChemBioChem 22, 1205-1209 (2021).

Jonathan Schwach, Mustafa Abdellatif, Dr. Andreas Stengl. More than Toxins—Current Prospects in Designing the Next Generation of Antibody Drug Conjugates. Frontiers in Bioscience-Landmark 27, 240 (2022).

Marina Able, Marc-André Kasper, Binje Vick, **Jonathan Schwach**, Xiang Gao, Saskia Schmitt, Belay Tizazu, Amrei Fischer, Sarah Künzl, Marit Leilich, Andreas Stengl, Michael von Bergwelt-Baildon, Jonas Helma-Smets, Dominik Schumacher, Christian P. R. Hackenberger, Katharina S. Götze, Irmela Jeremias, Heinrich Leonhardt, Michaela Feuring and Karsten Spiekermann. Effective eradication of acute myeloid leukemia stem cells with FLT3-directed DNA-damaging duocarmycin antibody drug conjugate. Accepted at Leukemia (2024)

Table of Contents

1 Summary

Cancer has been a major focus of pharmaceutical research, yet this disease remains infamous for its highly challenging treatment. The main reason lies in the high heterogeneity not only due to the variety of cancer types but also due to the vast genomic and epigenomic diversity in the patients themselves. The success rates of common treatments such as chemotherapy strongly depend on the cancer type and clinical profile of the patient. Treatment can lead to adverse effects due to lack of specificity towards cancer cells. Thus, the aim of modern cancer therapy is the development of personalized treatment options that directly target cancerous tissue. Key challenges that need to be solved are the quick and reliable determination of differentially expressed proteins and cancerogenic mutations as well as the development of effective cancer-specific agents.

Antibodies directly target cell surface structures such as overexpressed proteins and thereby offer a promising avenue for personalized cancer therapy. By combining specificity-conferring antibodies with other effector molecules, antibody drug conjugates employ the strengths of both moieties. However, the development of therapeutic antibodies and even more so antibody drug conjugates is a time-consuming and complicated process that starts with the identification and expression of suitable antigens, generation and characterization of binders, chemical conjugation, *in vitro* and *in vivo* characterization and concludes with the successful passing of clinical trials - a process which takes more than a decade for the development of a single therapeutic molecule.

Due to these time constraints and the requirement for expertise from different fields, the work presented in this thesis contributes to collaborative projects at three different stages of the development of antibody therapeutics: First, we identify and characterize novel antibodies against overexpressed T cell antigens in acute lymphoblastic leukemia using hybridoma technology. We implement an optimized workflow to screen for binders that recognize surface-presented antigens, allowing for the future generation of antibody drug conjugates or chimeric antigen receptors. Second, to address the problem of profiling antigen-surface expression, we present a novel conjugation technique to generate nanobody oligonucleotide conjugates. Using a chemo-enzymatic conjugation strategy based on enzymatic functionalization via tubulin-tyrosine ligase and click chemistry, we show that our method can effectively conjugate single stranded DNA and PNA to antibody fragments. We utilize confocal microscopy to demonstrate reversible hybridization of fluorescent, complimentary strands which in the future enables multiplexed detection of antigens by repeated cycles of hybridization, imaging and removal of the fluorescent strand. In addition, our conjugation technique could be used to generate antibody siRNA conjugates which are currently under investigation for therapeutic use by directly interfering with protein expression on the mRNA level. Lastly, we perform pre-clinical characterization of a Flt3-directed antibody drug conjugate to target cancer stem cells in acute myeloid leukemia. Cancer stem cells proliferate slowly and pose a challenging target to treat with commonly used anti-proliferative drugs such as MMAF. To this end, we generated and thoroughly characterized humanized antibody variants of an αFlt3 rat antibody using chromatography, ELISA, fluorescence microscopy and flow cytometry. In a collaborative effort duocarmycin was identified as a suitable payload for killing resting cells and improved *in vitro* activity of our antibody drug conjugate over the respective MMAF-conjugate against Flt3-positive cell lines and in a patient-derived xenograft model. Our data provides evidence that resting cells such as cancer stem cells can be efficiently targeted with a Flt3-targeting antibody drug conjugate conjugated to duocarmycin.

2 Zusammenfassung

Die Krebstherapie stellt bis heute einen Schwerpunkt der pharmazeutischen Forschung dar. Eine besondere Schwierigkeit ergibt sich bei der Behandlung von Krebs durch die hohe Heterogenität dieser Krankheit, die sich zum einen aus der großen Vielzahl an unterschiedlichen Krebstypen, zum anderen aus der hohen genomischen und epigenomischen Vielfalt der Patienten speist. Heutige Breitbandtherapien wie beispielsweise der Einsatz von Chemotherapeutika ermöglichen vielen Patienten eine Heilung oder zumindest eine zwischenzeitliche Reduktion der Tumorlast. Trotz vieler Erfolge existieren jedoch bis heute deutliche Defizite in der konventionellen Krebstherapie: Neben unzureichend anschlagenden Therapien entfaltet sich die Wirkung der Therapeutika im gesamten Körper anstatt nur an tumorösem Gewebe, was zu schweren Nebenwirkungen durch unspezifische Wechselwirkung mit gesunden Zellen führen kann. Daher ist und bleibt eine schnelle und zuverlässige Bestimmung des klinischen Profils wie beispielsweise der kanzerogenen Mutationen und überexprimierten Proteinen sowie die Entwicklung von effektiven und krebsspezifischen Therapeutika eine zentrale Herausforderung der modernen Krebstherapie.

Antikörper stellen einen eleganten Ansatz der modernen, personalisierten Krebsmedizin dar. Sie sind in der Lage Oberflächenstrukturen wie beispielsweise überexprimierte Proteine auf Krebszellen zu erkennen und sind eine wichtige Molekülklasse für die Krebsdiagnostik und -therapie. Als eine Weiterentwicklung von therapeutischen Antikörpern haben sich Antikörper-Wirkstoffkonjugate etabliert. Diese neue Klasse von Therapeutika kombiniert die hohe Spezifität von Antikörpern mit weiteren Effektormolekülen und erlaubt einen völlig neuen Einsatz dieser Effektoren. Nichtsdestotrotz ist die Entwicklung solcher Antikörper-Wirkstoffkonjugate ein komplizierter und zeitintensiver Prozess, der von der Identifizierung und Herstellung von Antigenen über die Generierung und Charakterisierung von Bindemolekülen, der Konjugation zu einem Wirkstoff, der *in vitro* und *in vivo* Charakterisierung des Konjugats bis hin zum Abschluss der klinischen Phasen reicht. Für gewöhnlich dauert die Entwicklung eines einzigen Therapeutikums bis zur klinischen Zulassung über ein Jahrzehnt.

Aufgrund dieser zeitlichen Einschränkungen und der benötigten Expertise aus unterschiedlichen Forschungsfeldern werden in dieser Arbeit Beiträge zu kollaborativen Projekten an drei unterschiedlichen Punkten der Therapeutikaentwicklung vorgelegt: Zum einen werden mittels Hybridomatechnologie Antikörper identifiziert und charakterisiert, die gegen überexprimierte Antigene auf T-Zellen gerichtet sind und zur Behandlung von akuter lymphoblastischer Leukämie eingesetzt werden können. Der Arbeitsablauf wurde dahingehend optimiert, Antikörper zu isolieren, die oberflächenexprimierte Antigene erkennen. Daher eignen sich die identifizierten Antikörper besonders zur Generierung von Antikörper-Wirkstoffkonjugaten oder chimären Antigenrezeptoren. Zweitens wird eine neue Konjugationsstrategie vorgestellt, die die Konjugation von Einzeldomänenantikörpern mit Oligonukleotiden ermöglicht und somit die Bestimmung von personalisierten Expressionsmarkern in Krebsgewebe erleichtert. Mittels einer chemoenzymatischen Konjugationsstrategie, welche eine enzymatische Ligationsreaktion der Tubulin-Tyrosinligase mit chemischer Click-Chemie kombiniert, konnten einzelsträngige DNA- und PNA-Moleküle an Antikörperfragmente konjugiert werden. Mit Hilfe von Konfokalmikroskopie konnte gezeigt werden, dass fluoreszierende Komplementärstränge reversibel an das Konjugat gebunden werden können, was zukünftig die Detektion einer Vielzahl an Zielstrukturen durch wiederholte Zyklen von Hybridisierung, Bildgebung und Entfernen des fluoreszenten

Komplementärstranges ermöglicht. Ein neu aufkommender Therapieansatz ist der Einsatz von Antikörper-siRNA-Konjugaten, welche die direkte Manipulation von Proteinexpressionslevel auf Ebene der mRNA erlauben. Die hier vorgestellte Konjugationsstrategie könnte zusätzlich zur Herstellung von Antikörper-therapeutischen Oligonukleotidkonjugaten verwendet werden. Zuletzt fokussiert sich diese Arbeit auf die präklinische Charakterisierung eines gegen Flt3 gerichteten Antikörper-Wirkstoffkonjugats zur Abtötung von Krebsstammzellen in Akuter Myeloider Leukämie. Aufgrund ihrer geringen Teilungsrate zeigen Krebsstammzellen eine erhöhte Resistenz gegenüber üblichen antiproliferativen Wirkstoffen wie beispielsweise MMAF. Hierzu wurden humanisierte Varianten eines αFlt3 Antikörpers, welcher aus der Ratte stammt, generiert und mittels Chromatographie, ELISA, Fluoreszenzmikroskopie und Durchflusszytometry charakterisiert. In Kollaboration mit anderen Arbeitsgruppen wurde Duocarmycin als Wirkstoff identifiziert, der im Vergleich mit etablierten Toxinen wie MMAF eine erhöhte Aktivität gegen sich langsam teilende Zellen wie beispielsweise Krebsstammzellen aufweist. Dieses Ergebnis konnte in *in vitro* Versuchen mit Flt3 positiven Zellen und in Xenograftmodellen mit Krebszellen demonstriert werden. Damit zeigt diese Arbeit auf, wie Krebsstammzellen und sich langsam teilende Krebszellen mit einem gegen Flt3 gerichteten Antikörper-Wirkstoffkonjugat abgetötet werden können.

3 Introduction

3.1 Defining Cancer – Prevalence and Hallmarks

Cancer has emerged as one of the leading causes of death in modern societies. Cancer, besides cardiovascular diseases and infectious diseases, is one of the top three causes of death worldwide and the most prevalent cause of death in industrialized countries such as most of Europe and North America[1-3]. Due to population aging and overall growth, cancer incidence and cancer related deaths are predicted to double within the next 40-50 years[4-6], putting further emphasis on the development of therapeutics for this disease.

The causes of cancer are manifold: On a population level, obesity, physical inactivity, and consumption of certain products such as alcohol and tobacco have been shown to increase the risk of developing cancer[7-9]. On a cellular level, risk factors such as chronic inflammation[10], viral infections[11], hormone levels and gene variants that occur either naturally or are induced by mutagenesis after DNA damage[12,13] have been shown to promote carcinogenesis.

While "cancer" describes a conglomerate of highly diverse and heterogeneous diseases, all cancers arise from the patient's own tissue. Notably, cancers can form from any tissue in the body and spread to other locations in a process termed "metastasis". In a landmark paper, Hanahan and Weinberg formed a mental framework to understand cancer as a disease by summarizing a set of traits, termed "hallmarks", that are common across all cancer types[14]. These hallmarks, by now updated twice[15,16], mostly focus on aberrant cell division and exceptional cell survivability by dysregulation of cell cycle, metabolism and high plasticity of the genome both by direct mutagenesis as well as epigenetic reprogramming. Gaining one or multiple of these hallmarks can be induced by a variety of factors and changes within the cell, therefore giving no clear indication for the initial cause. Furthermore, a tumor is not a static entity. Current research suggests that tumor cells undergo constant evolution of their genome and phenotype[17,18]. This leads to an exceptionally high heterogeneity between patients even within the same cancer type as well as the ability of the cancer to acquire resistance to treatment. The multitude of factors leading to carcinogenesis, combined with the genetic individuality of each patient and the evolutionary changes of tumorous cells over the course of the disease, makes it impossible to find a "one-fits-all" solution for cancer treatment.

3.1.1 Classical Cancer Treatment

Cancer has been known to mankind for centuries. However, its treatment options have been very limited due to lack of molecular understanding of the disease and its formation. The discovery that cancer is composed of cells has been as late as the 19th century. The rise of molecular biology opened the door wide for the development of ever-improving treatments[19-21]. Common treatments that are still used to this day include surgical removal, radiation therapy, chemotherapy, and hormone therapy. Surgery was one of the first approaches to remove tumorous tissue. However, surgical removal has a lot of disadvantages: Firstly, only solid tumors can be removed, rendering all non-solid tumors such as blood cancer incurable by this method. Secondly, removal of the tumor can pose a serious risk for the health of the patient if the site is within or near a vital organ such as the brain that could be damaged during the operation. Lastly, relapses of the tumor can occur if not all tumorous tissue has been removed or the tumor has already metastasized to other parts of the body. Radiation therapy uses ionizing radiation to infer damage on the tumor and has emerged as a promising treatment for certain cancer types. However, side effects such as neurological damages are commonly reported both as a short- and long-term[22,23]. In

chemotherapy, small molecule drugs are administered to halt growth and force apoptosis of the tumor. Since the drug is administered systemically, side effects of the drug can also occur in the whole body. Additionally, it has been shown that chemotherapy is biased towards the killing of fast growing cells, rendering slowly growing tumors or a slowly growing subpopulation hard to treat[24,25].

3.1.2 Acute Leukemia: Biology and Treatment

A common type of cancer that to date is mostly treated by combined chemotherapy is Leukemia. This type of cancer originates from cells of the hematopoietic and lymphoid systems. While overall a rare type of cancer, leukemia, especially the subtypes "acute lymphoblastic leukemia" (ALL) and "acute myeloid leukemia" (AML), is the most prevalent cancer type in children and young adults[26].

ALL is caused by abnormally proliferating blood cells of the lymphoid branch with B-ALL representing approximately three quarters of all cases and T-ALL representing the remainder. Similar to AML, the majority of ALL cases is developed during childhood and represents one of the major causes for malignancy related deaths in children[27]. After the age of 50, a second spike in prevalence of ALL occurs[27]. While 90% of patients that developed ALL in childhood can be cured with no detectable trace of cancer long-term, about half of adult patients with ALL relapse and face highly limited therapeutic options and bad prognosis[27,28]. ALL is classified by the World Health Organization into B-ALL and T-ALL, with the first being further subcategorized according to genetic translocations, which are common in ALL and a major predictor for prognosis[29].

As discussed previously, age has been found to be one of the most important prognostic markers for treatment and long-term survival. Other major markers include the immunophenotype and the blood cell count[30]. Additionally, genetic aberrations contribute to the development and diagnostics of ALL. These include chromosomal alterations often by translocation and fusion of genes as well as point mutations of key regulators. One prominent example is the rearrangement of Histone-lysine N-methyltransferase 2A, also known as mixed-lineage leukemia, that has been associated with poor prognosis and, despite a generally low mutation rate in ALL patients, shown to contribute majorly to malignant transformation[31,32]. Another notable example is the BCR-ABL1 fusion protein, often termed "Philadelphia chromosome". This mutation leads to a constitutive activation of the kinase domain and is often present in B-ALL with its prevalence significantly correlating with increasing age of the patient[33]. Mutation of BCR-ABL1 was initially associated with poor prognosis, but therapeutic outcome has been significantly improved with the use of tyrosine kinase inhibitors. In summary, the mutational burden and genetic profile strongly determine the risk group and overall prognosis of the patient, with a wide variety of mutations having been described in relation with ALL[33,34].

To date, the treatment strategy of ALL consists of chemotherapy using vincristine, corticosteroids or anthracycline and asparaginase for induction and consolidation[35]. These treatment regiments have been developed for pediatric ALL and only slowly find adaption for adult ALL, representing one possible factor to the still poor outcome of adult ALL. When complete remission is achieved, the standard of care is the maintenance of chemotherapy to reduce the risk of relapse. Patients falling into a high-risk group usually undergo hematopoietic stem cell transplantation (HSCT) if medically indicated[28,36]. Patients developing a relapse after initially successful induction therapy undergo an intensified treatment regimen. However, relapsed patients currently face very poor prognosis and short median survival[37]. Scientists have therefore been looking towards novel therapies such as antibody therapeutics and antibody drug conjugates (ADC) to improve the outcome especially for

relapsed patients. To this end, Blinatumomab is one of these solutions for B-ALL that has been approved both in the USA and Europe. Blinatumomab is a bispecific T cell engager (BiTE) that binds to CD3 on the T cell surface and CD19 on the B cell surface. It's proposed mechanism is the induction of proximity between a potentially malignant B cell and cytolytic T cells[38]. Inotuzumab ozogamicin represents an FDA- and EMA-approved antibody drug conjugate combining an αCD22 antibody with the DNA-damaging agent calicheamicin and has greatly improved survival especially of relapsed patients, albeit with significant toxicities in initial studies [39]. Apart from these, multiple ADCs are in clinical trials. However, most efforts focus on B-ALL due to the higher prevalence among ALL patients. Currently, there is no approved antibody therapeutic for patients with T-ALL, posing a significant risk for these patients due to a lack of options when experiencing a relapse.

Similar to ALL, AML is induced by malignant blood cells stemming from the myeloid line that includes red blood cells, platelets, and white blood cells that are not part of the B and T cell lines. Standard treatment consists of induction chemotherapy to achieve complete remission followed by either post-remission chemotherapy or allogenic HSCT. The World Health Organization subclassifies AML into six broad groups based on lineage of the tumor, chromosomal translocations and genetic mutations[40]. These groups correspond to different risk profiles which determine the patient's exact treatment plan based on the progression and mutagenic burden of the tumor. Underlining the high heterogeneity of this disease, AML has been associated with a multitude of genetic mutations. Nucleophosmin (NPM1) is a protein that shuttles between the nucleus and cytoplasm and mutated in about 30% of patients with AML and a favorable prognostic marker. Among other functions, NPM1 stabilizes the tumor suppressors Arf and p53 and contributes to the degradation of the Myc oncogene. Mutations of NPM1 can lead to altered cellular localization and loss of function, thereby promoting tumor formation[41]. Mutations in isocitrate dehydrogenases (IDH) 1 and 2 occur in 20% of AML patients. IDH mutations result in a new enzymatic function of the IDH enzymes, leading to the production of 2-hydroxyglutarate, which in turn promotes to DNA hypermethylation and aberrant gene expression[42,43], representing an epigenetic component to AML. A second link to epigenetics are the enzymes DNA methyltransferase 3 (DNMT3) and Tet methylcytosine dioxygenase 2 (TET2). DNMT3A and DNMT3B are important regulators to control methylation levels of the genome. Mutations in AML are loss of function mutations, leading to dysregulated epigenetic modification of the genome and gene expression[44,45]. TET2 catalyzes the hydroxylation of 5-methylcytosine to 5-hydroxymethylcytosine as a first step in a demethylation cascade, thereby regulating genomic methylation levels and gene expression[46,47].

Another important protein with high mutational burden in AML is FMS-like tyrosine kinase 3 (Flt3) with mutations occurring in approximately 30% of AML patients[48]. Flt3 is a membrane bound receptor tyrosine kinase that – like other receptor tyrosine kinases – becomes catalytically active upon ligand-induced dimerization. Usually, Flt3 is expressed on immature hematopoietic progenitors, including monocytes, myeloid precursors and precursor B-cells[49]. Structurally, Flt3 consists of an extracellular domain, a transmembrane domain, a juxtamembrane domain and the tyrosine kinase region that itself consists of three domains: Two catalytic domains which are spaced apart by an inter-kinase domain. The C-terminal catalytic region further contains a peptide loop – termed activation loop – that forms contact with the neighboring Flt3 molecule in the dimer[50]. Flt3 plays an important role in hematopoiesis and cell survival. Activation of Flt3 leads to downstream signaling via the JAK/STAT[51], PI3K/AKT and MAPK/ERK[52] pathways. In AML, two common mutations of Flt3 have been identified: internal tandem duplications (ITD) and tyrosine

kinase mutations. ITDs are in-frame insertions of variable length into the juxtamembrane domain or first catalytic region[53]. ITDs in the juxtamembrane domain cause conformational changes that allow dimerization and activation in a ligand-independent manner[54]. Mutations in the tyrosine kinase domain lead to a constitutively activated kinase function that induces constant downstream signaling.

Patients with AML are categorized into risk groups with favorable, intermediate or poor prognosis, depending on their age, general health and mutational profile. Until recently, first line treatment consists of the "3+7" regimen, meaning treatment with anthracycline for three days followed by cytarabine for an additional seven days. Afterwards, HSCT is performed if the initial induction therapy proved successful[55]. The better molecular understanding of AML has led to the development of new drugs and treatments. Hypomethylating agents such as 5-azacytidine are being explored for treatment of AML to remove epigenetic imprints by the aforementioned mutations in the epigenetic machinery. However, a clear indication which AML patients benefit from this type of treatment remains elusive[56,57]. Tyrosine kinase inhibitors have been developed specifically for the inhibition of signaling in patients carrying Flt3 mutations. Type I inhibitors such as midostaurin are used for patients carrying either ITD or tyrosine kinase mutations. They bind near the activation loop or ATP binding site of active Flt3. Type II inhibitors such as Quartizinib work by binding near the ATP binding site of inactive Flt3. These types of inhibitors are only active against ITD mutations[58]. The use of tyrosine kinase inhibitors in patients with Flt3 mutations has led to an overall better response and longer survival[59]. Nevertheless, many patients experience a relapse after the initial treatment[60,61]. Relapsed AML shows a strong clonal evolution, acquiring multiple additional mutations compared with the initial AML clone[62], which is accompanied by poor prognosis, putting further pressure on the development of novel drugs for the treatment of AML. One challenge of kinase inhibitors is the high promiscuity towards their targets, leading to inhibition of other kinases not only in cancer cells, but also healthy cells. These off-target effects are common with many small molecule therapeutics that are currently used in cancer therapy. The development of therapeutics with high specificity would represent a major improvement in the treatment of cancer in general and acute leukemia in particular.

3.2 Antibody-based therapeutics

Delivering drugs in a highly targeted and specific manner has been the focus of physicians for over a century. When Paul Ehrlich postulated his concept of the "magic bullet" more than 100 years ago, he was referring to drugs that are able to distinguish between structures and therefore tell apart healthy from unhealthy cells[63]. At the time, antibody research was still in its infancy. Nevertheless, remarkable advances have been made already: In 1890, Paul Ehrlich's colleagues, Emil von Behring and Kitasato Shibasaburo, developed the diphtheria antitoxin from horse serum[64]. Whilst unknown at the time, today we know that the active ingredient of this antitoxin were antibodies. Although Ehrlich's concept of his "magic bullet" is not limited to antibodies, this class of molecules delivers a multitude of desirable characteristics and prerequisites to achieve a better and more personalized medicine.

Human antibodies are categorized into five different classes – IgA, IgE, IgD, IgG and IgM – each fulfilling a specialized role such as secretion in mucus or circulation in the blood and lymph system. Each protein consists of two heavy and two light chains forming a Y-shaped quaternary structure, whereas the heavy chain determined the class of the antibody (figure 1). Inter- and intramolecular disulfide bonds further stabilize the antibody. Heavy and light chain each consist of

a variable domain and constant region. The variable domains together form the antigen-binding site, also termed paratope, that specifically recognize and bind the antigen molecule via its corresponding epitope. Contact to the antigen is made mainly via three loops within each variable domain termed complementary determining regions (CDR). Each “arm” of the Y-shaped antibody is formed by an antigen-binding fragment (Fab) that consists of the variable domains and further includes the constant domain of the light chain and the CH1 domain of the heavy chain. With each antibody consisting of two identical Fab fragments, a single antibody molecule can bind two epitopes simultaneously. Lastly, the longer heavy chains form the hinge and Fc (fragment crystallizable) region, which are important for downstream signaling and activation of the immune system.

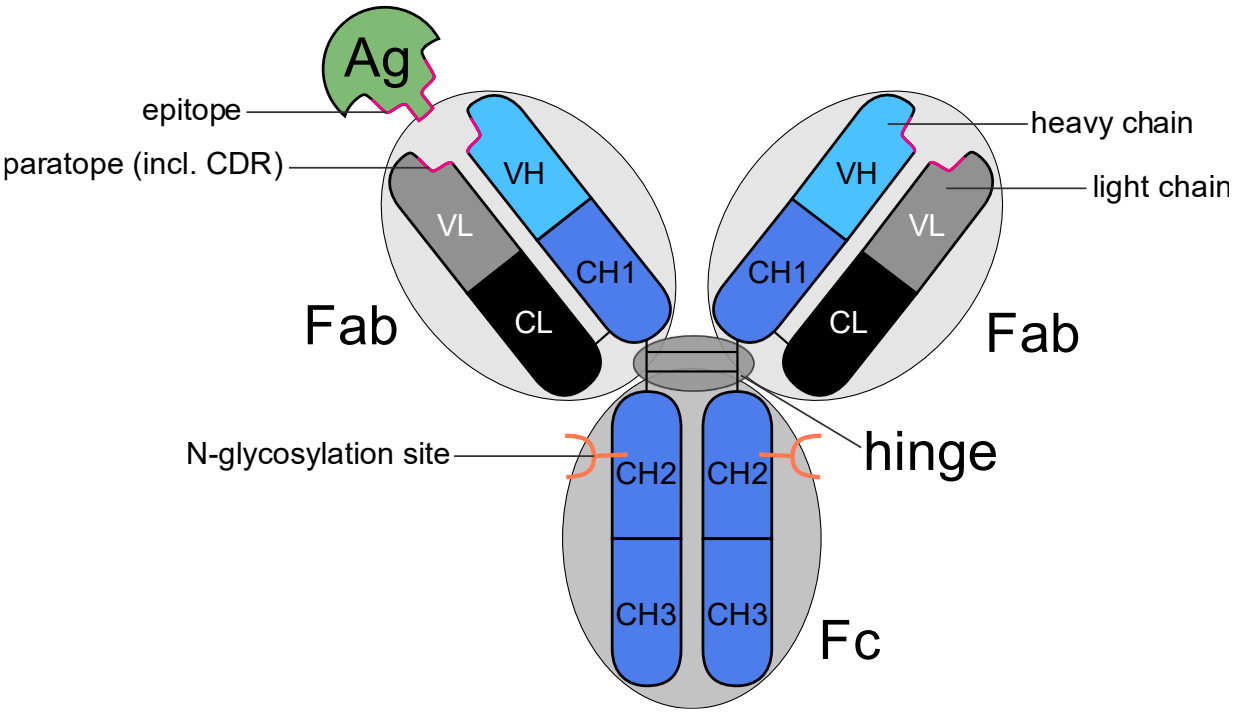

Figure 1: Structure of an IgG antibody. An IgG antibody consists of two identical heavy and two identical light chains that arrange in the classical Y-shaped structure. This tertiary structure is stabilized by the formation interchain disulfide bridges with the heavy chains connecting near the hinge region to each other and to their respective light chain. Each heavy chain consists of four domains: the variable domain V_H, and the constant domains C_H1, C_H2 and C_H3. The light chain consists of two domains: The variable domain V_L and the constant domain C_L. Each variable domain of both heavy and light chain contains three CDRs that are the defining contributors to antigen binding. The variable domains constitute the antigen-binding site, termed paratope, that specifically recognizes the structure on the antigen (Ag), the epitope. The variable domains together with C_H1 and C_L form the antigen-binding fragment (Fab) of the antibody, whereas the constant domains C_H2 and C_H3 of both heavy chains form the crystallizable fragment (Fc) that is also the site of post-translational N-glycosylation at the C_H2 domain. The hinge region is situated between the Fab fragments and the Fc fragment and creates a linker to allow for structural flexibility.

Antibodies are an integral part of the humoral immune system. They carry two main characteristics, making them interesting as therapeutic agents: First, they bind their target with high specificity, and second, they bind it with high affinity. In the body, antibodies are produced by B cells that secrete a soluble form of their B cell receptor (BCR). Each B cell carries its own unique receptor. During B cell maturation, heavy and – at later stages of development – light chain undergo a complex process of joining together multiple gene fragments from the genetic antibody locus, combined with directed and limited mutation. This yields a diverse repertoire of naïve BCRs that can recognize a large variety of structures on pathogens. This process of BCR repertoire generation allows the immune system to respond to novel, unknown pathogens and forms the foundation of antibody-mediated immunity.

Upon recognition of the antigen via the BCR, the B cell starts to proliferate and differentiate into plasma cells that specialize in antibody secretion or long-living memory B cells that can be reactivated if the antigen is encountered at a later stage in life again. Additionally, the antibody undergoes a process called somatic hypermutation, wherein further mutations are introduced to improve the affinity to its target. During the course of the immune response, B cells that initially produce mostly IgM and IgD molecules perform a class-switch to usually IgG, which is the most abundant antibody class in blood and forms a major pillar of the adaptive immune response.

By binding to their recognized structure, antibodies inactivate and mark the pathogen for destruction by the immune system. Clearance of the pathogen is carried out through multiple mechanisms: The Fc part of the IgG acts as a docking station for the complement system, leading to complement-dependent cytotoxicity (CDC). Furthermore, the antibody provides a signal via the Fc part for phagocytes and cytolytic T cells to neutralize the bound target, which are termed antibody-dependent cellular phagocytosis (ADCP) and antibody-dependent cellular cytotoxicity (ADCC), respectively[65,66]. Therefore, by their biological design and function, antibodies lend themselves to be used as naturally occurring therapeutics.

3.2.1 Antibody Formats in Cancer Therapy

These favorable characteristics of IgG antibodies combined with their relative ease of generation via immunization of animals made IgG antibodies the first antibody moiety to be investigated as therapeutics. To date, the vast majority of FDA- and EMA-approved antibody therapeutics relies on the IgG backbone. However, some disadvantages of using full-length antibodies as therapeutics such as low tissue penetrance, labor-intensive generation procedure and the ethically controversial killing of animals incentivized the development of alternative methods to generate antibodies.

The advent of display techniques on phage, yeast and ribosomes allowed for rapid in-vitro screening of libraries containing billions of different binders such as single chain variable fragments (scFv), Fabs and single domain antibodies (sdAb). These alternative formats exhibit different characteristics than classical antibodies, which will discussed in the upcoming chapters. Additionally, bispecific antibodies (bsAb) and ADC not only promise to increase specificity and potency, but also allow for new modes of action of future therapeutics. While our understanding of different antibody formats is still expanding, researchers today can access an increasingly large toolset to tailor therapeutics for specialized requirements.

3.2.1.1 Classical Antibodies

As previously stated, the vast majority of approved antibody therapeutics relies on the IgG class. In humans, IgG antibodies are further divided into the subclasses IgG1, IgG2, IgG3 and IgG4, with each class carrying slight variations in their sequence, structure, glycosylation, and effector functions. These effector functions are mainly mediated by the Fc region of the antibody and include CDC, ADCC and ADCP as well as Fc receptor (FcR) binding. Most therapeutic antibodies utilize the IgG1 subclass with some drugs being designed as IgG2 and IgG4. Interestingly, although IgG3 exhibits strong effector functions, so far no therapeutic has been successfully developed based on this subclass due to higher rates of proteolysis and aggregation and short half-life, which require extensive engineering[65,67].

The IgG1 subclass, being the most abundant IgG subclass in blood, has established itself as the gold standard for antibody therapeutics development, due to its ability to activate multiple immune

mechanisms at the same time. IgG1 and IgG3 can effectively trigger complement activation via the C1q protein, leading to the formation of the membrane attack complex and thereby neutralization of the pathogen[68]. Binding affinity to the Fc gamma receptors (FcγR) FcγRI (CD64), FcγRIIa (CD32a), FcγRIIb (CD32b), FcγRIIc (CD32c), FcγRIIIa (CD16a) and FcγRIIIb (CD16b), varies with the IgG subclass. These receptors are present on multiple cell types of the immune system. FcγRIII is present on macrophages, neutrophils and natural killer cells and a main mediator for ADCC[69]. Again, IgG1 and IgG3 show the strongest affinity for FcγRIII, whereas IgG2 and IgG4 do not show strong activation of ADCC[70]. IgG1 also shows strong binding to the neonatal FcRn, which has been shown to increase recycling rate and thereby improve serum half-life[71,72].Taken together, the choice of antibody class has large implications regarding stability and activation pathways of the immune system. Researchers must decide which mechanisms of action are desirable for the treatment and which could pose a detriment for the patient. The high efficacy and multi-faceted mechanisms of action of IgG1 have made it a prime choice for antibody therapeutic development.

In 1975 Köhler and Milstein laid the foundation for modern antibody therapy when they established murine cell lines secreting monoclonal antibodies by hybridoma technology[73], which made it possible to produce antibodies of a single, defined specificity. Generally, targets for antibody therapeutics should be i) expressed either exclusively expressed, overexpressed or differentially expressed on the surface of the targeted cell to allow distinction between healthy and non-healthy cells, ii) the target should be abundant in the absolute expression level and iii) the target should be essential for cell growth or survival to reduce the formation of resistance. Binding of the antibody does not only mark the bound antigen for destruction by the immune system, which can be seen as an indirect mechanism, it also creates the possibility for direct manipulation of the target. Direct manipulation includes i) inhibiting ligand binding, usually by binding near the ligand binding site of the receptor, ii) inhibition of dimerization, thereby interfering with downstream signaling and iii) induced internalization and depletion of the bound receptor[74]. Current antibody therapeutics targeting e.g. epidermal growth factor receptor block both ligand binding and receptor dimerization to induce apoptosis[75].

The first antibody to be approved was OKT3 in 1986. This murine IgG2a antibody suppresses the immune system of patients receiving organ transplants by targeting the CD3 T cell antigen, inducing apoptosis of the T cell[76]. While OKT3 showed the potential of antibodies in therapy, it also induced the production of human anti-mouse antibodies (HAMA) that were detectable three weeks after initial treatment, leading to increased clearance of the OKT3 antibody and allergic reaction for the patient[77,78]. These reactions represent common side effects towards fully murine antibodies[79,80]. Increasing the share of human sequences in the protein will lead to reduction of immunogenicity and has therefore been an early focus to create safer and more potent antibody therapeutics. To this end, researchers replaced the murine constant regions with human constant regions yielding a chimeric antibody consisting of human constant, but murine variable domains[81]. Further improvements have been achieved by humanization through CDR grafting[82] (figure 2). In this approach, monoclonal antibodies can be isolated from mice or other non-human organisms. Then, the CDRs are grafted into an antibody framework of human origin. This approach minimizes the amount of non-human and therefore potentially immunogenic sequences in the antibody. Humanization of the antibody has led to vast reduction in immunogenicity, although data suggests that even fully humanized sequences can lead to immune reactions[83].

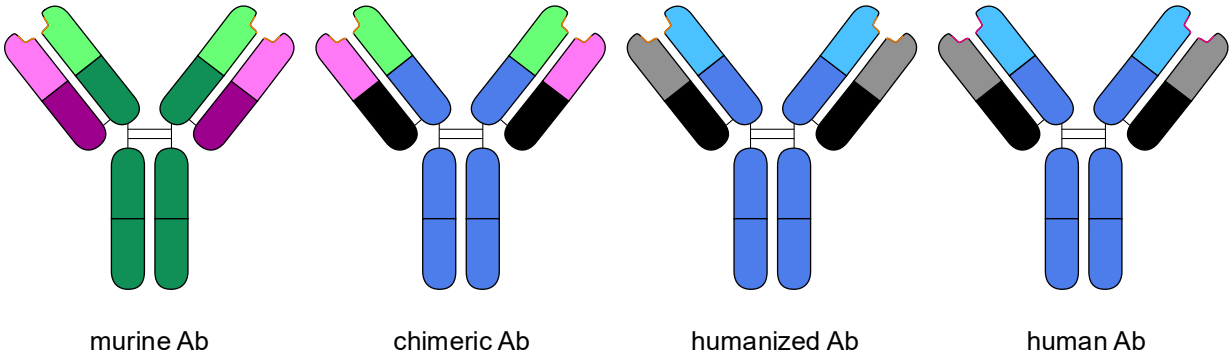

Figure 2: Structural differences between murine, chimeric, humanized and fully human antibodies. Murine antibodies are often the basis for generation of new antibodies by hybridoma technology but cause immune responses in humans. Chimeric antibodies represent a mixture of murine and human features. Usually, the variable domains are transferred from the murine antibody to a human backbone containing fully human constant domains of both heavy and light chain. A humanized antibody contains ideally only the murine CDR sequences, whereas even the variable domains are built on a human framework. Fully human antibodies do not contain foreign sequence features and must be isolated from human B lymphocytes or *in vitro* libraries via display techniques. Murine heavy chain is depicted in green, murine light chain in purple and murine CDR in orange. Human heavy chain is depicted in blue, human light chain in black/grey and human CDR in magenta.

Today, next generation sequencing, the development of transgenic mice carrying human antibody sequences and in-vitro display techniques such as phage display allow the isolation of fully human sequences either from patients, animals, or in-silico libraries, respectively. These advances enable the development of antibody therapeutics that are better tolerated by patients. Modern therapeutics therefore show a clear trend towards not only humanized and human full-length antibodies, but also other formats with different characteristics than the classic IgG antibody.

3.2.1.2 Novel Formats: Bispecifics and Antibody Fragments

Antibody therapeutics have enabled a huge leap forward in the fight against cancer. However, this does not come without limitations. These include a lack of efficacy manifested in incomplete remissions as well as relapses with acquired resistance to antibody treatment[84-86]. A major reason for acquired resistance is tumor heterogeneity: Even within the same tumor, cells will exhibit expression of the targeted antigen at varying levels, depending on the progression of the disease, mutational burden and tumor microenvironment[87]. Antibody treatment will therefore preferentially target those tumor cells with high antigen expression, naturally selecting potential survivors with low or non-existent expression. These survivors might seed the regrowth and lead to a relapse of the tumor. Further resistance mechanisms include altering antigen shuttling and internalization or differential intracellular signaling[88-90]. Another major issue of cancer immunotherapy is the non-exclusive expression of the target antigen. Being able to identify an antigen that is exclusively expressed on tumorous, but not on healthy cells, is unfortunately rare. Thus, current therapies resort to overexpressed antigens. However, healthy cells expressing the antigen, albeit at a lower level, are still targeted by the therapeutic, creating adverse side effects. Finally, solid tumors present a physical barrier that impede the diffusion of large molecules like full-length antibodies, leading to reduced tissue penetration and impeded exposure of the tumor cells to the antibody.

These problems have sparked interest in the development of novel formats (figure 3). Bispecific antibodies target two antigens with the aim to increase specificity towards the tumor and reduce the likelihood of the tumor becoming resistant. Smaller formats like Fab, scFv and sdAb (i.e. nanobodies) promise to increase tissue penetration due to their naturally smaller size[91,92]. Unlike full-length antibodies, the discovery of these molecules is compatible with display techniques in

phage and yeast, allowing for large libraries and more rapid protocols compared to full-length antibodies acquired via animal immunization.

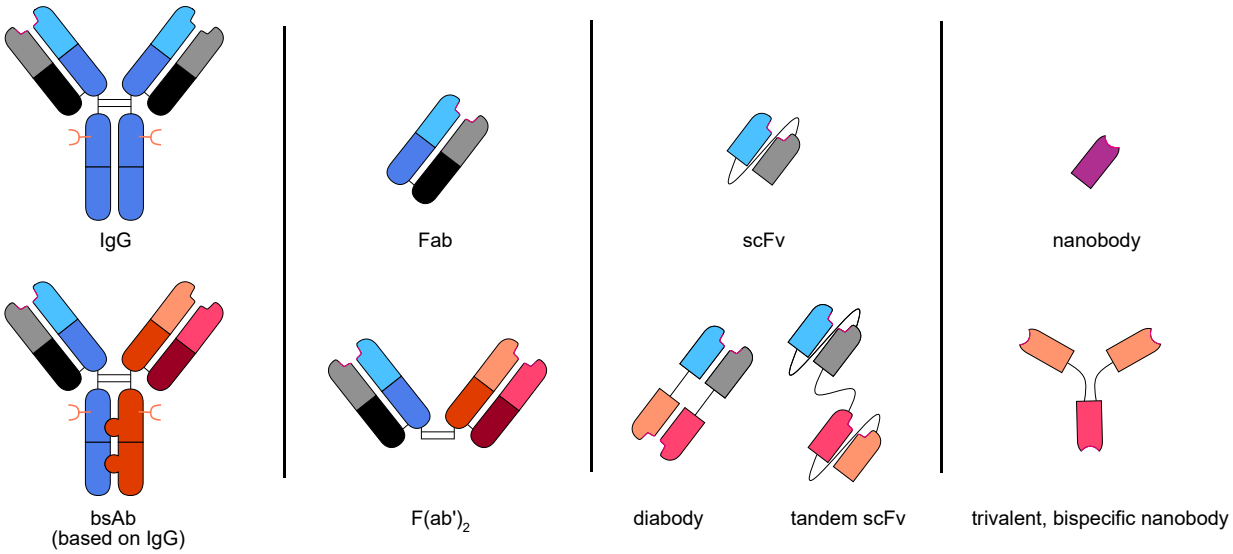

Figure 3: Different formats of antibody-based therapeutics and selected bispecific versions that are already in clinical use or under investigation. Left to right: full length IgG antibody and a bispecific antibody based on IgG using the "knob into hole" technology; antigen-binding fragment (Fab) and a bispecific F(ab')$_2$ fragment linked via the hinge region; single-chain variable fragment (scFv) and bispecific a diabodies and tandem scFv; nanobody and a trivalent, bispecific nanobody.

The word "bispecifics" is an umbrella term for therapeutics that combine specificity against two or more different epitopes. The epitopes can either be present on the same cell or two antigens on two different cells. Biparatopic binders are a subgroup of bispecifics that target two different epitopes on the same antigen. Bispecifics are not confined to a special format or type of antibody fragment. On the contrary, building blocks of different formats are often combined to produce a bispecific therapeutic. Bispecifics can be generated either by chemical conjugation[93-95] or by genetic engineering. One major branch of research focuses on the generation of bispecific full-length IgGs. IgG antibodies are bivalent by nature, therefore introducing a second specificity theoretically does not require the introduction of artificial linkers or structures. However, since both specificities need to be expressed within the same cell, homodimerization of chains with the same specificity is possible and reduces the yield of the bispecific product. A common solution to this problem is the enforcing heterodimerization of chains with different specificities using the "knob into hole" approach: Here, the interfaces of both chains are altered to create protruding amino acids in one chain (knobs) and empty pockets (holes) on the other chain to create sterical hinderance for homodimerization[96,97]. Bi- and multispecific IgGs have been shown to successfully target tumor cells 25 years ago[98]. The FDA and EMA have originally approved Catumaxomab for treatment of malignant ascites. Catumaxomab is a trifunctional antibody targeting epithelial cell adhesion molecule on tumor cells, CD3 on T cells and natural killer cells and macrophages via the Fc region. By bringing those three cells in close proximity to each other, the antibody stimulates the killing of the tumor both via ADCC and ADCP[99]. Although Catumaxomab has been withdrawn from the market, it showed the potential of multispecific IgGs for treatment of cancer.

Fabs consist of the complete light chain, paired with the VH and CH1 domains of the heavy chain. This makes them much smaller in size with about ~55 kDa, leading to higher tissue penetration but also faster renal clearance[100], an effect that is further enhanced by the lack of FcRn-mediated recycling. While some antibodies and especially ADCs can cause toxicities due to unspecific

uptake via FcRs[101,102], Fabs are thought to provide a solution due to the lack of the Fc region. Fabs are monovalent, bind their target at a 1:1 ratio and are therefore unable to crosslink multiple antigens. Common sources of Fabs are monoclonal antibodies from hybridoma and binders derived from libraries by *in vitro* selection. Design of those selection libraries is especially complicated due to the high combinatorial variability that can be introduced into three CDRs each on the heavy and light chain, creating six highly variable regions that contribute to antigen recognition. This variability is beyond the scope of currently constructible libraries. Thus, common approaches resort to utilization of an invariant light chain with variability introduced into the CDR3 of the heavy chain. While not as stable as full-length antibodies, Fabs are more stable than scFvs due to the interaction of the CH1-CL domains[103]. Steps towards increasing serum half-life have been made by PEGylation or fusion of the Fab to albumin, which allows FcRn-mediated recycling of the fusion protein[104,105]. $F(ab')_2$ fragments are a variation, consisting of two Fab fragments joined together via the hinge region. This construct is bivalent – like a full-length antibody – with improved tissue penetration but lacks the Fc region and associated effector functions. The bivalency of $F(ab')_2$ molecules can be exploited to produce a bispecific agent with each arm recognizing a different antigen. Fabs have been the first antibody fragment to be explored and approved by the FDA and EMA with four constructs being in clinical use to date. However, no Fab has so far been approved for cancer treatment, which might be partially caused by the lack of Fc-mediated activation of the immune system. Therefore, approved Fabs so far rely on direct manipulation of their targets via blockage of receptor signaling. All four approved Fab therapeutics follow this strategy. Abciximab, receiving approval in 1994 as the first therapeutic Fab, prevents blood clot formation by inhibiting the binding of platelet receptor GPIIb/IIIa to von-Willebrand factor and fibrinogen[106]. Ranibizumab is a vascular endothelial growth factor A-binding Fab for the treatment of macular degeneration and macular edema, blocking signaling of this receptor pathway[107]. Certolizumab pegol has been approved for treatment in Crohn's disease and rheumatoid arthritis. It represents a Fab conjugated to polyethylene glycol to increase half-life and binds to tumor necrosis factor a, preventing inflammatory signaling[108]. Lastly, Idarucizumab has been approved as an anti-anticoagulant that binds to and thereby blocks signaling of the anticoagulant dabigatran[109].

Besides Fabs, scFvs have become a popular format for therapeutics. With only about 25-30 kDa, they represent a class of antibody fragments roughly half the size of Fabs. scFvs consist of only the variable domains of both heavy and light chain connected by a short peptide linker to prevent dissociation of both domains. Their small format makes them highly interesting for *in vitro* discovery and expression in bacteria, although in combination with the lack of the Fc region the problem of fast renal clearance is further excacerbated[110], necessitating repeated administration of scFv-based therapeutics in short intervals. Selection of the linker is of special importance for scFvs and influences solubility, folding and quaternary structure. One of the most common linkers is based on glycine and serine. These amino acids have minimal side chains, resulting in high flexibility, while the hydroxy group of serine confers hydrophilicity to the linker. However, studies suggest that commonly these repetitive glycine-serine linkers can cause dimerization[111] and increase immunogenicity[112]. Linker length is also a major determinant of multimerization. Short linkers do not allow enough flexibility for both variable domains to make contact within the same molecule and multimerize with the variable regions of a second molecule instead. The linker length can be exploited for the production of scFv complexes containing two (diabody), three (triabody) or even four molecules in complex[113,114]. This strategy not only allows for the production of multivalent binders, but also bi- and multispecific therapeutics. Multispecific scFvs can also be generated by

genetic fusion of two scFvs via another linker (tandem scFv). Due to their small size, low cost of expression and ease of engineering, scFvs have become a popular tool for the discovery of novel therapeutics or as fusion partners with other molecules[115], with an especially notable role as the antigen-binding domain in chimeric antigen receptors[116].

Like Fabs, the lack of the Fc region does not allow scFvs to initiate secondary immune responses via CDC, ADCC and ADCP. So far, only two scFv-based therapeutics have been approved by the FDA and EMA for cancer therapy. Both therapeutics use a novel class as therapeutics: BiTEs. BiTEs are bispecific molecules with one molecule targeting a T cell surface antigen, while the other one recognizes a tumor associated antigen. This creates spatial proximity between the immune and cancer cells, leading to activation of the T cell and release of granzyme and perforin. BiTEs thereby improve killing and enhance reduction of the tumor. Blinatumomab was the first BiTE to be approved in 2015 for B-ALL. It is a tandem scFv and targets the CD19 B cell antigen and the CD3 T cell antigen. Treatment of patients with relapsed and refractory ALL with Blinatumomab has led to improved survival for patients[38,117]. Even more innovative was the development of Tebentafusp that has been approved only recently in 2022. This therapeutic is a fusion protein of an scFv and the soluble part of a T cell receptor that recognizes a peptide of the melanoma-associated antigen gp100 for the treatment of metastatic uveal melanoma[118].

Although scFvs are stripped of all domains that do not contribute towards recognition of the antigen, they are not the smallest commonly used format yet. sdAb such as nanobodies derived from camelid heavy chain antibodies[119] or isolated from artificial libraries based on human frameworks have become a staple both for therapeutic research over the last decades. With full-length antibodies on one side, sdAbs represent the other end of the spectrum: They are only 13-15 kDa small and structurally extremely simple. As their name suggests, sdAbs consist of only a single domain that contributes to binding of the antigen and completely lack a second chain. Their simple structure allows discovery campaigns in phage display and expression at low cost in bacterial systems. In stark contrast to human frameworks, camelid nanobodies are soluble without the need for a second domain due to the exchange of multiple hydrophobic amino acids to polar, hydrophilic ones[120]. Although these mutations could suggest high immunogenicity in humans, it has been shown that some camelid frameworks create no or only minor immune responses[121]. Nevertheless, some frameworks benefit from humanization to minimize their risk profile for therapeutic use[122]. Nanobodies are structurally unique in the way they bind to their targets: Whereas classic antibodies form a cavity for binding their target, the antigen recognition surface of nanobodies is rather flat with often the CDR3 loop protruding outwards of the domain[123,124], which suggests that nanobodies might recognize different surfaces on antigens than binders derived from classical antibodies.

Unlike previously discussed formats, no sdAb has been FDA- or EMA-approved as a therapeutic in- and outside of the field of cancer therapy. However, Ozoralizumab has been approved in Japan for treatment of rheumatoid arthritis. Ozoralizumab is a trivalent construct carrying two specificities, with two domains targeting TNFa, while the last domain binds to serum albumin to enhance half-life and improve tissue distribution at inflammatory sites[125]. Nanobody therapy is still in its infancy. Due to the lack of Fc-mediated signaling, nanobody therapy has to rely on manipulation of signaling pathways by blocking receptor-ligand interactions[126,127] or function as activators in BiTE-like formats[128,129].

3.2.1.3 Antibody Drug Conjugates

A common motif especially in formats lacking the Fc region is the vastly reduced possibility to induce killing of the tumor cells, which poses a major hindrance for the development of antibody-based therapeutics. While full-length antibodies exhibit enhancer effector functions via CDC, ADCC and ADCP, they often fail to penetrate sufficiently into the tumor or are not effective enough to eradicate tumor cells before the development of resistances. Increasing the dosage of drug is also only possible to a certain degree before side-effects become too severe and the damage by adverse side effects outweighs the danger of the initial disease. The therapeutic index describes the differences in dosage between effective treatment of the disease and the onset of severe side effects. Ideally, a broad therapeutic index is achieved when the drug is effective even at low dosage and no or little side effects are observable at high dosage. Therapeutic antibodies have allowed tremendous improvements in cancer therapy. However, they are often used in combination with other drugs such as chemotherapeutics or radiation therapy as their efficacy as is insufficient. Simply put: Their therapeutic index is too narrow to be used as a standalone treatment.

Conceptually, ADCs present themselves as an ideal solution. They consist of three units: the binding moiety, the drug (also termed payload or cargo) and a linker to connect both. Although most understand the term ADC synonymously with the conjugate of an antibody to a small molecule toxin, the term ADC has a broader interpretation. The “drug” part of the ADC can refer to other types of molecules, including cytokines, protein toxins, proteolysis targeting chimeras (PROTAC) and oligonucleotides (ON). The most common form of ADCs are antibody-toxin conjugates. The toxins used in these conjugates are highly potent small molecules that otherwise would be too toxic for systemic administration. Here, the ADC combines the high specificity of the antibody with the exceptional potency of a toxin. This represents the strength and premise of ADC technology: Fusing together two vastly different molecules to create a novel function that none of these molecules alone could have achieved.

Internalization is a crucial step for most ADCs. After binding to the cell surface, the ADC gets internalized and transported to the endosome. In the endosome, the drug gets released by acidification, enzymatic cleavage or complete degradation of the antibody. After release from the endosome, the drug can reach its final destination by molecular diffusion and – depending on the mechanism of action – induce apoptosis by inhibition of the cytoskeleton, cause DNA damage or interfere with critical steps in cellular metabolism.

The attachment of other molecules to the antibody will alter the biophysical characteristics of the whole conjugate. For example, most currently used small molecule toxins are highly hydrophobic, leading to aggregation of the conjugated product. In contrast, oligonucleotides are hydrophilic but strongly charged and physically large molecules. The drug to antibody ratio describes how many drug molecules are attached to each antibody molecule. While most ADCs will consist of a heterogeneous mixture containing molecules of different DARs, the average DAR is still an important characteristic for both efficacy and stability. Technologies to generate specific DARs and the correct determination of the DAR is therefore of utmost importance[130,131].

3.2.2 Generation of Antibody Drug Conjugates

The desire to create ADCs gave rise to a completely new set of challenges. Whereas therapeutic antibodies could be expressed naturally or fused on a genetic level, the generation of ADCs required the attachment of two chemically distinct moieties by chemical conjugation. Reactions

that include biomolecules such as proteins have special requirements: i) the reaction must take place in aqueous solutions since these are the natural environment of proteins and strong organic solvents will lead to protein denaturation, ii) the reaction must take place in approximately neutral pH since highly acidic or basic pH ranges will lead to unfolding and denaturation and iii) the reaction must take place in comparatively mild conditions with regards to the use of oxidative, reductive, electrophilic and nucleophilic agents due to the abundance of amino acid side chains that could be chemically altered and affect the functionality of the protein. This necessitated a design process rooted deeper in biochemistry than molecular biology. Since the inception of ADCs, the core questions to be answered have remained the same: Where is the drug attached? How is the drug attached? And how can the drug be efficiently released? A smart conjugation design with high chemo- and site-selectivity is essential because site of attachment and conjugation chemistry have major impacts on stability and biodistribution of the drug[132,133]. Strategies for the generation of ADCs include the usage of proteinogenic amino acids, both naturally occurring and genetically engineered, as well as chemo-enzymatic approaches (figure 4).

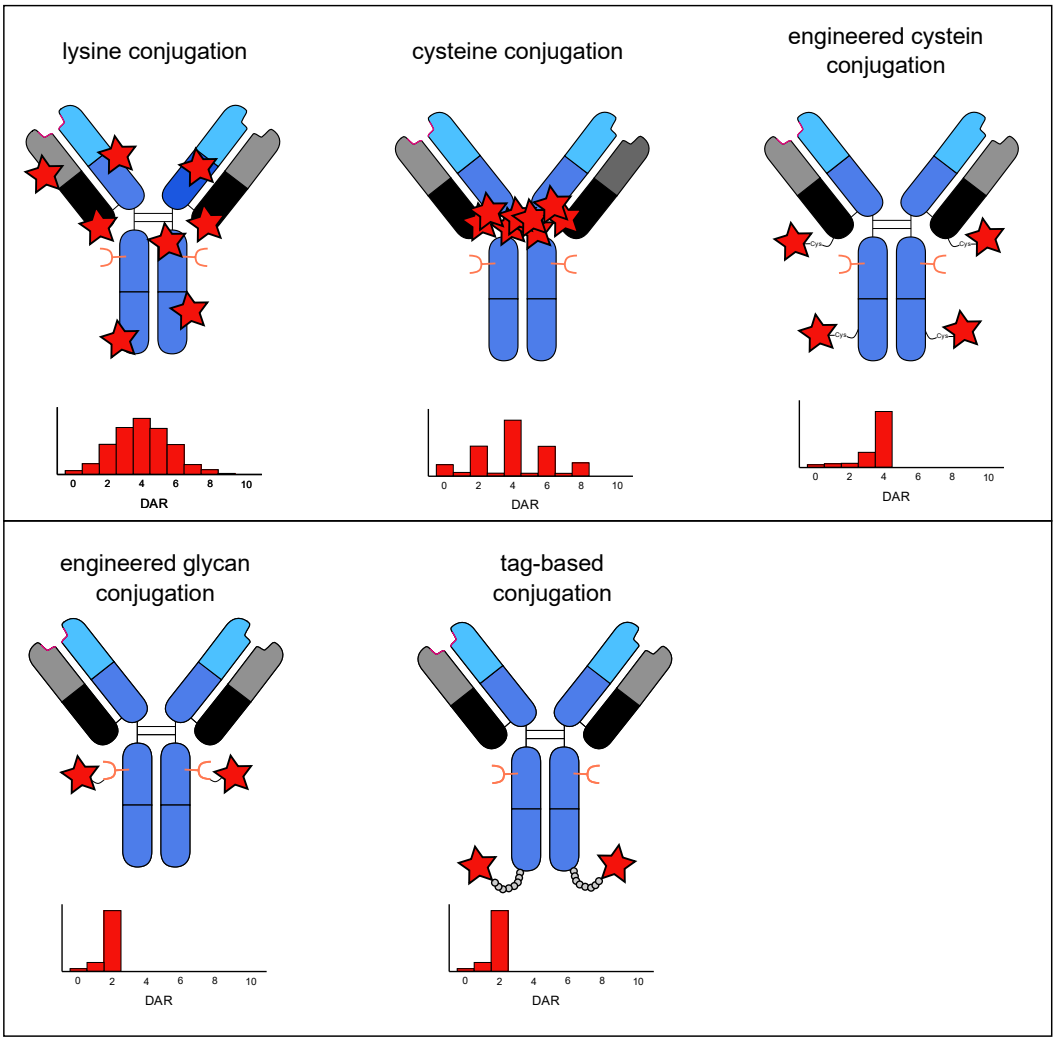

Figure 4: Conjugation methods commonly used for the generation of ADCs. Top panel: Conjugation via proteinogenic amino acids. When conjugating the ε-amine group of naturally occurring lysine residues, neither the position of the drug, nor the drug to antibody ratio can be controlled well. Lysine conjugation leads to highly heterogenic products containing a variety of DARs. Cysteine conjugation targeting intermolecular disulfide bridges leads to a much more defined distribution of DARs and improved site-selectivity over lysine conjugation. Conjugation via engineered cysteine represents a further improvement regarding site-selectivity and yields a product of very defined DAR with relatively little other DAR species in the product. Bottom panel: Chemo-enzymatic conjugation strategies. Conjugation of engineered glycans allows for site-specific attachment of the drug with little variation in DAR. Similarly, tag-based approaches such as Sortase A and tubulin tyrosine ligase are also able to achieve ADC products of defined DAR.

3.2.2.1 Conjugation via Proteinogenic Amino Acids

Many of the 20 canonical natural amino acids such as threonine, glutamic acid, aspartic acid, glutamine and asparagine carry nucleophilic amide, hydroxyl or carboxyl groups that are commonly used in organic chemistry as handles for reactions. Although many of these charged amino acids are even found in the active pocket in enzymes, it is the chemical microenvironment at the reaction site that increases their reactivity with the educts. For bioconjugation in aqueous solutions, only few amino acids allow conjugation in pH-neutral and mild reaction conditions. Historically, two amino acids have been prime targets for bioconjugation: the e-amine group of lysine and the thiol group of cysteine. These functional groups exhibit high nucleophilicity at near neutral pH, are abundant in natural proteins and accessible on the protein surface due to their polarity.

Many amine reactive agents have been described and are commonly used for functionalization of the lysine side chain: isocyanates and isothiocyanates, acyl azides, imidoesters, carbodiimides, aldehydes and phosphine derivatives[134]. The first and until today by far most commonly used agents are based on the electrophilic N-Hydroxysuccinimide[135]. NHS ester reactions are fast even at room temperature, work in various amine-free buffers of slightly basic conditions (pH 8.0-8.5, usually well tolerated by most proteins) and form stable amide bonds with the lysine side chain with the succinimide functioning as a stable leaving group. NHS groups are regularly used to attach small chemical molecules such as fluorophores, biotin, toxins and bifunctional linkers to proteins and peptides. A major disadvantage of NHS ester labeling is the neutralization of the positively charged lysine as well as their propensity for side reactions towards histidine, serine, threonine, and tyrosine, creating undesired side products and attachment sites on the protein[136]. Additionally, NHS esters hydrolyze rapidly in water, especially at basic pH, necessitating high excesses of reagents. To address some of the downsides of NHS esters, novel conjugation methods such as 2-(2-styrylcyclopropyl) ethanal[137], azaphilones[138] and diazonium terephthalates[139] have been recently described. While lysine-based conjugation strategies provide a quick and reliable way to attach other molecules to proteins, the high abundance of lysines on the surface makes it near-impossible to control both the site-specific attachment, as well as the number of molecules that react with the protein. This leads to highly heterogenous products with varying DARs and differently decorated molecules even if they carry the same amount of drug. Since these characteristics are of special importance for the generation of ADCs, the current field is moving away from lysine conjugation for the production of therapeutics.

A potential solution to this issue is the conjugation via thiolate groups of cysteines. Cysteines are much rarer in proteins compared to lysines, naturally limiting the number of attachment sites. With a pK_a of 8.2, a significant portion of cysteine is deprotonated and forms the highly nucleophilic thiolate ion[140]. Furthermore, cysteines engage in the formation of disulfide bridges to stabilize the tertiary and quaternary structure of proteins. Antibodies have multiple disulfide bridges. For example, an IgG antibody contains one intrachain disulfide bridge in each domain and four interchain disulfide bridges with two of these connecting the CL domain of the two light chains with the hinge region of their respective heavy chain and the remaining two connecting the two heavy chains. The interchain disulfides are buried within the structure, making them less accessible for chemical functionalization. In contrast, the interchain disulfides are solvent exposed and all concentrated in the hinge region. This yields a high control over both the site of attachment, making cysteine conjugation strategies much more site-specific, and the maximally achievable DAR. Michael acceptors such as maleimides and vinyl sulfones as well as aziridines and arylating agents are common for cysteine functionalization, with maleimides being most frequently used[134]. Maleimides, while structurally similar to NHS, contain an alkene moiety that introduces ring strain

and thereby increases the electrophilicity of the site. Although they are able to label primary amines, the reaction with thiolates is kinetically preferred at neutral pH, leading to a high chemoselecivity for cysteine[140]. Similar to NHS-ester conjugation, many chemicals are readily available with functional maleimide groups or other cysteine reactive moieties. Brentuximab vedotin and Trastuzumab emtansine, two FDA- and EMA-approved therapeutic ADCs, rely on cysteine chemistry. However, it has been shown that maleimide conjugates undergo hydrolysis and thiol-exchange reactions, transferring their payload to albumin and other proteins containing sulfhydryl groups, which can lead to toxic side effects[141-143]. Efforts have been made to create more stable linkers for cysteine chemistry that do not undergo thiol exchange reactions including conjugation via ethynylphosphonamidates, N-aryl maleimides, N-phenyl maleimides and N-Methyl-N-phenylvinylsulfonamides[144-149]. A major advantage for cysteine-based conjugation chemistry is the ability to engineer conjugation sites. The replacement of cysteine with the structurally similar but less nucleophilic serine is well tolerated by many proteins. Replacing surface exposed, undesirable cysteines with serines and introducing new cysteines at desired positions in the antibody enables complete control over the attachment site and the amount of available functional groups. This strategy has been employed e.g. in Genentech's "Thiomab" platform[150] for the generation of ADCs[151,152]. These engineered antibodies have been shown to have improved serum stability over maleimide conjugates[153]. Nevertheless, the exact position of the engineered cysteine is of utmost importance and heavily influences the stability of the conjugate [154,155].

While cysteine chemistry provides an improvement over lysine-based conjugation techniques, the reduction of intra- and intermolecular disulfide bridges removes a stabilizing characteristic for antibodies. Although the position and abundance of cysteines is much more defined, cysteine conjugation will still lead to a heterogenous mixture of ADCs with different DARs and attachment sites.

Worth mentioning are some papers that report other side chains such as tyrosines have been for protein functionalization[156,157]. However, these reactions are far less commonly used and ADC research mostly relies on conjugation via lysines and cysteines.

3.2.2.2 Chemo-Enzymatic Conjugation

Another way to introduce reactive handles into proteins is the utilization of enzymes often in combination with chemical functionalization. Enzymes catalyze the reaction of their substrates upon recognition of specific structures or sequences. High specificity of these reactions is achieved either by the structure of the enzymes and substrates themselves, withholding any wrongly shaped or charged substrate from entering the active pocket of the enzyme, or by compartmentalization of reaction spaces within the cell, allowing only desired substrates into the compartment. Generally, enzymes are unable to recognize the entire structure of their substrate, but only a small recognition motif. This fact can be exploited, since it makes enzymes blind towards everything else, as long as they find their recognition motif.

One of the first and best-known enzymes for enzymatic functionalization of proteins is BirA. BirA recognizes a stretch of 15 amino acids (GLNDIFEAQKIEWHE), called the AviTag, and catalyzes the ligation of biotin to the lysine in the recognition sequence via a BirA-biotin intermediate state[158]. BirA has been optimized for various purposes and is widely employed for the biotinylation of proteins, often in tandem with multimerization or detection via avidin, in different fields of research[159-161]. The beauty of enzymatic system is that the position and number of recognition sequences define how many functionalities can be attached. In many cases, the catalyzing enzyme shows promiscuity towards variations of its substrate, allowing the introduction of chemical

handles for further reactions. This leads to a two-step process of the enzymatically catalyzed reaction to introduce a reactive handle to the protein, followed by a chemical reaction for the conjugation of a small molecule.

For the generation of ADCs, multiple enzyme systems have been reported. Microbial transglutaminase forms isopeptide bonds between lysines and glutamine and has been employed for the generation of ADCs[162]. Interestingly, the surface-exposed lysine residues of IgG1 are not recognized by this enzyme. However, deglycosylation of amino acid Q295 renders it accessible for modification by transglutaminase[163,164]. Alternatively, the antibody can be engineered with a recognition motif (Q-tag)[133].

Sortase A is another popular and widely used enzyme for functionalization of proteins. While the original function is the crosslinking of peptidoglycan structures on the cell wall of bacteria, it has first been reported for protein functionalization in 2004[165]. Sortase A is a transpeptidase that recognizes the LPXTG motif on the first and poly-glycine chain on the second substrate and acts by cleaving of the LPXTG motif between tyrosine and glycine, followed by ligation of the tyrosine to the poly-glycine of the second substrate. Sortase A-mediated protein functionalization allows for modification of both the N- and C-terminus and has been successfully employed for the generation of ADCs[166-169].

Other strategies target the glycosylation structure of antibodies by the remodeling of N-glycans with mutant endoglycosidase[170], the usage of glycotransferases and engineered sugars[171,172]. These methods are elegant since they do not require sequence engineering of the antibody and instead use native structures. However, glycan engineering is a technically challenging endeavor. Additionally, native glycosylation is important for antibody functionality and alterations thereof have been implied to potentially increase immunogenicity[173,174].

Lastly, tubulin tyrosine ligase (TTL) has been employed for protein functionalization and generation of ADCs[95,175-177]. While the original function is the ligation of tyrosine to the C-terminus of tubulin, a short 14 amino acid long patch rich in glutamic acids (VDSVEGEGEEEGEE) at the C-terminus is sufficient as a recognition motif. TTL has a broad substrate tolerance[178], allowing the introduction of a variety of chemical handles for subsequent functionalization reactions.

3.2.2.3 Classes of Payloads

Most ADCs focus on the conjugation of antibodies to small, toxic molecules to induce apoptosis in the target cell. These toxins have seen great clinical success over the last decades. Interestingly, to this date there are only few toxins available for use in ADCs. Only few toxins fulfill the strict requirements necessary to be considered for usage in ADCs: They have to be both potent without causing severe side effects, soluble and must not be metabolized in the body. Moreover, the structure of these toxins is highly complex and making them chemically available for bioconjugation is an equally complex task. This has posed a major roadblock for ADC development, because a limited number of available toxins corresponds to only few modes of actions that can be employed against tumors, leaving patients and physicians alike out of options if the tumor becomes resistant against a certain toxin. To this end, researchers are actively exploring other drug classes like cytokines, protein toxins, PROTACs and ONs (figure 5).

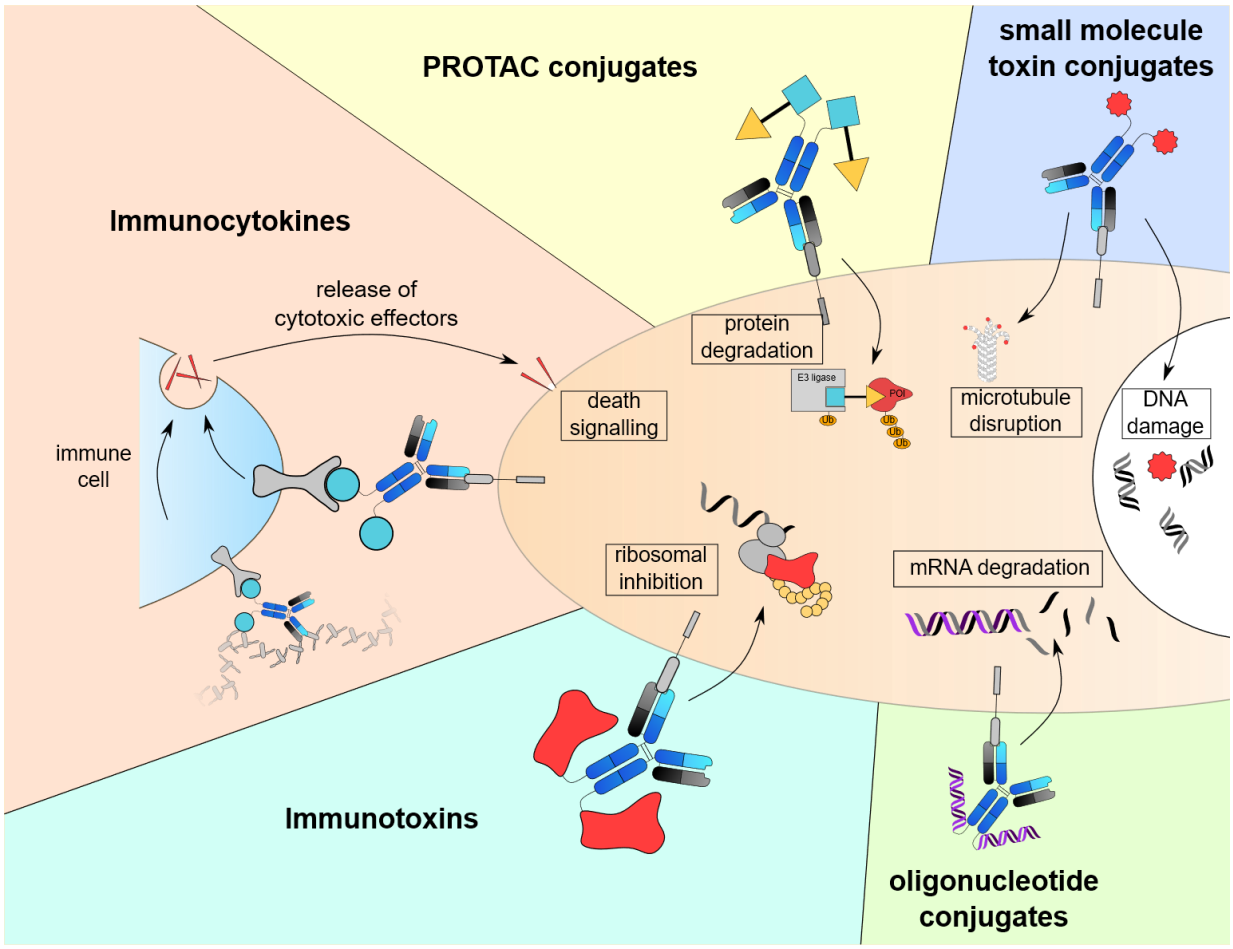

Figure 5: Overview of different ADC payloads that are in clinical use or under investigation. Most classic ADCs based on small molecule toxins disrupt the cytoskeleton or inflict DNA damage, triggering apoptosis of the cell. PROTACs are small, bifunctional molecules binding both to an E3 ligase and the protein of interest (POI) that should be targeted for degradation. They induce protein degradation by forcing spatial proximity between the E3 ligase the POI. Immunocytokine-based ADCs function by binding to the target cell and signaling to immune cells via the cytokine-fusion partner at the same time. This triggers the release of cytotoxic effectors like perforin or direct induction of apoptosis of the cancer cell. Immunotoxin-conjugates function similarly to small molecule toxins but utilize a cytotoxic protein. Current research focuses on Pseudomonas exotoxin A, which inhibits protein translation at the ribosomal level by ribosylation of elongation factor 2. Oligonucleotide ADCs deliver siRNAs to the cell, leading to degradation of the complementary RNA and thereby inhibit protein translation. Adapted from Schwach et al. 2022[179]

To understand which benefits novel drug classes could bring to the table, it is necessary to first understand the role and function of small molecule toxins in ADC therapy. Small molecule toxin ADCs need to be internalized. The moment of drug release depends on the linker between the antibody and the toxin. When using non-cleavable linkers, drug release occurs after complete degradation of the antibody[180], leaving the toxin attached to a residual amino acid which can negatively affect biodistribution and potency[181]. An improvement are cleavable linkers that are sensitive to acidification, reduction of a disulfide within the linker[182,183] or lysosomal proteases of the cathepsin family[184]. One of the most common linkers for ADC development uses the cathepsin cleavable valine-citrulline motif in combination with a para-amino benzyloxycarbonyl spacer. These linkers are called self-immolative since they undergo spontaneous 1,6-elimination after cleavage by cathepsin, leaving only the free toxin without residual atoms of the linker.

Most approved therapeutic ADCs use one of two classes of toxins: Microtubule inhibitors and DNA damaging agents. Auristatins (including the well-established toxins MMAE and MMAF), maytansinoids and tubulysins are part of the first class. They disrupt the cytoskeleton either by preventing the hydrolysis of GTP that is necessary for tubulin polymerization or by directly binding

to tubulin and thereby inhibiting polymerization[185,186]. This disruption in microtubule formation leads to dysfunction of important cell functions like cell division and cellular transport along microtubuli[187]. The second class, DNA damaging agents, includes calicheamicin, anthracylin, duocarmycin, camptothecin derivatives (e.g. exatecan) and pyrrolobenzodiazepines. They initiate DNA damage within the cell via various mechanisms: Pyrrolobenzodiazepin and duocarmycin lead to alkylation and crosslinking of DNA. Calicheamicin directly leads to strand breaks and derivatives of camptothecin inhibit the DNA religation step of topoisomerases after the enzyme induced temporary strand breaks in order to unwind the DNA during transcription and replication. Lastly, anthracylin inflicts DNA damage via intercalation into the double helix.

A major difference between microtubule inhibitors and DNA damaging agents is thought to be their ability to target resting cells. Due to the fact that the damage to a cell might not be as severe if it is not dividing, DNA damaging agents are thought to be more potent than microtubule inhibitors[188,189], although this does not appear to be a general truth with some studies publishing different results[190]. Some toxins such as MMAF are membrane-permeable, allowing them to move across membranes with ease. This enables an easier endosomal escape after drug release but also allows the toxin to diffuse out of the cell after it has already undergone apoptosis. These free toxin molecules can then inflict damage in neighboring cells, an effect that has been termed “bystander effect”. Although this can clearly lead to apoptosis of healthy cells in proximity to the tumor, the bystander effect generally enhances the cytotoxicity and allows the targeting of heterogenous tumors in which not all cells express a sufficient level of antigen[191-193]. Interestingly, the highly related toxin MMAE is not membrane permeable. In some cases, ADCs using MMAE have been reported to have ocular toxicities, a side effect that might be related to unspecific uptake and accumulation of the drug within the cell[194,195]. Since most small molecule toxins are highly hydrophobic, they have a strong influence on the overall biophysical characteristics of the ADC, making them more instable and prone to aggregation and affects renal clearance rate with high DARs being removed first. Overloading of the antibody with toxin can thereby have an overall negative effect *in vivo* with currently approved ADCs suggesting an optimal DAR of 3-4[196,197], although this will depend on the hydrophobicity of the toxin.

Antibody-protein toxin conjugates are an upcoming alternative to small molecule toxins. Since both partners are proteins, they can be expressed as a fusion protein, completely abolishing the need for chemical conjugation methods and yielding a highly homogenous product. With Moxetumomab pasudotox, one representant of this type of ADCs has already reached approval for the treatment of hairy cell leukemia[198]. Moxetumomab pasudotox is a fusion of an anti-CD22 scFv and a modified version of *Pseudomonas* exotoxin A (PE). PE binds and inhibits elongation factor 2 by ADP-ribosylation, leading to inhibition of protein translation[199,200]. The bacterial origin of PE has caused significant problems regarding immunogenicity which necessitated the development of de-immunized versions of the protein toxin[201,202]. PE-based ADCs have been in clinical trials against EpCAM with initial promising results[203,204]. This proves that PE-based ADCs can be a powerful tool for cancer therapy. Besides PE, diphtheria toxin has become a focus of protein toxin ADCs. Diphteria toxin employs a similar mechanism as PE by stalling ribosomal translation via inhibition of EF2. A bispecific diphteria toxin-based ADC has seen promising results using scFvs against CD19 and CD22 in patient derived xenograft models and first clinical evaluations[205,206]. Similarly, the toxin has been fused to tandem scFvs targeting EpCAM and HER2 for treatment of colorectal cancer[207], to biparatopic PSMA-binding scFv for the treatment of prostate cancer[208] and a tandem scFv for the treatment of gliablastoma[209]. Although not all these studies could show sufficient tumor regression, they provide evidence that diphtheria toxin might establish itself as a second alternative to PE in the near future.

PROTACs are an especially interesting moiety that are under investigation for ADC generation. PROTACs are small molecules with two functionalities: First, they bind their target protein, and second, they bind an E3 ligase, forming a tertiary complex. The induced spatial proximity of the complex leads to ubiquitination of the target protein and its destruction via the proteasomal complex. A hallmark of PROTACs is their catalytic mode of action, theoretically allowing for extreme cytotoxicity with only few internalized molecules. While common small molecule toxins act on their targets at a 1:1 stoichiometry, the catalytic mode of PROTACs makes them theoretically the ideal moiety for ADCs regarding efficacy. PROTACs are currently held back by a disadvantageous pharmacokinetic profile, poor tissue selectivity and often insufficient cell permeability[210,211]. While the latter will remain an issue for PROTAC-ADCs, the tissue selectivity and pharmacokinetics can be improved by conjugation to an antibody in a similar fashion to classic ADCs using small molecule toxins. It has been shown that the regulation of E3 ligase activity can promote tumorigenesis and vice-versa, that tumor cells regulate the expression of certain E3 ligases[212,213]. This could provide another layer of specificity for PROTAC-ADCs by targeting E3 ligases that are upregulated in the targeted tumor type. Currently used E3 ligases include the Von-Hippel-Lindau ligase[214-216] and Cereblon[217,218]. The field of PROTAC ADCs is still in its infancy, with only few studies available to date that are often limited to *in vitro* studies. Nevertheless, the proof of concept of PROTAC ADCs has been shown in using a Trastuzumab-based PROTAC to degrade the chromatic reader bromodomain-containing protein 4[219], while another group could show similar proof of concept to degrade serine/threonine-protein kinase 2[220]. The pharmaceutical company Genentech has also undertaken a larger study regarding conjugation methods and stability of PROTAC ADCs[221-223], which showed reasonable stability and potent anti-tumor efficacy in mouse studies, further reinforcing the potential of PROTAC-ADCs for future therapeutic use.

Another interesting moiety that is being explored are antibody-cytokine fusions, also termed immunocytokines. Cytokines are a diverse group of molecules involved in cell-to-cell signaling and strong modulators of the immune system. Cytokines can activate and inhibit the cytotoxic potential of specific immune cell populations and studies have reported effective cancer treatment with free cytokines. Interferon a has been approved for adjuvant treatment of high-risk melanoma patients with other cytokines such as granulocyte-macrophage colony-stimulating factor, IFN g, IL-7, IL-12, and IL-21 being in multiple clinical trials[224]. The major downside of cytokine therapy is the systemic administration and undirected activation of immune cells that will receive signaling triggers both in- and outside of the tumor location. The therapeutic index for many cytokines is very narrow, with low dosages being ineffective and high dosages leading to severe adverse effects[225-228]. This narrow window forces cytokines into a “supportive” role in cancer treatment, being given only as combinational therapy in concert with chemotherapy or radiation therapy. It has been hypothesized early on that antibody-cytokine fusions could eliminate the lack of specificity and provide a major improvement for cytokine therapy. Their mechanism is slightly resembling the BiTE-format, with one moiety targeting the cancer cell and the other partner targeting an immune cell, leading to immune cell activation and induced apoptosis of the tumor cell. However, while BiTEs induce apoptosis by mere proximity, cytokine-ADCs directly provide activation signals to the immune cell. Cytokine-ADCs differ in two major ways from all previously discussed ADC types: Firstly, internalization of the Cytokine-ADC is a detriment to its function. To maximize efficacy, the cytokine should be presented on the tumor surface for as long as possible. This allows cytokine-ADCs to use different targets than classical ADCs that rely on internalization. Second, they do need to directly recognize an antigen on the tumor surface. Tumor cells are able to alter their microenvironment, including the extracellular matrix[229,230]. In addition to cytokine-ADCs that bind to tumor cells, this enables the development of antibodies that are directed against tumor-specific features of the extracellular matrix and thus activating the immune cells at the

tumor site. Another advantage of using cytokines as cargo is the large array of readily available cytokines. This allows the choice of cytokine according to susceptibilities of the tumor. Similar to protein toxin ADCs, immunocytokines can be expressed as one fusion protein. With the exception of the linker peptide, they do not utilize foreign or artificial sequences, resulting in low immunogenicity. Immunocytokines are one of the best explored ADC groups with combinations of multiple cytokines and antibody formats. However, no immunocytokine has seen approval yet. Several cytokine ADCs have been tested based on interleukin 2 targeting classical surface antigens such as CD20 and EpCAM[231-233], interleukin 12 in combination with an anti-fibronectin scFv[234] with another group using the same scFv fragment as heterotrimer with two scFv molecules[235]. Other cytokines that have been used as fusion partners with antibodies include granulocyte-macrophage colony-stimulating factor and interleukin 15[236] and interferon g[237] being able to show efficient tumor killing *in vitro* and in mice. Due to the different modes of action compared to classical ADCs, immunocytokines bear a large potential for immunotherapy of cancer.

Lastly, antibody oligonucleotide conjugates (AOC) will be discussed. Short-interfering and antisense RNA molecules are well established tools in research to manipulate the stability of RNA in the cell. Despite their lack of specificity, some have been approved by the FDA, although none in a cancer-related background. A significant downside of these drugs is that they regularly fail to address cells outside of the liver, severely limiting the number of use cases[238]. As shown by the first AOC entering clinical trials in 2022[239], antibodies could provide a solution to the limited spectrum of targetable cells by providing the specificity and altering the pharmacokinetics of oligonucleotide-based drugs. The promise of oligonucleotides is huge: Their high customizability allows to alter the expression virtually any given protein in the cell, enabling the targeting of intracellular and genetic characteristics of cancer cells. However, the use of ONs comes with downsides. Oligonucleotides are large fragments of heavy molecular weight and extremely negative charge. These properties will severely alter the characteristics of the AOC. While the charge of the ON increases the solubility of the conjugate, the oligonucleotide will be unable to cross membranes[240,241], an issue that is especially crucial during the endosomal escape after degradation of the antibody, potentially necessitating co-treatment with additional agents to enhance endosomal escape[242-245]. AOCs can be generated using standard conjugation of lysines[246,247] or cysteines[248]. In addition to chemical conjugation, the negative charge of the ON enables the attachment to positively charged carrier molecules such as proteamine[89,249] or poly-arginine[246]. While studies provide proof-of-concept, that AOC treatment affects gene expression, a common denominator is the low efficacy of the treatment, likely caused by insufficient endosomal escape[89,248,250]. Despite those setbacks, many new treatments have yielded ambivalent results in the beginning that have only been resolved after years of continuous optimization. The target-specific delivery of oligonucleotides represents a highly researched field in- and outside of therapeutic applications.

3.3 Aims of this Study

Over the last decades, improved treatment regimen and deeper understanding of the underlying molecular mechanisms has resulted in higher survivability and longer survival times for leukemia patients. Still, there remains a significant portion of non-responding individuals and patients experiencing relapses with the tumor often exhibiting resistance against the previously applied treatment. While the number of ADCs in clinical trials is rapidly increasing, they dwarf against the sheer number of malignancies with highly heterogeneous expression patterns even within the same cancer type. Despite all progress, we have to realize that to this day, modern cancer

treatment still largely relies on surgical removal, radiotherapy and chemotherapy – approaches that cause severe side effects, often offer limited success and can rarely be tailored to the specific cancer profile of the individual. Our options for precise and personalized medicine are limited. We need to expand our toolkit.

The time-consuming and highly collaborative nature of the development of antibody therapeutics compels parallel development of multiple steps along the development pipeline. Therefore, this work covers multiple aspects at different stages of antibody and ADC development. First, we aim to generate antibodies against a set of ALL associated antigens to explore their use as ADCs in the future. Furthermore, we refine an existing antibody directed against Flt3 for the treatment of AML that has shown promising results in mice. To this end, we employ humanization of the variable regions and characterize the resulting candidates by chromatography and ELISA to find the most suitable lead candidate. This lead candidate will be subsequently conjugated with small molecule toxins and the cytotoxic activity assessed *in vitro*. Lastly, this work aims to establish and evaluate the functionality of a new protocol to generate antibody fragment-oligonucleotide conjugates via chemo-enzymatic conjugation that could be used for diagnostics and the generation of therapeutic antibody-oligonucleotide conjugates.

4 Material and Methods

4.1 Material

4.1.1 Buffers and Solutions

	Compound	Concentration	
4x Lämmli buffer	SDS	350	mM
	Bromophenol blue	0,5	% (m/v)
	Glycerol	33	% (v/v)
	Tris-HCl 0.5 M (pH 6.8)	50	mM
6x DNA loading buffer	Glycerol	30	% (v/v)
	Tris-HCl (pH 8.0)	20	mM
	EDTA	60	mM
	SDS	0,48	% (m/v)
	Bromphenol blue	0,25	% (m/v)
NiNTA binding buffer pH = 8,2	Tris-HCl	20	mM
	NaCl	250	mM
	Imidazole	20	mM
	ß-ME (add for TTL purification only)	3	mM
NiNTA elution buffer pH = 8,2	Tris-HCl	20	mM
	NaCl	250	mM
	Imidazole	500	mM
	ß-ME (add for TTL purification only)	3	mM
TTL storage buffer pH = 7,0	MES/K or MOPS	20	mM
	KCl	100	mM
	MgCl2*6H2O	20	mM
	L-Glutamate	50	mM
	L-Arginine	50	mM
	ß-ME	3	mM
Osmotic lysis buffer pH = 8,0	Tris-HCl	100	mM
	EDTA	1	mM
	Sucrose	20	% (m/v)
10x TAE	Tris-HCl	400	mM
	Acetic acid	1,148	% (v/v)
	EDTA pH 8,0	10	mM
10x CuAAC buffer pH = 7,4	CuSO4	2,5	mM
	THPTA	12,5	mM
	Aminoguanidine	50	mM
	Na-Ascorbate	50	mM
Ab Binding buffer pH = 7,5	NaH2PO4	20	mM
	NaCl	50	mM
	EDTA	1	mM
Ab Elution buffer pH = 3,0	Na-Citrate	100	mM
Neutralization buffer pH = 9,0	Tris-HCl	1000	mM
5x TTL reaction buffer pH = 7,0	MES	100	mM
	KCl	500	mM
	MgCl2	50	mM

FACS buffer **pH = 7,0**	PBS BSA	1x 0,1	 % (m/v)
AEX binding buffer **pH = 7,5**	Tris-HCl	20	mM
AEX elution buffer **pH = 7,5**	Tris-HCl NaCl	20 1000	mM mM
Imaging buffer **pH = 8,0**	PBS NaCl	1x 500	 mM

4.1.2 Commercial Antibodies

Antibody	Clone or Cat. No.	Supplier
αhCD2-PE	RPA-1.10	eBioscience
αhCD5-APC	L17F12	BioLegend
αhCD7-APC	6B7	BioLegend
αhCD28-APC	CD28.2	BioLegend
αhTRAT1-APC	TRIM-04	Novus Biologicals
αhTSPAN7-APC	B2D	Novus Biologicals
αhCCR9-APC	L053E8	BioLegend
polyclonal goat anti-mouse IgG-AF647	115-605-164	Jackson ImmunoResearch
polyclonal goat anti-mouse IgG-HRP	115-035-071	Jackson ImmunoResearch

4.1.3 Primers

ID	Primer name	Sequence 5'-3'	Predicted T_m [°C]	Use
35	SMART template switch-oligo	AAGCAGTGGTATCAACGCAGAGTACATrGrGrG	-	reverse transcription
36	SMART mIGK RT	ttgtcgttcactgccatcaatc	53	reverse transcription
37	SMART mIGL RT	ggggtaccatctaccttccag	56	reverse transcription
38	SMART mIGHG RT	agctgggaaggtgtgcacac	56	reverse transcription
39	SMART universal PCR	aagcagtggtatcaacgcagag	55	RT-PCR primer for antibody amplification
40	SMART mIGK PCR	acattgatgtctttggggtagaag	54	RT-PCR primer for antibody amplification
41	SMART mIGL PCR	atcgtacacaccagtgtggc	54	RT-PCR primer for antibody amplification
42	SMART mIGHG PCR	gggatccagagttccaggtc	56	RT-PCR primer for antibody amplification

43	HK_CD2_GA-cloning_FW	ttctctaggcgccggaattcATGAGCTTTCCATGTAAATTTGTAGCC	55	antigen cloning into pMIG/pMIY
45	HK_CD5_GA-cloning_FW	ttctctaggcgccggaattcATGCCCATGGGGTCTCTGC	55	antigen cloning into pMIG/pMIY
47	HK_CD7_GA-cloning_FW	ttctctaggcgccggaattcATGGCCGGGCCTCCGA	54	antigen cloning into pMIG/pMIY
49	HK_CD28_GA-cloning_FW	ttctctaggcgccggaattcATGCTCAGGCTGCTCTTGGC	56	antigen cloning into pMIG/pMIY
78	HK_CD2_GA-cloning_RV #2	gagttttctcgaggttaacgTTAATTAGAGGAAGGGGACAATGAGTT	55	antigen cloning into pMIG/pMIY
79	HK_CD5_GA-cloning_RV #2	gagttttctcgaggttaacgTTACAGCCTCTGAGCCCCAT	54	antigen cloning into pMIG/pMIY
80	HK_CD7_GA-cloning_RV #2	gagttttctcgaggttaacgTCACTGGTACTGGTTGGGGG	56	antigen cloning into pMIG/pMIY
81	HK_CD28_GA-cloning_RV #2	gagttttctcgaggttaacgTCAGGAGCGATAGGCTGCG	55	antigen cloning into pMIG/pMIY
96	G4S-FC-Strep-TT-pcDNA3.1_FW	GGTGGCGGTGGCTCGC	56	antigen cloning into pcDNA3.1
97	G4S-FC-Strep-TT-pcDNA3.1_RV	gcggccgccactgtgctggatTCACTCCTCGCCCTCCTC	55	antigen cloning into pcDNA3.1
98	CD2-FCStrepTT_GA-pcDNA#2_FW	tgtggtggaattctgcagatATGAGCTTTCCATGTAAATTTGTAGC	53	antigen cloning into pcDNA3.1
99	CD2-FCStrepTT_GA-pcDNA#2_RV	ttgggcgagccaccgccaccGTCCAGACCTTTCTCTGGAC	54	antigen cloning into pcDNA3.1
100	CD5-FCStrepTT_GA-pcDNA#2_FW	tgtggtggaattctgcagatATGCCCATGGGGTCTCTG	53	antigen cloning into pcDNA3.1
101	CD5-FCStrepTT_GA-pcDNA#2_RV	ttgggcgagccaccgccaccGTTTGGATCCTGGCATGTGAC	54	antigen cloning into pcDNA3.1
102	CD7-FCStrepTT_GA-pcDNA#2_FW	tgtggtggaattctgcagatATGGCCGGGCCTCCGA	54	antigen cloning into pcDNA3.1
103	CD7-FCStrepTT_GA-pcDNA#2_RV	ttgggcgagccaccgccaccGAGGGCAGAGGCTGCTG	54	antigen cloning into pcDNA3.1
104	CD28-FCStrepTT_GA-pcDNA#2_FW	tgtggtggaattctgcagatATGCTCAGGCTGCTCTTGGC	56	antigen cloning into pcDNA3.1
105	CD28-FCStrepTT_GA-pcDNA#2_RV	ttgggcgagccaccgccaccCTTAGAAGGTCCGGGAAATAGG	55	antigen cloning into pcDNA3.1
249	CH2_LALA_mutagenesis_wOH_FW	gctgctGGCGGACCTTCCGTGTTC	55	human IgG1 LALA mutagenesis
250	CH2_LALA_mutagenesis_RV	TTCTGGAGCAGGACATGGAG	54	human IgG1 LALA mutagenesis

251	CH1-mid_XagI_FW	agctgctctgggctgcctggtCAAGGACTACTTTCCTGAGCCTG	57	human IgG1 LALA mutagenesis
252	hinge_LALA-mutagenesis_RV	acggaaggtccgccagcagcTTCTGGAGCAGGACATGGAGG	56	human IgG1 LALA mutagenesis

Melting temperatures were predicted using the Oligo Calculator tool 3.1.9 (https://www.bioinformatics.org/JaMBW/3/1/9/index.html).

4.1.4 Functionalized Oligonucleotides

Name	Sequence 5'-3' / N-C	Functionalization
DNA docking strand	TAACTGGACTTCATC	5' azide
PNA docking strand	TAACTGGACTTCATC	N-term N3-acetic acid
DNA imager strand A594	GATGAAGTCCAGTTA	3' AF594
DNA imager strand A647	GATGAAGTCCAGTTA	3' AF647
DNA non-complementary	GTTCATGTGCTGATT	3' AF647

DNA docking strand (azide-DNA) was ordered from metabion (Martinsried, Germany), PNA docking strand (azide-PNA) was ordered from Panagene (Daejeon, South Korea), oligonucleotides conjugated to fluorophores (imager strands and non-complementary) were ordered from Eurofins Genomics (Ebersberg, Germany).

4.2 Methods

4.2.1 Molecular Biology Methods

4.2.1.1 Polymerase Chain Reaction

Polymerase chain reaction has been performed using Phusion polymerase (Thermo Fisher Scientific) according to the manufacturer's instructions in 25 µl total volume using 1 ng of template. GC reaction buffer was used if the product had a GC-content of more than 65% or if initial amplifications using HF buffer were unsuccessful. PCRs were performed on a Mastercycler pro (Eppendorf) according to the following program:

Table 1: Thermocycler program for standard polymerase chain reaction using Phusion polymerase.

Step	Temperature [°C]	Duration [s]	
Initial Denaturation	98	10	
Denaturation	98	10	cycle 35x
Annealing	1 °C below predicted primer T_m	10	
Elongation	72	30 s / 1 kb	
Final Extension	72	300	
Hold	4	-	

5 µl of each PCR product were run on an agarose gel to confirm correct size of the PCR product. Samples were processed using NucleoSpin Gel and PCR Clean-up kit (Machery-Nagel) prior to digestion, Gibson assembly or by Eurofins Genomics or stored short-term at 4 °C or frozen until further usage.

4.2.1.2 Colony PCR

Colony PCR was performed in a total volume of 20 µl using MyTaq Red DNA polymerase (Bioline) according to the manufacturer's instructions. Bacterial colonies were picked from a plate and

shortly dipped into 15,6 µl ddH_2O before inoculating a 2 ml culture for miniprep. Per sample, 4,44 µl master mix containing 4 µl of 5x Red reaction buffer and each 0,2 µl of 10 µM forward and reverse primer were added. PCRs were performed on a Mastercycler pro (Eppendorf) according to the following program:

Table 2: Thermocycler program for colony polymerase chain reaction using MyTaq polymerase.

Step	Temperature [°C]	Duration [s]	
Initial Denaturation	98	10	
Denaturation	95	15	cycle 35x
Annealing	1 °C below predicted primer T_m	30	
Elongation	72	30 s / 1 kb	
Final Extension	72	300	
Hold	4	-	

10 µl of each PCR product were run on an agarose gel to confirm correct size of the PCR product.

4.2.1.3 Digestion

Digestions have been performed using the FastDigest restriction enzyme system (Thermo Fisher Scientific) according to the manufacturer's instructions for 1 h at 37 °C. For cloning of DNA fragments into the vectors pMIG and pMIY (antigens for transduction of Ba/F3 cells), vectors and inserts were digested using EcoRI and XhoI for subsequent ligation. For cloning into pcDNA3.1 (antigen-Fc-Strep-TT fusion proteins for recombinant expression and chimeric antibodies), vector was digested using EcoRV for subsequent cloning via Gibson assembly. Digested DNA was run on agarose gels, isolated and purified using the NucleoSpin Gel and PCR Clean-up kit (Machery-Nagel) and concentration determined on a NP80 spectrophotometer (Implen). Samples were stored frozen until further usage.

4.2.1.4 Ligation

Ligation was performed using T4 ligase (Thermo Fisher Scientific) according to the following table:

Table 3: Pipetting scheme for ligation.

Compound	Amount
Linearized vector DNA	100 ng
Insert DNA	3:1 molar ratio over linearized vector DNA
10x T4 Ligase buffer	2 µl
T4 DNA Ligase	1 U
ddH_2O	to 20 µl

Ligation mix was incubated for 1 h at 37 °C. Transformation into JM109 bacteria (generated in-house) was performed by incubating 5 µl of the ligation mix with 50 µl bacterial suspension on ice for 20 min, followed by heat shock at 42 °C for 30 s, addition of 1 ml LB medium and incubation at 37 °C, 600 rpm for 1 h before plating on LB agar plates containing suitable antibiotic.

4.2.1.5 Gibson Assembly

For Gibson assembly, the NEBuilder kit was used (New England Biolabs) according to the manufacturer's instructions but all volumes and the amount of DNA scaled down to one fifth. The Gibson assembly mixture has been incubated at 50 °C for 1 h in a Mastercycler 2000 thermocycler

(Eppendorf). Transformation into NEB5a bacteria was performed by incubating 0,4 µl of the Gibson assembly mix with 5 µl bacterial suspension on ice for 20 min, followed by heat shock at 42 °C for 30 s, addition of 500 µl LB medium and incubation at 37 °C, 600 rpm for 1 h before plating on LB agar plates containing suitable antibiotic.

4.2.1.6 DNA and RNA Isolation

Small scale DNA isolation ("miniprep") was performed using home-made solutions from small scale bacterial cultures up typically up to 3 ml. Bacteria were harvested by centrifugation at 5000 g for 1 min, resuspended in 100 µl miniprep solution I (50 mM Glucose, 20 mM Tris, 10 MM EDTA, 100 µG/ml RNase A, pH 8,0) and lysed in 200 µl miniprep solution II (0,2 M NaOH, 1% SDS) for 5 min at room temperature. Samples were neutralized with miniprep neutralization solution (5 M Kac, pH 4,8), centrifuged at 10.000 g for 10 min and supernatant transferred to a clean tube. Plasmids were precipitated with 1 ml ice-cold pure EtOH and centrifuged at 10.000 g for 10 min. Supernatant was discarded and the DNA pellet dried and reconstituted in ddH_2O. Concentration and purity was measured on the NP80 spectrophotometer (Implen) and samples were sent to Eurofins Genomics for sequencing to verify correct integration of the construct.

Large scale DNA isolation ("midiprep") was performed using the NucleoBond Xtra Midi kit (Machery Nagel) according to the manufacturer's instructions from bacterial cultures up typically up to 250 ml. Concentration and purity was measured on the NP80 spectrophotometer (Implen) and samples were sent to Eurofins Genomics for sequencing to verify correct integration of the construct.

RNA isolation was performed using the NucleoSpin RNA kit (Machery Nagel) according to the manufacturer's instructions from approximately one million antibody-expressing hybridoma cells. 10 µl of isolated RNA were used for quality assessment on a 12 % agarose gel and concentration and purity was measured on the NP80 spectrophotometer (Implen).

4.2.1.7 Isolation of Antibody Sequences from Hybridoma by Chain-specific Reverse Transcription and PCR

Isolation was based on a published protocol with slight adaptations[251]. For reverse transcription, RNA samples were diluted to 50 ng/µl and the following reaction was assembled using the SMARTScribe Reverse Transcriptase kit (Takara Bioscience):

Table 4: Pipetting scheme for reverse transcription

Compound	Amount
RNA	2 µl (100 ng)
5x SMARTScribe buffer	2 µl
Chain specific RT primer (10 µM)	1 µl
dNTPs (10 mM)	1 µl
DTT (20 mM)	1 µl
Template-switch oligo (100 µM)	0,3 µl
SMARTScribe Reverse Transcriptase	0,5 µl
ddH2O	to 10 µl

Separate reactions were prepared for light and heavy chain. For heavy chains, the SMART mIGHG RT primer was used that covers all murine IgG1 and IgG2 antibody subclasses. For light chains, the SMART mIGK RT was used that covers all murine kappa subclasses. The reaction was incubated at

42 °C for 70 min followed by inactivation at 70 °C for 5 min. 1,5 µl of cDNA product were used as template to assemble a PCR reaction mix using Phusion polymerase according to the manufacturer's instructions. The SMART universal PCR primer was used as forward primer, the SMART mIGHG PCR as reverse for heavy chain and the SMART mIGK PCR as reverse for light chain, respectively. Afterwards, the following PCR program was run:

Table 5: Thermocycler program for touch-down polymerase chain reaction using Phusion polymerase.

Step	Temperature [°C]	Duration [s]	
Initial Denaturation	98	10	
Denaturation	98	15	cycle 10x
Annealing	start at 63, step down 0,5/cycle	30	
Elongation	72	45	
Denaturation	98	10	cycle 15x
Annealing	56	30	
Elongation	72	45	
Final Extension	72	420	
Hold	4	-	

5 µl of each PCR product were run on an agarose gel to confirm correct size of the PCR product. Samples were processed using NucleoSpin Gel and PCR Clean-up kit (Machery-Nagel) prior to sequencing by Eurofins Genomics.

4.2.1.8 SDS Polyacrylamide Gel Electrophoresis (SDS-PAGE)

5 µg of protein or protein conjugate were mixed with Lämmli buffer and heated to 95 °C for 5 min. Samples were run using a 6 % stacking gel and 15 % separating gel at 120 V for 2 h. Gel was stained in 0,25 % Coomassie solution and destained in destaining buffer (50 % ethanol, 10 % acetic acid, 40 % ddH_2O). Gels were imaged on an Amersham Imager 600 (Amersham) gel imager.

4.2.1.9 Enzyme-Linked Immunosorbent Assay

Nunc Maxisorp 96-well plates (Thermo Fisher Scientific) have been coated with 50 µl antigen diluted in PBS to a concentration of 1 µg/ml at 4 °C overnight. Wells have been blocked with 250 µl blocking buffer (0,5% BSA in PBS) at room temperature for 1 h and washed 2x with 250 µl PBS-T buffer consisting of 0,05% Tween-20 (Carl-Roth) in PBS. A dilution series of the antibody in blocking buffer was prepared ranging from 10 µg/ml to 0,04 ng/µl with 1:4 dilution steps. 100 µg of the respective dilution were added to the well and incubated at room temperature for 2 h, followed by 5x washing with 200 µl PBS-T. HRP-coupled goat anti-mouse secondary antibody (Jackson ImmunoResearch) was diluted in blocking buffer, 100 µl of diluted secondary antibody added to each well and incubated at room temperature for 1 h, followed by 5x washing with 200 µl PBS-T. 1-Step Ultra TMB ELISA (Thermo Fisher Scientific) was diluted 1:5 in ddH_2O and 100 µl of the solution added to each well, followed by incubation at room temperature for 5-10 min. Plates were measured on a Tecan Infinite 1000 multi-well plate reader system at an absorbance of 450 nm.

4.2.1.10 Bacterial Protein Expression

GBP-TT was expressed in a pHEN6c vector backbone with an N-terminal pelB sequence followed by a 6x His-tag in JM109 cells. Bacteria were cultured in 1 l LB/Ampicillin medium at 37 °C, 180 rpm until reaching an OD_{600} of 0,6-0,8. Protein expression was induced using 1 mM IPTG and bacteria incubated overnight. Bacteria were harvested by centrifugation at 5000 g for 10 min. The pellet was resuspended in 25 ml NiNTA binding buffer supplemented with 25 µg/ml DNase I (Applichem) and

100 µg/ml lysozyme (Sigma-Aldrich) (final concentrations) and incubated for 2 h at 4 °C under constant rolling. Bacteria were further sonicated using a Brandson 450D Sonifier with 7 pulses of 8 s each at 40% amplitude. Lysed cells were pelleted at 20.000 g for 30 min. The supernatant was sterile filtered using a 0,2 µm sterile filter and further used for purification by His-tag-based metal affinity chromatography.

4.2.2 Protein Purification and Chemistry

4.2.2.1 His-tag-based Metal Affinity Chromatography

Purification of His-tagged proteins was carried out on an Äkta Pure System (Cytiva) with connected system pump and fraction collector. A HisTrap HP 5 ml column (Cytiva) was equilibrated in 5 CV of ddH_2O and 5 CV of NiNTA binding buffer. The cleared and filtered lysate was loaded onto the column at a flowrate of 3 ml/min followed by an addition of 20-30 ml of NiNTA binding buffer to the lysate reservoir to ensure complete loading of the sample and flushing of the tubing. The column was then washed with 10 CV of NiNTA binding buffer at 5 ml/min, followed by a gradient elution from 0-100% NiNTA elution buffer over 20 CV at 5 ml/min. Fractions were collected as fixed volumes of 1 ml. Respective fractions were collected, pooled and concentrated using an Amicon Ultra-4 Centrifugal filter (10.000 MWCO, Merck Milipore) until a final sample volume of 2-2,5 ml was reached. The buffer was subsequently exchanged to PBS using PD-10 desalting columns (Cytiva) according to the manufacturer's instructions. Concentration was measured using an NP80 spectrophotometer (Implen). Samples were stored at -80 °C for long-term storage or 4 °C as a working stock.

4.2.2.2 Protein A-based Affinity Chromatography

Purification of antibodies and Fc-tagged proteins was carried out on an Äkta Pure System (Cytiva) with connected system pump and fraction collector. A MabSelect SuRe (Cytiva) column was equilibrated in 5 CV of ddH_2O and 5 CV Mab binding buffer. The filtered supernatant was loaded onto the column at a flowrate of 0.5 ml/min. The column was subsequently washed at 1 ml/min with 10 CV of binding buffer. Elution was performed as a one-step elution at 1 ml/min with 10 CV elution buffer and directly eluted into a prepared vessel containing neutralization buffer for neutralization to a final pH of 7- 7.5. Respective fractions were collected, pooled and concentrated using Amicon Ultra 0.5 mL Centrifugal Filters (10.000 MWCO, Merck Milipore) until a final sample volume of less than 130 µl was reached. For humanized antibodies based on aFlt3 20D9, the buffer was exchanged by 0.5 ml Zeba Spin desalting columns (Thermo Fisher Scientific, 7 MWCO) to sterile filtered antibody storage buffer. For antibodies purified from murine hybridoma supernatant or buffer was exchanged to PBS in the last step. Concentration was measured using an NP80 spectrophotometer (Implen). All protein samples were frozen at -80 °C for long-term storage or stored at 4 °C as a working stock.

4.2.2.3 Size Exclusion Chromatography

Size-exclusion chromatography was carried out on an Äkta Pure System (Cytiva) with connected system pump and fraction collector. A Superdex 200 Increase column (Cytiva) was equilibrated in 5 CV of ddH_2O and 1 CV of PBS. Protein sample was centrifuged at 10.000 g for 10 min before injection into the sample loop. Per run, a maximum of 250 µl were injected onto the column from a 500 µl injection loop by flushing the loop with 1,5 ml of PBS at a flow rate of 0,5 ml/min. Elution was performed at a constant flow rate of 0,5 ml/min for 1,3 CV. Respective fractions were collected, pooled and concentrated using Amicon Ultra-4 Centrifugal Filters (10.000 MWCO, Merck Milipore) until a desired concentration was reached. Concentration was measured using an NP80 spectrophotometer (Implen). Samples were stored at -80 °C for long-term storage or 4 °C as a working stock.

4.2.2.4 Anion Exchange Chromatography

Preparative anion exchange chromatography was performed on an Äkta pure (Cytiva) with connected system pump and fraction collector. A ResourceQ column (Amersham Pharmacia Biotech) was equilibrated in 5 CV of ddH_2O and 5 CV of AEX binding buffer. Per run, a maximum of 250 µl of crude conjugation product were injected onto the column from a 500 µl injection loop by flushing the loop with 3 ml of AEX binding buffer at a flow rate of 1 ml/min. Elution was performed by linearly increasing the concentration of AEX elution buffer from 0% to 50% over 20 CV followed by 100% buffer B for 5 CV. Respective fractions were collected, pooled and concentrated using Amicon Ultra 0.5 mL Centrifugal Filters (10.000 MWCO, Merck Milipore) until a final sample volume of less than 130 µl was reached.

and protein absorption measured at 280 nm. Peak fractions were collected, concentrated using Amicon Ultra Centrifugal Filters (0.5 ml, 3 NMWL, Merck Millipore) and buffer exchanged to 1x PBS using Zeba Spin desalting columns (7 MWCO).

4.2.2.5 Copper-catalyzed Ligation of Nanobodies and Oligonucleotides

O-propargyl-L-tyrosine incubated with GBP-TT and TTL in a reaction using 298 µM GBP-TT, 29,8 µM TLL (10x molar excess of GBP-TT over TTL) and 10 mM O-propargyl-L-tyrosine in TTL reaction buffer and incubated for 3 h at 30 °C. Afterwards, 0.5 ml Zeba Spin desalting columns (Thermo Fisher Scientific, 7 MWCO) were used according to the manufacturer's instructions to remove free O-propargyl-L-tyrosine and exchange the buffer to PBS. For analytical AEX, conjugation of azide-DNA to alkynyl-GBP was performed by incubating 40 µM alkynyl-GBP with a 4x molar excess of azide-DNA. For analytical AEX, conjugation of azide-PNA to alkynyl-GBP was performed by incubating 60 µM alkynyl-GBP with a 2x molar excess of azide-PNA. For preparative AEX, 70 µM alkynyl-GBP was incubated with a 2x molar excess of azide-DNA. Reactions were performed for 1 h at 25 °C in CuAAC reaction buffer which contained the following components in final concentrations: 0,25 mM $CuSO_4$, 1,25 mM THPTA, 5 mM aminoguanidine, 20 mM sodium ascorbate and 20 mM MOPS buffer at pH 7,0. After incubation, quenching of the reaction was achieved by addition of 50 mM EDTA and samples buffer exchanged to PBS using Zeba Spin desalting columns (Thermo Fisher Scientific, 7 MWCO) according to the manufacturer's instructions. Conjugation to 6-fluorescein azide (6-FAM) was performed as a control using 10 mM 6-FAM and samples buffer exchanged as described above. Reaction products were analyzed by SDS-PAGE with densitometric analysis using the GelAnalyzer software (GelAnalyzer 19.1, www.gelanalyzer.com, by Istvan Lazar Jr., PhD and Istvan Lazar Sr., PhD, CSc) or further processed by AEX.

4.2.2.6 Antigen Binding and Imager Strand Annealing/Dissociation Assay

Immobilization of eGFP was performed in 96-well µClear plates multiwell plates (Greiner) at room temperature for 1 h at a concentration of 5 µM, followed by a blocking step with blocking solution (PBS + 1% BSA) for at room temperature for 1 h after which all wells were washed twice in PBS-T containing PBS + 0,05% Tween-20 (Carl Roth). GBP-DNA and GBP-PNA conjugate were added at a concentration of 7,5 µM and incubated at room temperature for 1 h. Wells were washed thrice in PBS-T and fluorophore labeled imager strands (complementary probe labeled with Atto594, non-complementary probe labeled with Atto647, both probes were synthesized by Eurofins Genomics) annealed at room temperature for 30 min at a concentration of 10 µM and washed another three times with PBS-T before read-out.

For *in vitro* binding assays on cells, adherent HEK293F cells transfected with eGFP-actin or untransfected wild type control cells were seeded into 96-well µClear plates multiwell plates (Greiner). Cells were fixed with PBS + 4% PFA at room temperature for 10 min, washed twice with PBS-T and permeabilized with PBS + 0,25% Triton X-100 (Sigma-Aldrich) at room temperature for

10 min. Wells were washed twice in PBS-T, 7,5 µM GBP-oligonucleotide conjugate added and incubated at room temperature for 1 h before washing thrice with PBS-T. Fluorophore labeled imager strands (complementary probe labeled with Atto594, non-complementary probe labeled with Atto647, both probes were synthesized by Eurofins Genomics) were annealed at room temperature for 30 min at a concentration of 10 µM. Dissociation was induced by incubating the samples in PBS + 50% formamide at room temperature for 2 h. Wells were washes thrice in PBS-T and imager strands re-annealed as described above with incubation time increased to 1 h. All samples were washed another three times with PBS-T before read-out.

Measurements were performed on a Tecan Infinite 1000 multiwell plate reader system with excitation wavelengths at 488 nm (eGFP), 603 nm (Atto594) and 646 nm (Atto647). Emission was recorded at 509 nm, 626 nm and 664 nm, respectively. All measurements were performed in duplicates and the mean fluorescence intensity calculated.

4.2.2.7 Accelerated Aging Assay to Determine Antibody Stability

Antibodies were diluted to 1 mg/ml and 0.1 % sodium azide was added to prevent bacterial growth. Samples were aliquoted into three tubes each for incubation at 4 °C, 25 °C and 37 °C, respectively. After one, two and four weeks of incubation, samples were taken for each condition and centrifuged at 10.000 g for 10 min prior to analysis by HPLC-SEC.

4.2.3 Cell Culture and Cell-based Assays

4.2.3.1 Standard Cell Culture Procedures

HEK293F cells were cultured in HEK TF medium (Xcell) supplemented with 8 mM L-Glutamine (Sigma-Aldrich) in autoclaved glass shaking flasks ranging from 125 ml to 500 ml volume at 37 °C, 8% CO_2 and 120 rpm. Cell density was kept between 0,25 Mio/ml and 2 Mio/ml for standard cultivation. HEK293F were transitioned to adherent culture by transfer into DMEM medium (Sigma-Aldrich) supplemented with 10% FBS (Gibco). Cells in adherent culture were split 2-3 times a week at ratios of 1:5 to 1:10 by incubation with Trypsin/EDTA solution (Sigma-Aldrich) for 5 min at 37 °C.

Phoenix Eco cells were cultured in DMEM medium (Sigma-Aldrich) supplemented with 10% FBS (Gibco) at 37 °C and 5% CO_2. Cells were split 2-3 times a week at ratios of 1:5 to 1:10 by incubation with Trypsin/EDTA solution (Sigma-Aldrich) for 5 min at 37 °C.

ExpiCHO cells were cultured in ExpiCHO medium (Thermo Fisher Scientific) in autoclaved glass shaking flasks ranging from 125 ml to 500 ml volume at 37 °C, 8% CO_2 and 120 rpm. Cell density was kept between 0,25 Mio/ml and 2 Mio/ml for standard cultivation.

Ba/F3 cells were cultured in RPMI1640 medium (Sigma-Aldrich) supplemented with 10% FBS (Gibco) and 10 ng/µl murine IL-3 (Peprotech) at 37 °C and 5% CO_2. Cell density was kept between 0,1 Mio/ml and 1 Mio/ml for standard cultivation.

All cells were frozen in Bambanker freezing medium (Nippon Genetics) with 10 million cells per vial in 1 ml freezing medium. Cells were thawed in 9 ml room temperature PBS and centrifuged at 300 g for 5 min. Supernatant was removed and cells resuspended in an appropriate volume of medium for seeding.

4.2.3.2 Transfection of ExpiCHO and HEK293F Cells for Protein Expression in Mammalian Cells

Humanized antibodies based on aFlt3 20D9 were expressed using the ExpiCHO expression (Thermo Fisher Scientific). CHO cells were subcultured to a maximum of 2 Mio. cells/ml in a 125 ml shaking flask and incubated at 37 °C, 8 % CO2, 180 rpm. Expression was performed using the

standard expression protocol according to the manufacturer's instructions. In brief: One day prior to transfection CHO cells were split to 3 Mio. cells/ml and incubated overnight. On the day of transfection, cells were diluted to 6 Mio. cells/ml in a volume of 25 ml. Transfection was performed with a total of 20 µg DNA (10 µg of each heavy and light chain plasmid) diluted in 1 ml OptiPRO SFM (Thermo Fisher Scientific). In parallel, 80 µl of ExpiCHO transfection reagent were diluted in 920 µl OptiPRO SFM. Diluted DNA and transfection reagent were mixed and incubated for 3 min before addition to the CHO cells. One day after transfection, 6 ml of feed medium and 150 µl of enhancer reagent were added. Expression was typically performed for 7-10 d before harvesting the supernatant and sterile filtering it using a 0,22 µm sterile filter prior to purification. If larger quantities of antibody were needed, all volumes were scaled by a factor of 2-3 and cells were cultured in an appropriately larger flask.

Fc-fusion proteins of CD2, CD5, CD7 and CD28 were expressed in HEK293F cells. HEK293F cells were subcultured to a maximum of 2 Mio. cells/ml in a 125 ml shaking flask and incubated at 37 °C, 8 % CO2, 180 rpm. Transfections were carried out in volumes ranging from 50 ml to 500 ml at a cell density of 1 Mio. cells/ml depending on the expression yield of the respective protein. Per 1 ml of cell culture, 1,5 µg of plasmid DNA and 3 µg of linear polyethylenimine (PEI) (MW 25.000, Polysciences) were used. PEI and DNA were separately diluted in OptiPRO SFM (Thermo Fisher Scientific) with each dilution equaling to a maximum of 5% of the pre-transfection cell culture volume. Diluted PEI and diluted DNA were mixed and incubated at room temperature for 30 min before addition to the cells. Expression was typically performed for 4-7 d before harvesting the supernatant and sterile filtering it using a 0,22 µm sterile filter prior to purification.

4.2.3.3 Transfection of Phoenix ECO Cells for Ecotropic Virus Production and Transduction of Ba/F3 Cells

Phoenix Eco cells were seeded into 6-well cell culture plates and transfected at approximately 40% confluency using 7,5 µg of pMIG or pMIY plasmid with the respective antigen insert using Freestyle MAX reagent (Thermo Fisher Scientific) according to the manufacturer's instructions. After 24 h, the medium was aspirated and exchanged for fresh complete DMEM. Viral supernatant was harvested after another 48 h. 1 Mio. Ba/F3 cells were seeded in 1,5 ml complete Ba/F3 medium, mixed with 1,5 ml viral supernatant and centrifuged at 30 °C for 90 min at 300 g. Ba/F3 cells were sorted 2 d post transduction, and resorted another 7 d after the first sort.

4.2.3.4 Fluorescence-Activated Cell Sorting (FACS)

Transduced Ba/F3 have been harvested and washed 3x in sterile filtered FACS buffer (PBS + 0,1% BSA). Cells were resuspended in 2 ml sterile FACS buffer and strained through a 35 µm nylon mesh prior to sorting. Sorting has been performed on a FACS Aria cell sorter (BD Biosciences) with a four laser setup of 405 nm, 488 nm, 561 nm and 640 nm using the following filter sets: V450/50, V525/50, V610/20, V660/20, V710/50, V780/60, B530/30, B710/50, YG582/15, YG610/20, YG670/14, YG710/50, YG780/60, R670/30, R730/45, R780/60. Sorting has been performed on GFP and YFP signal using the 488 nm laser for excitation and the B530/30 filter for emission.

4.2.3.5 Antibody-based Cell Staining and Flow Cytometry

Screening of hybridoma supernatants was performed 10-12 d after fusion. Transduced Ba/F3 were harvested and washed 2x in sterile filtered FACS buffer (PBS + 0,1% BSA) containing 0,1% sodium azide. 15.000 wild type Ba/F3 cells were mixed with 15.000 antigen-transduced Ba/F3 cells in a total volume of 40 µl and deposited in a V-bottom 96-well plate (Falcon). 40 µl of hybridoma supernatant was added incubated on ice for 20 min. 120 µl of FACS buffer were added to the plate and cells centrifuged at 300 g, 5 min. Cells were washed a further 2x with 200 µl FACS buffer. Cells were resuspended in 40 µl secondary staining solution consisting of goat anti-mouse secondary

antibody conjugated to AF647 (Jackson ImmunoResearch) and 1 µg/ml DAPI for 20 min on ice. 160 µl of FACs buffer were added to the plate and cells centrifuged at 300 g, 5 min. Cells were washed a further 2x with 200 µl FACS buffer. Finally, cells were resuspended in 130 µl FACS buffer and strained through a 35 µm nylon mesh prior to analysis. As positive control, commercial antibody conjugated to APC was used to confirm antigen expression and mixing ratio of the Ba/F3 cells. As a negative control, the Ba/F3 mix was incubated with secondary staining solution without prior incubation with any primary antibody.

When using purified murine or chimeric antibodies, primary staining was performed in 40 µl FACS buffer at a concentration of 1 mg/ml. The rest of the staining protocol performed as described above.

Analysis has been performed on a FACS Fortessa cytometer (BD Biosciences) with a four laser setup of 405 nm, 488 nm, 561 nm and 640 nm using the following filter sets: V450/50, V525/50, V610/20, V660/20, V710/50, V780/60, B530/30, B710/50, YG582/15, YG610/20, YG670/14, YG710/50, YG780/60, R670/30, R730/45, R780/60. When using the HTS plate reading module, 70 µl of sample were read in at a speed of 3 µl/s with 2 washes of 200 µl autoclaved ddH_2O between samples.

4.2.3.6 Internalization Assay using AF647-Conjugated Antibody and Confocal Microscopy

CD5-presenting Ba/F3 cells were seeded into an 8-well slide with glass bottom (Ibidi) for live cell microscopy at a density of 400.000 cells per well and stained for 20 min on ice with 10 µg of purified antibody. Cells were washed 2x with FACS buffer and stained for 20 min on ice with goat anti-mouse secondary antibody conjugated to AF647 (Jackson ImmunoResearch). Cells were then washed 2x with FACS buffer and incubated for 0 h and 2 h, respectively, before imaging. Spinning disk confocal microscopy was performed on a Nikon TiE microscope equipped with a Yokogawa CSU-W1 spinning disk confocal unit (50 µm pinhole size), an Andor Borealis illumination unit, Andor ALC600 laser beam combiner (405 nm / 488 nm / 561 nm / 640 nm), and Andor IXON 888 Ultra EMCCD camera. The microscope was controlled by software from Nikon (NIS Elements, ver. 5.02.00). Images were acquired with a pixel size of 217 nm using a Nikon CFI Apochromat TIRF 60x NA 1.49 oil immersion objective (Nikon). The emission of eGFP and the pHrodo Deep Red dye was captured by using a 525/50 nm and a 700/75 nm filter, respectively.

4.2.3.7 Internalization Assay using pHrodo-Conjugated Antibody and Confocal Microscopy

Conjugation of goat anti-human secondary antibody with pHrodo Deep Red TFP-ester (Thermo Fisher Scientific) was performed according to the manufacturer's instructions. 1 µg of humanized 20D9 #3 antibody was pre-incubated with 1 µg of conjugated secondary antibody at room temperature for 30 min. 400.000 Ba/F3 cells transduced with human Flt3 or empty vector as control (kindly supplied by AG Spiekermann, LMU) were seeded in 400 RPMI1640 medium supplemented with 10% FBS and 10 ng/µl murine IL-3 (Peprotech) and the formed complex added to the medium. At time points 0 h, 5 h and 24 h, samples were transferred to an 8-well slide with glass bottom (Ibidi) for live cell microscopy. Spinning disk confocal microscopy was performed on a Nikon TiE microscope equipped with a Yokogawa CSU-W1 spinning disk confocal unit (50 µm pinhole size), an Andor Borealis illumination unit, Andor ALC600 laser beam combiner (405 nm / 488 nm / 561 nm / 640 nm), and Andor IXON 888 Ultra EMCCD camera. The microscope was controlled by software from Nikon (NIS Elements, ver. 5.02.00). Images were acquired with a pixel size of 217 nm using a Nikon CFI Apochromat TIRF 60x NA 1.49 oil immersion objective (Nikon). The

emission of eGFP and the pHrodo Deep Red dye was captured by using a 525/50 nm and a 700/75 nm filter, respectively.

4.2.3.8 Confocal Microscopy of fixed HEK293F cells expressing Lamin-B1 after DNA Hybridization

HEK293F cells were transfected in suspension culture with pMCP-eGFP-LaminB1 plasmid at a density of 1 Mio. cells/ml using 2,5 µg DNA/ml and Freestyle MAX reagent (Thermo Fisher Scientific) according to the manufacturer's instructions. 1 d after transfection, cells were transitioned into adherent culture using DMEM/F12 medium (Sigma-Aldrich) supplemented with 10% FBS (Gibco), seeded into an 8-well slide with glass bottom (Ibidi) and incubated overnight. Cells were fixed with PBS + 4% PFA at room temperature for 10 min, washed twice with PBS-T and permeabilized with PBS + 0,25% Triton X-100 (Sigma-Aldrich) at room temperature for 10 min. Cells were washed in PBS and blocked in blocking buffer containing PBS + 5% BSA at room temperature for 1 h. AEX purified nanobody-DNA conjugate was diluted in blocking solution to a concentration of 16,6 µM, added to the sample and incubated at 4 °C over night. Samples were washed twice in PBS. Imager strand was diluted to 10 nM in imaging buffer and added to the cells and incubated at room temperature for 5 min before washing twice with imaging buffer. Samples were imaged on a confocal microscopy setup as described below. Samples were washed twice in 0,01x PBS. Imager strand was removed by stripping twice in stripping buffer (PBS + 30% formamide) with incubation at room temperature for 3 min in each stripping step. Before restaining, samples were washed twice in PBS.

Spinning disk confocal imaging of HEK293F cells was performed on a Nikon TiE microscope equipped with a Yokogawa CSU-W1 spinning disk confocal unit (50 µm pinhole size), an Andor Borealis illumination unit, Andor ALC600 laser beam combiner (405 nm / 488 nm / 561 nm / 640 nm), and Andor IXON 888 Ultra EMCCD camera. The microscope was controlled by software from Nikon (NIS Elements, ver. 5.02.00). Images were acquired with a pixel size of 217 nm using a Nikon CFI Apochromat TIRF 60x NA 1.49 oil immersion objective (Nikon). eGFP, Alexa594 and Alexa647 were excited for 500 ms using the 488, 561 and 640 nm laser lines, respectively. The emission of eGFP, Alexa594 and Alexa647 was captured by using a 525/50 nm, a 600/50 nm and a 700/75 nm filter, respectively. On top of that, differential interference contrast (DIC) images were acquired.

Confocal microscopy of HeLa Kyoto cells was performed by Ksenia Kolobynina (AG Cardoso, TU Darmstadt). Images were acquired using a Leica TCS SP5II confocal laser scanning microscope (Leica Microsystems, Wetzlar, Germany) equipped with an oil immersion Plan-Apochromat x100/1.44 NA objective lens (pixel size in XY set to 100 nm, Z-step=290 nm) and laser lines at 488, 561 and 633 nm. For the second round of imaging cells were recorded as z-stacks with a z-spacing of 290 nm to find the exact plane corresponding to the first round of imaging.

5 Results

5.1 Generation of Antibodies against ALL-associated Targets

The generation of novel binders is most commonly done either via display technologies or hybridoma technology. In our studies, we opted to isolate antibodies from hybridoma cells. Although this means that the initially isolated binder is inherently non-human, this approach yields the advantage that the resulting binders are already in an IgG format and can be characterized as such from the very beginning. In brief, the generation of antibodies via hybridoma technology involves the immunization of mice with antigen, followed by sacrificing the mouse to harvest the spleen and immortalization of the isolated murine B cells by fusion with a myeloma cell line, yielding an immortal cell that possesses the ability to secrete antibodies into the culture medium. The presence of antigen-binding antibody in the medium is usually assessed via ELISA. The resulting cells are genetically instable, so that loss of the genetic locus coding for the antibody can occur during extended cell culture. The generation of a stable hybridoma cell line therefore involves repeated subculturing and re-testing of potential clones to test for antibody production. The earlier an interesting clone can be identified, the earlier the subculturing process can be started to avoid overgrowth by non-producing cells. This increases the overall chance to successfully establish a stable hybridoma cell line. Our aim in this project was to generate antibodies against the overexpressed ALL targets CD2[252,253], CD5[254,255], CD7[256,257] and CD28[258]. Since all of these antigens are surface-presented, we aimed to modify the established hybridoma workflow by including flow cytometry measurements to test surface-recognition of the antigen early into the hybridoma generation.

5.1.1 Expression and Purification of ALL-Antigens

To generate antigen for immunization and analysis, we aimed to express all antigens in the established HEK293 Freestyle (HEK293F) expression system, followed by Protein A chromatography on a fast protein liquid chromatography (FPLC) system. Utilization of a human cell line for expression ensures the correct post-translational modification of the antigen.

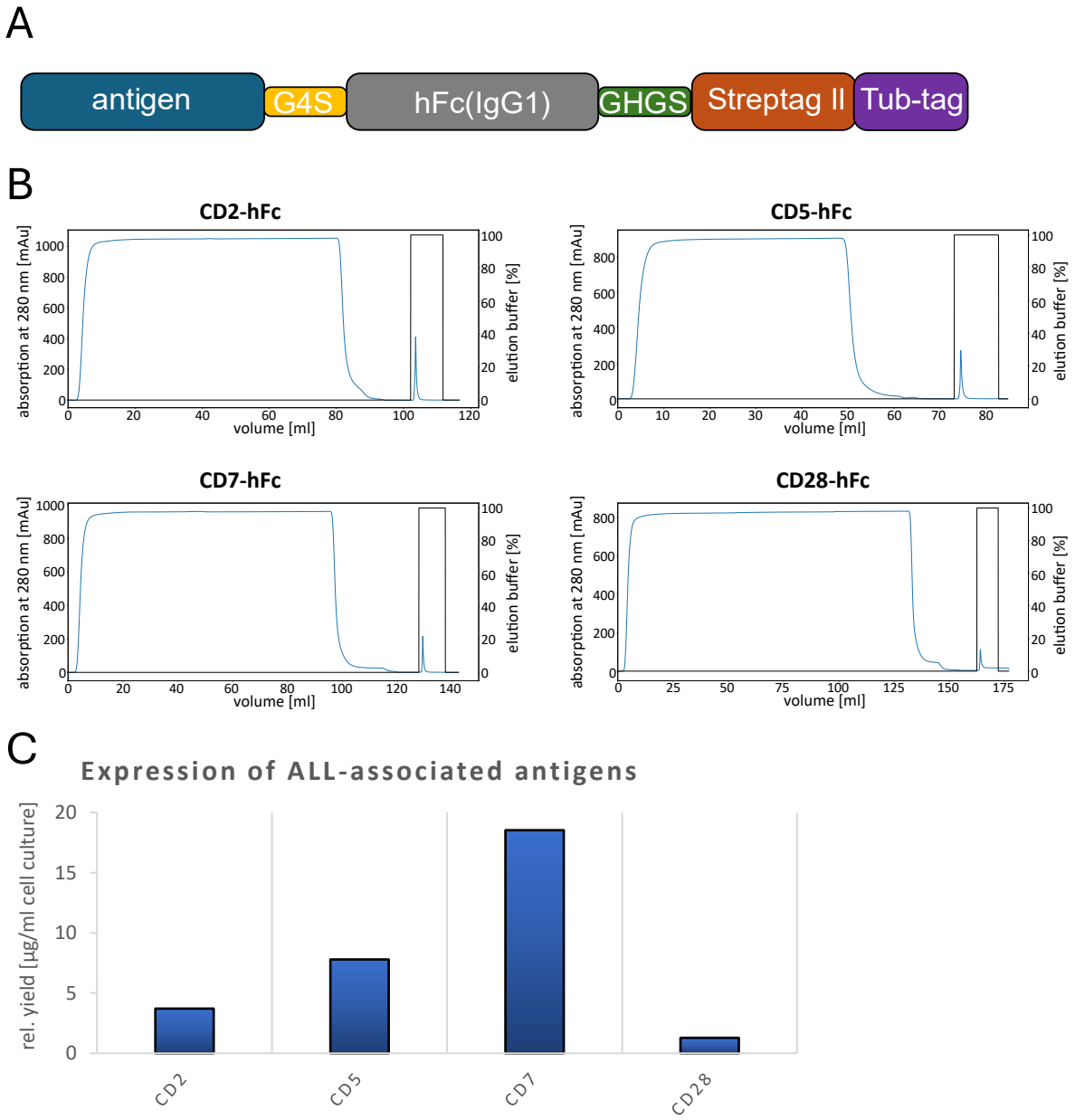

Figure 6: Expression and purification of the ALL-associated antigens CD2, CD5, CD7 and CD28 in HEK293F cells. (A) Schematic overview of the designed antigen (B) Chromatograms of protein A chromatography of all four antigens. The concentration of buffer B (elution buffer) is represented in grey. (C) Evaluation of expression yields. Cleared supernatant has been purified using Protein A FPLC after transient transfection of HEK293F cells and the relative yield calculated. Stark differences in expression yields have been observed. Whereas CD5 and CD7 yielded high amounts of protein, CD28 expressed poorly.

We decided to express as Fc-fusion proteins with a human IgG1 Fc domain. Fc fusion proteins have been shown to increase solubility of the antigen[259]. Additionally, in some cases Fc fusion proteins have been reported to yield superior immune response in mice[260], which is likely a combination of reduced renal clearance due to higher molecular weight and Fc-mediated recycling, as well as higher uptake by immune cells via FcγRs, leading to improved presentation of immunogenic antigens to the immune system. To reduce potential steric hindrance, the extracellular domain was separated via a single G4S linker from the human Fc region. In addition, we added a GHGS-linker in

conjunction with a Strep-Tag II and Tub-tag so that the antigen can be easily multimerized and modified in future studies (figure 6 A)

We managed to purify all four antigens from HEK293F cells (figure 6 B and C). However, we observed stark differences in expression yields, with CD7 showing the highest yields at about 18,5 µg/ml cell culture and CD28 showing the lowest with only 1,3 µg/ml.

5.1.2 Generation of Ba/F3 Target-expressing Cell Lines

In addition to ELISA screenings of hybridoma cells, we opted to integrate flow cytometry data into our discovery workflow, since the recognition of surface-presented antigens is much closer to the final application as an ADC than the recognition of recombinant protein on an ELISA plate. To this end, we engineered Ba/F3 cells to present the respective human antigen on the cell surface. This cell line is a murine pre-pro B cell line that is easy to handle and provides robust protein expression. Phoenix Eco cells were transfected with antigen cloned into either pMIG (CD2, CD5, CD28) or pMIY (CD7) vector to produce ecotropic MMuLV. This virus was then used to transduce Ba/F3 wild type cells to express surface-presented antigen and either GFP or YFP, respectively, as a transduction control (figure 7 A). Transduced cells were then sorted twice in 1-week intervals via Fluorescence-activated cell sorting (figure 7 B).

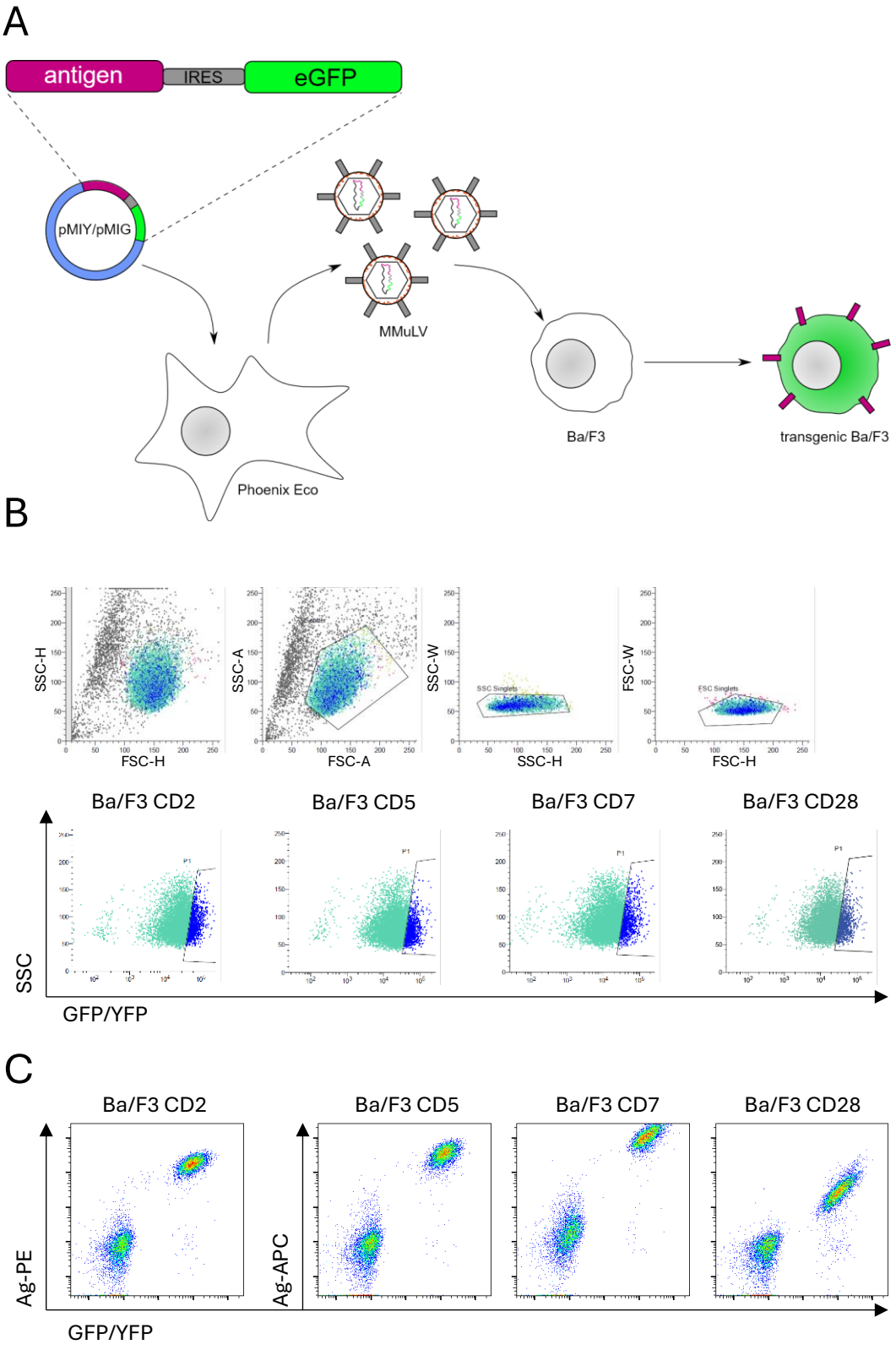

Figure 7: Generation of Ba/F3 target-expressing cell lines. (A) Design of the transcription cassette within the pMIG/pMIY vectors. All antigens are co-transcribed with either GFP or YFP separated by an IRES element. The fluorescent YFP/GFP acts as a transduction marker. (B) Schematic of the viral transduction of Ba/F3 cell line to produce transgenic, antigen-presenting cells. (C) Second sorting round of antigen-expressing engineered Ba/F3 cell lines. Representative gating strategy of Ba/F3 CD2 cells (top) and final sorting gate of all cell lines (bottom). (D) Validation of sorted cell lines using commercially available antibody directed against the respective antigen. Engineered, GFP-positive Ba/F3 cells have been mixed at a 1:1 ratio with wild type, GFP-negative Ba/F3 cells and stained with commercially available antibody. All antibodies recognized the engineered cell line, but not the untransduced wild type.

Although the IRES element does not force a 1:1 expression ratio between antigen and fluorescent protein, the fluorescence marker acts as a reliable control of antigen expression. After second sorting, we found only few cells that expressed the fluorescent marker but were not stained by commercial antibody. In all samples, the commercial antibody specifically recognized transduced cells, but not untransduced wild type (figure 7 C), suggesting that these cell lines can be used to screen novel antibodies generated by hybridoma technology.

5.1.3 Validation of Antibody Candidates

In the first experiments we applied both read-outs in parallel and only proceeded with clones that yielded signal in both ELISA and flow cytometry. However, this process proved to be inefficient. We found that overall very few clones were detected in flow cytometry but not ELISA, which does not justify the high investment of time and effort. To streamline the process, we proceeded to utilize ELISA as a pre-screening method. Clones that were positive in ELISA (experiment performed by Heinrich Flaswinkel, data not shown) were then further analyzed in flow cytometry to confirm binding to surface-presented antigen. To simultaneously validate binding specificity, we mixed antigen-presenting Ba/F3 cells with wild type Ba/F3 cells at a 1:1 ratio before staining with hybridoma supernatant.

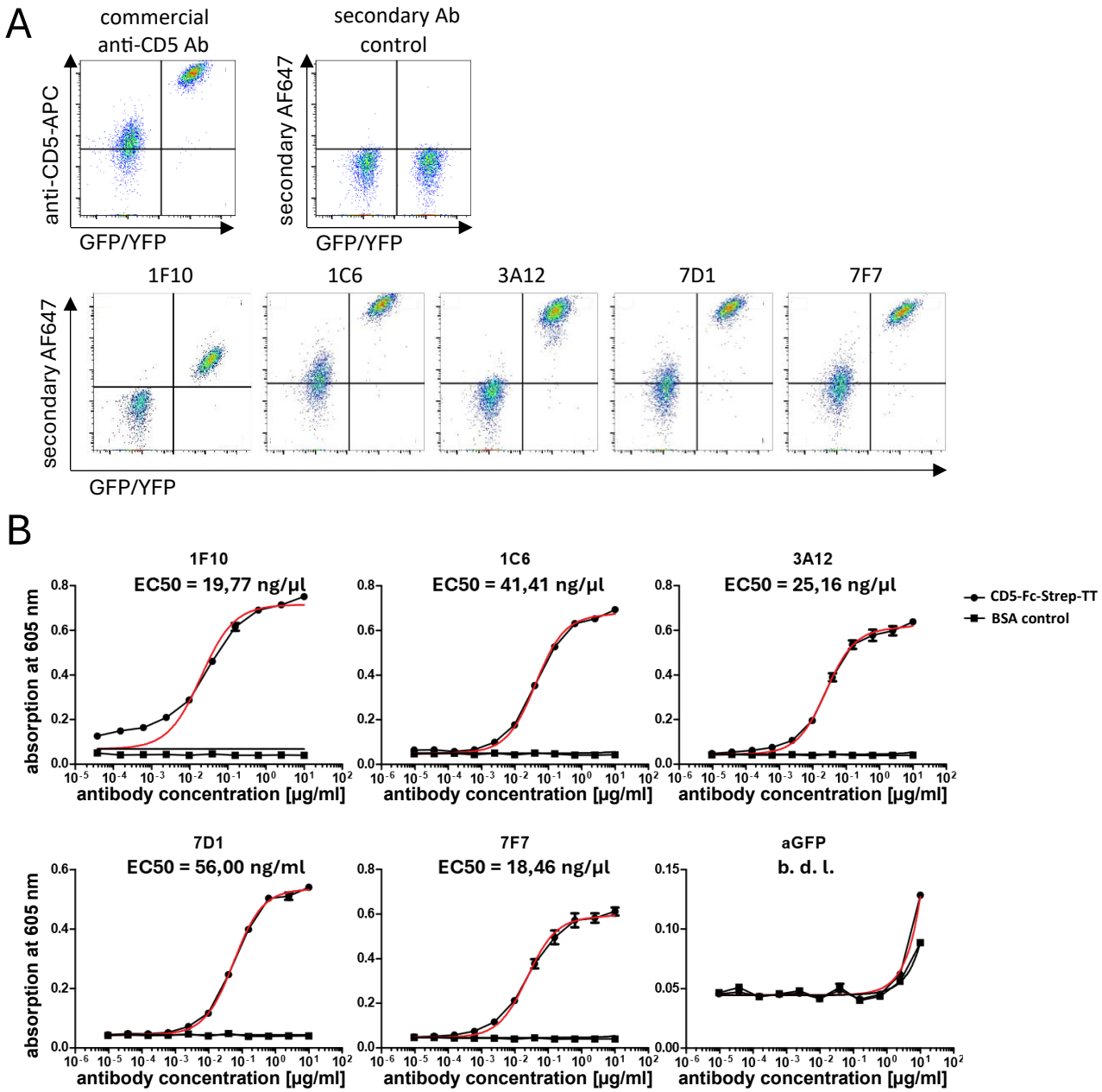

Figure 8: Identification and characterization by ELISA of hybridoma-derived murine antibodies on the example of CD5 antigen. (A) Flow cytometry data of the five isolated antibodies directed against CD5 in the first round of screening. Whereas most showed high signal towards CD5-presenting Ba/F3 cells, we observed some minor shifts in the wild type cell line in three out of five stainings. Samples have been pre-gated on single, live cells. (B) ELISA of the murine CD5 antibodies on recombinant CD5-Fc protein and anti-GFP antibody as control to determine the EC50 value. While minor differences could be detected, all antibodies showed similar binding strength towards recombinantly expressed CD5-Fc antigen. Error bars represent standard deviation. Fit represented as red sigmoid line. b.d.l. = below detection limit.

Using this workflow, we were able to identify antibodies directed against all four antigens. Figure 8 shows exemplary data and first characterization by ELISA of five isolated antibodies against CD5. In the initial screening, we observed minor unspecific binding to wild type Ba/F3 cells in almost all samples including the commercial positive control antibody (figure 8 A). Hybridoma clones that were positive in the initial ELISA and flow cytometry screening were subcultured until a stable clone was obtained (experiment performed by Heinrich Flaswinkel and Elisabeth Kremmer). Hybridoma supernatant has then been purified by Protein A chromatography to allow for determination of the EC50 value in ELISA (figure 8 B).

For all hybridoma clones, the antibody sequence has been obtained via RNA isolation, reverse transcription and PCR based on a previously published method [251] with minor modifications. The variable sequences have been genetically fused to a human IgG1 backbone to obtain a chimeric antibody. This antibody has been transiently expressed in HEK293 Freestyle cells and purified via Protein A chromatography. The chimeric antibodies have then been analyzed by cytometry to ensure that their ability to recognize the CD5 antigen has not been altered by chimerization (figure 9). In addition to wild type Ba/F3 cells, Ba/F3 cells transduced with CD2 have been used as an additional control. We observed no binding of either murine or chimeric antibody to CD2-presenting Ba/F3 cells. Minor binding to wild type Ba/F3 cells was observed only for murine antibody 7F7 but not chimeric one. Overall, the population shape of CD5-presenting Ba/F3 cells was less defined in murine antibody, which could be a result of prolonged storage of the antibody in the hybridoma supernatant during the isolation and characterization process.

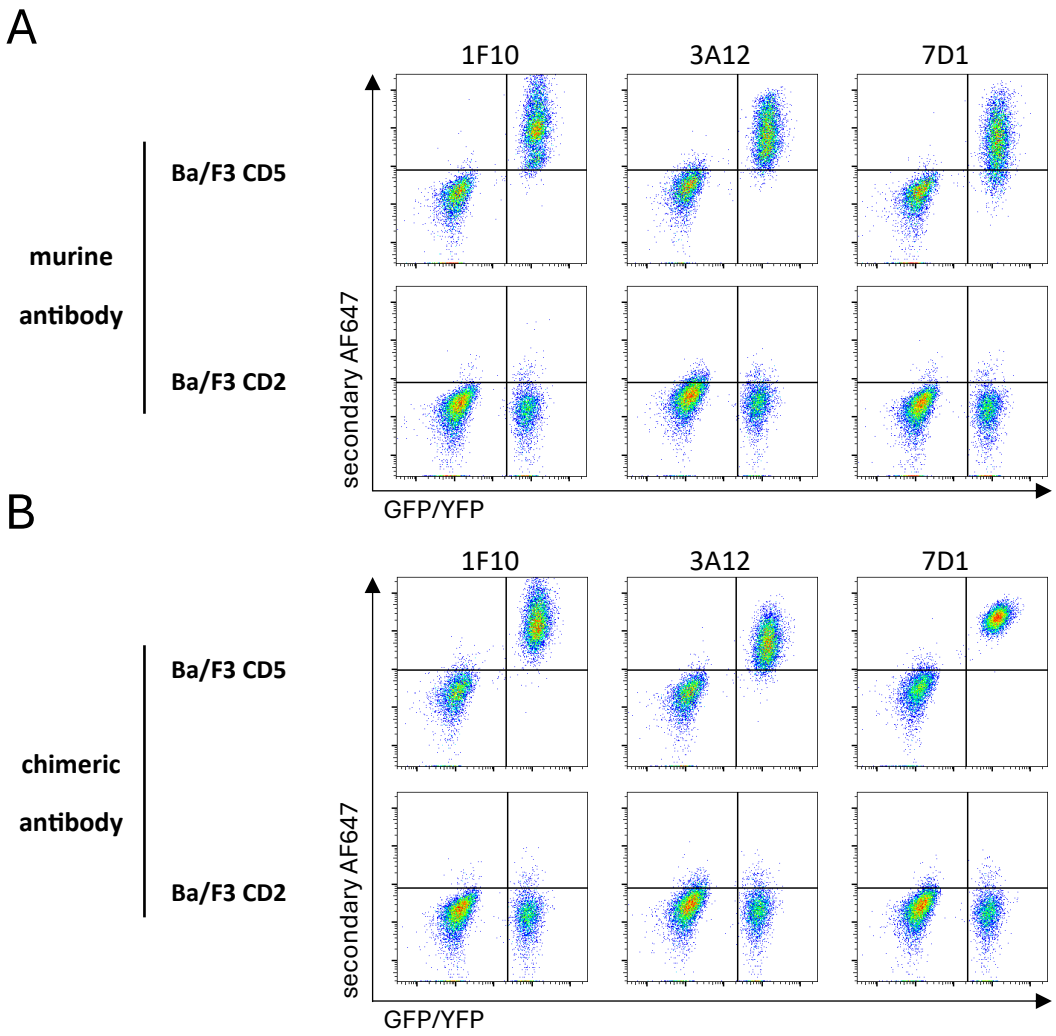

Figure 9: Comparison of murine aCD5 antibodies purified from hybridoma supernatant and recombinantly expressed chimeric antibodies. (A) Cytometric measurement of a mixture of CD5-presenting and wild type Ba/F3 cells stained with purified murine antibodies. All samples showed specific binding only towards transduced Ba/F3 cells but neither towards untransduced Ba/F3 cells nor CD2-presenting Ba/F3 cells. Samples have been pre-gated on single, live cells. (B) Cytometric measurement of a mixture of CD5-presenting and wild type Ba/F3 cells with purified chimeric antibodies. Staining of transduced Ba/F3 cells was more uniform compared to purified murine antibody. Samples have been pre-gated on single, live cells.

Since efficient internalization is a crucial step in the mechanism of action of ADCs, we used confocal microscopy to qualitatively assess the internalization of the isolated candidates. To this end, we stained CD5-presenting Ba/F3 cells with αCD5 antibody and an anti-mouse secondary antibody conjugated to AF647 and imaged either directly or after incubation for 2 h. At the 0 h time point, we observed staining only on the cell surface but were unable to detect any internalized antibody signal. After incubation for 2 h, the staining pattern on the cell surface changed from an even distribution across the cellular membrane to bright, focused spots on few areas of the cell. Additionally, we observed antibody signal in the intracellular space, usually on spots where the signal of cytosolic GFP is lower than in the surrounding area, which is in accordance with the lysosomal and endosomal transport of the antibody. The maximally observed signal was generally brighter after 2 h of incubation suggesting concentration of the antibody in the small spaces of the endosomes and lysosomes. Antibody 7D1 showed an overall weaker signal compared to 1F10 and 3A12, which could be due to worse binding kinetics as observed in ELISA. However, no such effect was observed in flow cytometry. Nevertheless, we observed internalization signal for 7D1. Using αGFP antibody as a control, we observed no binding the cell surface and hence no internalization, suggesting that the internalization is mediated by binding to CD5 and not an artifact of the formation of a complex between primary and secondary antibody.

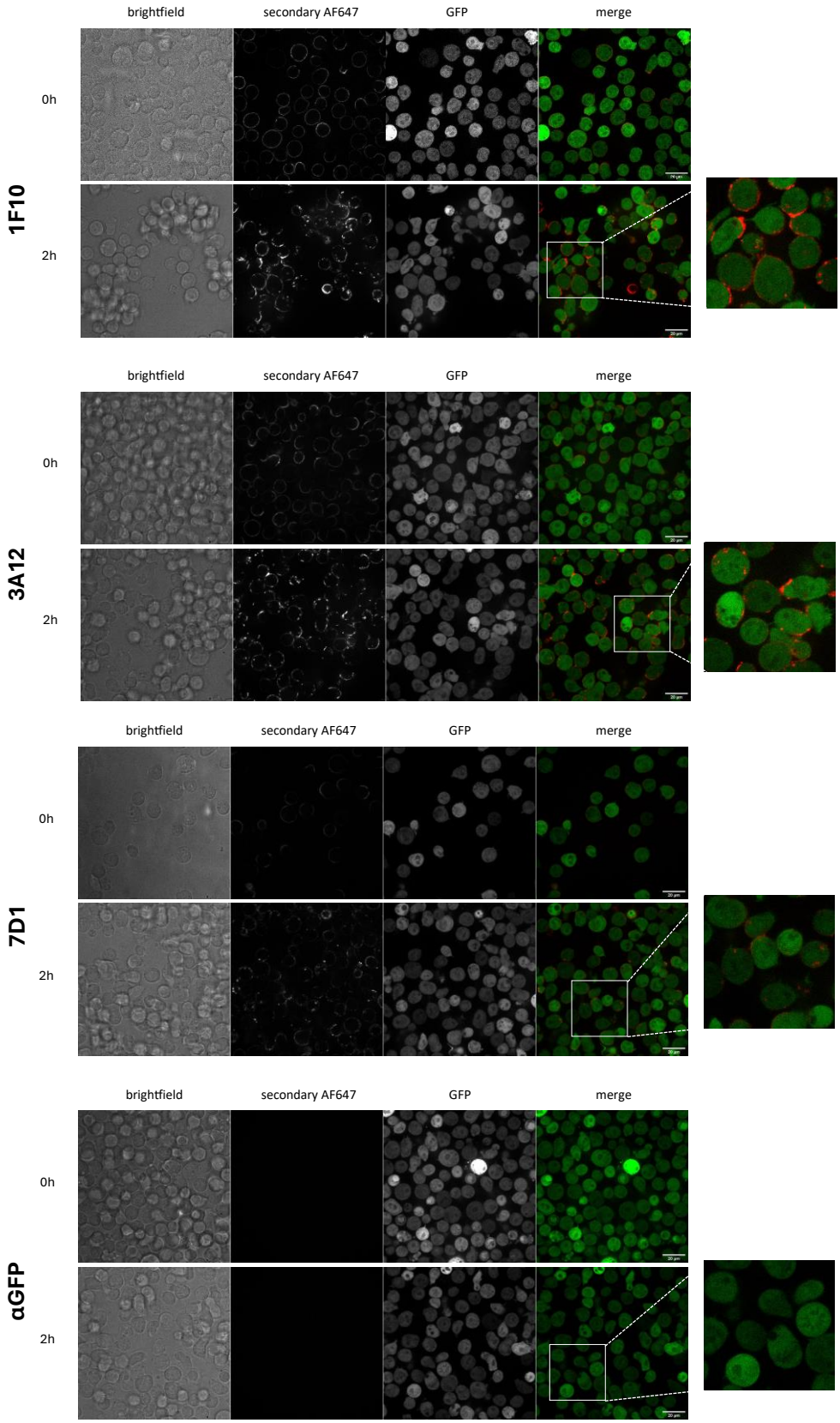

Figure 10: Internalization of αCD5 antibodies. Confocal microscopy of live CD5-presenting Ba/F3 cells. Cells were stained with the respective αCD5 antibody and an anti-mouse secondary antibody conjugated to AF647. Cells were then incubated at 37 °C, 5% CO_2 for 2 h. At the 0 h and 2 h time points, a sample was taken and imaged. At the 0 h time point, weak signal was detected only at the cell surface. In contrast, after 2 h incubation, signal was observed in spots both at the cell surface as well as in the intracellular space, suggesting internalization of the antibody complex. No internalization was observed using αGFP control antibody. Scale bar represents 20 µm. green overlay = GFP, red overlay = AF647.

In summary, we were able to implement an efficient workflow that integrates cell-surface recognition of the respective antigen in the first round of screening. Using this workflow, we were able to isolate hybridoma-derived antibodies against all four T-ALL associated antigens that recognize cell surface-presented antigen and are therefore of particular interest for the development of therapeutic ADCs.

5.2 Applications of Antibody Drug Conjugates

ADCs have seen a rise in interest over the last decade in medicine, especially for cancer therapy, but also for research applications. The generation of ADCs involves the conjugation of a drug to an antibody or antibody derivative, a step that comes after the identification and isolation of a suitable antibody. This work focused on two applications: First, the introduction of a novel conjugation strategy for AOCs with proof-of-concept use in fluorescent microscopy, and second, the pre-clinical development of a classical ADC for the targeting of cancer stem cells in AML.

5.2.1 Chemo-Enzymatic Functionalization of Nanobodies with DNA and PNA for Confocal Microscopy

Protein-oligonucleotide conjugates have seen interesting use cases in a multitude of fields, such as protein immobilization[261], bioanalytics[262-264] and material sciences[265-267]. Depending on the application, stoichiometry of protein and oligonucleotide, site of attachment and orientation are important for the generation of a functional product. As previously discussed, one particularly interesting idea is the usage of AOCs for therapeutic applications. However, due to the large size, strong charge and structural and chemical complexity, efficient conjugation and the production of a defined product is challenging.

5.2.1.1 TTL and Copper-Catalyzed Generation of Nanobody-Oligonucleotide Conjugates

We therefore aimed to employ Tub-tag® technology as a novel strategy to for the generations of AOCs. With this technology having been used for the successful conjugation of proteins to small molecules[178] protein-protein ligation[95], it provided a promising avenue for the conjugation of proteins to oligonucleotides and therefore broaden the toolset of AOC generation techniques.

The conjugation is a two-step process: First, TTL is co-incubated with the protein of interest carrying an engineered Tub-tag and an engineered variant of tyrosine containing a chemical handle for further functionalization. During the reaction, the TTL enzyme will incorporate the engineered tyrosine at the C-terminus of the Tub-tag. In a second step, the chemical handle on the engineered tyrosine can be used for functionalization of the protein of interest (Figure 11 A). Tub-tag technology therefore allows for highly site-specific conjugation of proteins with other moieties at a defined stoichiometric ratio of 1:1. As a proof of concept, we used the incorporation of O-propargyl-L-tyrosine into a Tub-tagged GFP-binding protein (GBP) as a model antibody fragment. After TTL-catalyzed incorporation of O-propargyl-L-tyrosine, free tyrosine and buffer components were removed by using desalting columns. Afterwards, Cu[I]-catalyzed alkyne-azide cycloaddition (CuAAC) for conjugation to azide-functionalized oligonucleotides (15 nucleotides) was performed. Furthermore, we aimed for the conjugation of both DNA and peptide nucleic acid (PNA) oligonucleotides to further broaden the usability of our system. As control reactions, we performed additional reactions containing no azide moiety or azide-modified 6-carboxyfluorescein (6-FAM) that allows tracking of conjugated nanobody in gel electrophoresis.

Analysis via sodium dodecyl sulfate polyacrylamide gel electrophoresis (SDS-PAGE) revealed a shift towards higher molecular mass in samples with 6-FAM, DNA and PNA (Figure 11 B). While the control reaction with 6-FAM appeared to be near-complete since no band of unfunctionalized nanobody was detectible and thus suggested efficient incorporation of O-propargyl-L-tyrosine, samples using DNA and PNA contained unfunctionalized nanobody. Interestingly, the mere incubation of alkyne-functionalized nanobody with CuAAC reaction buffer led to a minor shift despite the absence of any conjugation partner. This shift could be explained by oxidative damage of amino acid side chains by the reactive copper species, a commonly described feature in CuAAC-based bioconjugation[268]. Taken together, these data suggest that the Tub-tag technology provides an effective tool for the generation of AOCs. However, the presence of unconjugated nanobody in the final product presents a qualitative deficiency for downstream applications, since the unconjugated binders will still bind to their target and thereby block binding sites for AOCs. To improve the purity of our product, we further performed anion exchange chromatography (AEX). In the case of DNA, the phosphate groups of the deoxyribose-phosphate backbone add a strong negative charge to the conjugate, allowing for separation of conjugated.

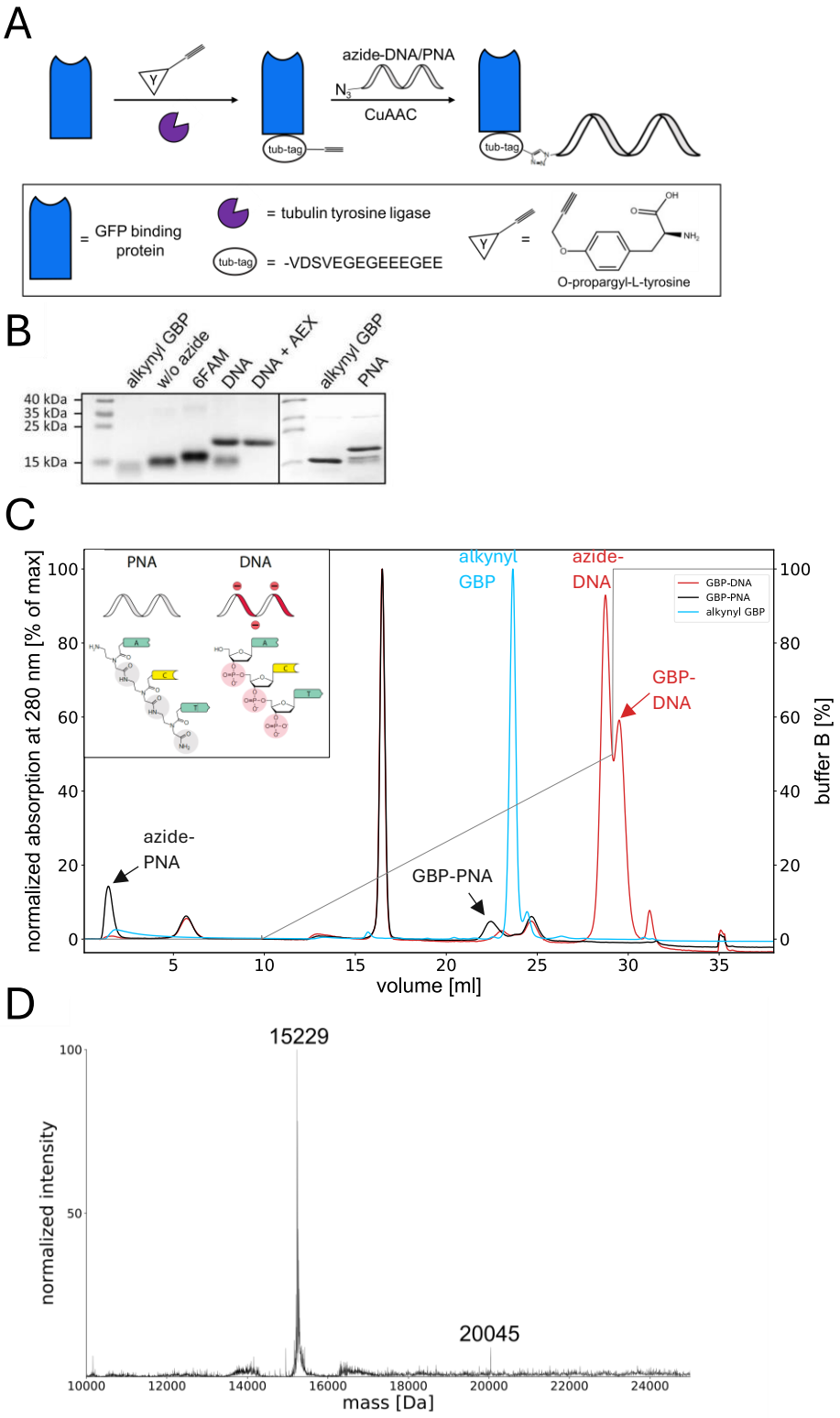

Figure 11: Generation of AOC using chemoenzymatic conjugation catalyzed by TTL and CuAAC. (A) Overview of Tub-tag mediated chemoenzymatic functionalization of nanobody in conjunction with CuAAC. **(**B) SDS-PAGE analysis of the Tub-tagged GBP after incorporation of O-propargyl-L-tyrosine and conjugation to 15 nucleotide long azide-DNA and azide-PNA oligonucleotides, respectively. (C) Preparative AEX using the conjugation products that are being shown in subfigure A. (D) Mass spectrometry measurement of nanobody-DNA conjugate (mass expected unconjugated nanobody 15030 Da, mass measured unconjugated nanobody 15229 Da; mass expected nanobody-DNA conjugate: 20047 Da, mass measured nanobody-DNA conjugate: 20045 Da). Mass spectrometry performed by Philipp Ochtrop (Leibniz-FMP, Berlin). Adapted from Schwach et al. 2021[177].

For nanobody-DNA conjugates, we observed a significant shift towards higher ionic strength. AEX enabled the separation of unconjugated alkynyl-nanobody from nanobody-DNA conjugate (Figure 11 B and C). However, separation of nanobody-DNA conjugate and free azide-DNA was not possible to baseline, leading to the presence of free azide-DNA in the final product. In line with the uncharged backbone of PNA, nanobody-PNA conjugate showed only a minor shift from unconjugated alkynyl-nanobody because no strong negative charge is introduced via the oligonucleotide (Figure 11 C). This is further seen in the instant elution of free azide-PNA, that is unable to bind to the column matrix. The earlier elution of nanobody-PNA conjugate compared to alkynyl-nanobody could be explained by steric shielding of the negative charges of the Tub-tag by the PNA molecule, leading to decreased interaction with the column matrix and thereby earlier elution. In summary, these results suggest that AEX is capable of removing free azide-PNA from the final product, but depletion of unconjugated alkynyl-nanobody is incomplete. This situation is reversed for nanobody-DNA conjugates, which can readily be separated from alkynyl-nanobody by AEX but retain contaminant azide-DNA. Mass spectrometry of nanobody-DNA conjugate that has not been purified via AEX qualitatively confirmed the conjugation of DNA to the nanobody (Figure 11 D). The intensities of detected peaks are not directly comparable to the intensity bands of the SDS-PAGE, because the oligonucleotide alters the ionization and flight characteristics of the molecule. Therefore, the intensity ratios in this measurement do not correspond to the conjugation efficiency.

5.2.1.2 Specific Binding of Nanobody-Oligonucleotide Conjugates to their Epitope and Complementary DNA strand

While the generation of nanobody-oligonucleotide conjugates via Tub-tag technology was successful, we next tested whether the conjugates were functionally active and could both still recognize GFP via the nanobody as well as specifically hybridize to a complementary fluorescently labeled DNA strand via the oligonucleotide moiety. This is especially important since the CuAAC step can oxidize amino acid side chains on the protein surface and thereby potentially alter or completely abrogate binding to the eGFP target. Similarly, oxidative damage to the oligonucleotide might impair the ability for hybridization with a complementary strand.

We were able to detect binding of the complementary probe (fluorescently labeled with Alexa Fluor 594) to eGFP, but not to the BSA control for both DNA- and PNA-nanobody conjugates, confirming functionality of the nanobody and oligonucleotide. Addition of a non-complementary probe (fluorescently labeled with Alexa Fluor 647) led to only minor signal increase, confirming that the hybridization is specific (Figure 12, top). A similar experimental setup using fixed and permeabilized untransfected HEK293F cells and HEK293F cells transfected with eGFP-actin, respectively, yielded similar results, with specific binding of the complementary probe (Figure 12, bottom). In this cell-based assay, we detected a generally increased background signal. This could be explained by unspecific binding to cellular structures and DNA-binding proteins that can unspecifically retain the probe via the sequence or the fluorophore. Interestingly, the PNA-nanobody conjugate yielded stronger signal in all samples when hybridized with the complementary probe. This is accordance with published data that shows increased melting temperatures of PNA-DNA duplexes[269], leading to stronger binding and less loss of fluorescence during the final washing steps.

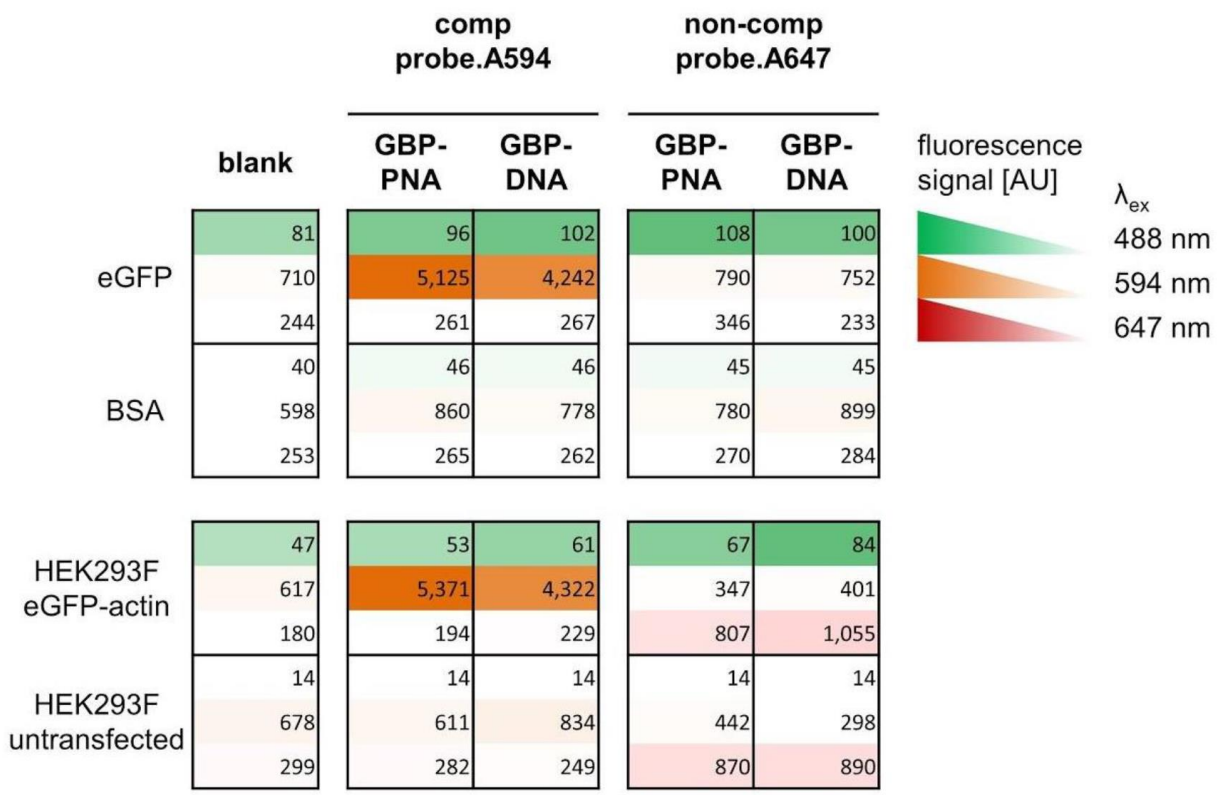

Figure 12: Binding of nanobody-oligonucleotide conjugates to purified eGFP and eGFP-actin transfected HEK293F cells in an ELISA format. Top: Binding of nanobody-oligonucleotide conjugates to purified eGFP and annealing of either a complementary fluorescent imager strand (comp probe.A594) or non-complementary fluorescent imager strand (non-comp probe.A647). Bottom: Binding of nanobody-oligonucleotide conjugates to either eGFP-actin expressing or untransfected HEK293F cells. Imager strands were used as in the top panels. Fluorescence signal intensity per well is represented by the respective color coding. Adapted from Schwach et al. 2021[177].

These results confirmed that the combination of Tub-tag technology and CuAAC is a suitable tool for the generation of functional AOCs. While a we could detect a minor shift of alkynyl-nanobody when incubated with CuAAC buffer in SDS-PAGE, suggesting that the protein surface is likely altered by oxidative damage which could lead to a different migratory speed in the gel, this observation did not translate into the functional readout and the binding capacity of GBP was not altered, or there was a sufficient amount of undamaged GBP in the final product allow efficient binding to eGFP.

5.2.1.3 Reversible Staining of Cellular Structures using Nanobody-Oligonucleotide Conjugates

Next, we set out to functionally test our conjugate for reversible staining in confocal microscopy. The length of the DNA strands and their sequence has been chosen so that the hybridization can be reversed under certain buffer conditions such as 50% formamide. This technique is used regularly for sequential staining of multiple structures and high-resolution microscopy[270,271]. To this end, we fixed and permeabilized HEK293F cells that were previously transfected with LaminB1-GFP and HeLa Kyoto cells that were previously transfected with PCNA-GFP. Cells were incubated with nanobody-DNA conjugate and excess conjugate was removed by washing with PBST. Cells were then incubated with the first fluorescent probe and imaged, followed by stripping with formamide buffer to break the hybridization of the nanobody-DNA conjugate. Samples were then stained with the second fluorescent probe using the same DNA sequence, but a different fluorophore and imaged again (Figure 13 A).

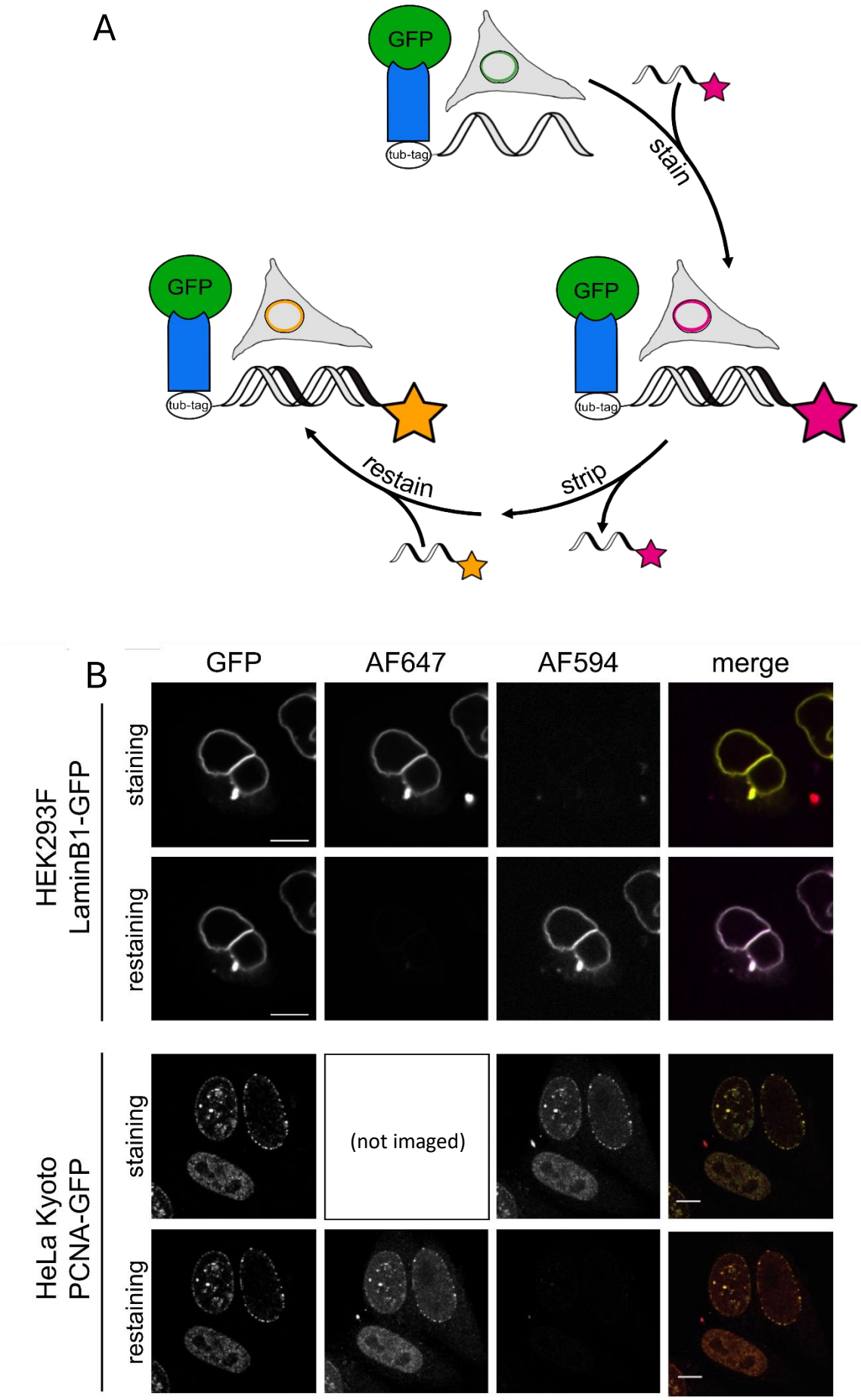
A
GFP
tub-tag
stain
GFP
tub-tag
GFP
tub-tag
restain
strip
B
GFP
AF647
AF594
merge
HEK293F
LaminB1-GFP
staining
restaining
HeLa Kyoto
PCNA-GFP
staining
(not imaged)
restaining

Figure 13: Nanobody-oligonucleotide conjugates are suitable for reversible staining of cells in fluorescence microscopy. (A) Schematic representation of the reversible staining principle. (B) Top: Staining of HEK293F cells expressing eGFP-LaminB1. eGFP-LaminB1 is stained by binding of the nanobody-DNA conjugate and subsequent annealing of a complementary imager strand leading to colocalized signal of imager strand and eGFP. Disruption of the interaction of imager and docking strand leads to almost complete removal of fluorescence, allowing for restaining with a complementary imager strand in a different channel. Bottom: Staining of HeLa Kyoto cells expressing eGFP-PCNA. Staining was performed identically to the top panel. Staining of HeLa Kyoto cells has been performed by Ksenia Kolobynina. Scale bars represent 10 µm. Red overlay = AF647. Magenta overlay = AF594. Adapted from Schwach et al. 2021[177].

We altered the staining sequence between HEK293F-LaminB1-GFP expressing cells and the HeLa Kyoto PCNA-GFP-expressing cells to ensure that the staining was reversible regardless of which probing strand was used first. While Lamin presents a target of relatively low complexity, being mostly present near the inner nuclear membrane, PCNA shows a more intricate pattern within the nucleus with multiple foci of high density both near the nuclear membrane as well as within the nuclear compartment. Both cell lines exhibited an almost perfect overlap in the GFP channel and the probes of both initial staining and restaining (Figure 13 B). We did not observe unspecific staining outside of the GFP-tagged proteins or unspecific binding of the AOC or probe to other parts of the cell. Most importantly, residual signal from the initial staining in the restaining was minimal, concluding that removal of the first probe was near-complete.

In summary, we were able to utilize Tub-tag technology for the generation of AOCs for conjugation of both DNAs and PNAs. We confirmed successful conjugation of the sample by SDS-PAGE, mass spectrometry and AEX chromatography. For DNA conjugates, AEX chromatography proved to be a successful strategy for the removal of unconjugated nanobody. However, free DNA could not be fully removed. In contrast, free PNA could be easily removed by AEX, but this purification technique proved insufficient for the separation of unconjugated nanobody from the AOC. While SDS-PAGE hinted at potential oxidative damage due to the CuAAC conjugation, our AOCs yielded specific signal in binding assays on recombinant protein and antigen-expressing cell lines. Finally, we could show that the hybridization of AOC and the fluorescent probe could be efficiently reversed using confocal microscopy. These results suggest that the AOCs produced with Tub-tag technology are fully functional and damage to both the nanobody protein and the oligonucleotide payload is minimal.

5.2.2 Development and Pre-Clinical Assessment of an αFlt3 ADC

Apart from AOCs which can be used in cancer research both for diagnostics and therapy, we developed a humanized ADC for the targeting of cancer stem cells, thereby representing a more classical approach to ADC therapy. Despite advances in the treatment of AML, particularly patients carrying Flt3 mutations such as the Flt3-ITD still have a poor prognosis. These patients would therefore greatly benefit from the development of a therapeutic drug directly targeting the overexpressed Flt3 antigen. Here, we use 20D9, an antibody that has previously been developed in our laboratory and has shown promising results in preclinical characterization studies in the ADC format, as a basis for further refinement. Shortcomings of the previous study was the reliance on a chimeric version of this antibody, a feature that can lead to human anti-mouse antibody response, as well as the usage of MMAF as a toxin that does not target cancer stem cells as efficiently, leading to relapse in patients even after initially successful treatment. Our aim is therefore to humanize the framework regions to reduce immunogenicity and select a suitable candidate for the development of a therapeutic ADC for treatment of Flt3-positive AML. Since the introduction of mutations in the framework region means altering the binding domain of the antibody, thorough testing and characterization to ensure safety and efficacy of the therapeutic. Additionally, we strive to develop

an ADC that is able to target cancer stem cells by using a different antibody-toxin combination than the previous study that is better able to address slowly dividing cells.

5.2.2.1 Humanization of an αFlt3 Antibody

Humanization of the 20D9 antibody was performed by Yumab GmbH (Braunschweig, Germany). Yumab uses in-silico humanization based on germline-optimized CDR grafting. This process aims to identify amino acids in the framework regions that are not common in humans. These amino acids will then be exchanged for amino acids that appear in the most closely related human germline sequences. CDR grafting is possible due to high identity between many murine, rat and human germline antibody sequences, allowing for a decrease in non-human structures with relatively few mutations. Additionally, another approach was taken by 3D-modeling of the rat antibody in order to identify surface displayed amino acids. By comparison with an antibody database, amino acids that differ from consensus sequences can be identified and mutated to more closely match the 3D structure of a human antibody.

Table 6: Overview of the degree of humanization as measured by GI of the antibodies used in this project.

Antibody	GI of VH [%]	GI of VL [%]	Mean (VL and VH)
rat wt	85,4	84,0	84,7
#1	91,0	89,3	90,2
#2	93,6	89,3	91,2
#3	100	89,3	94,7
#4	98,9	89,3	94,1
#5	91,0	95,2	93,1
#6	93,6	95,2	94,4
#7	100	95,2	97,6
#8	98,9	95,2	97,1
#9	91,0	100	95,5
#10	93,6	100	96,8
#11	100	100	100
#12	98,9	100	99,5
#13	91,0	96,4	93,7
#14	93,6	96,4	95,0
#15	100	96,4	98,2
#16	98,9	96,4	97,7

The in-silico humanization yielded four new humanized chains for each heavy and light chain variable regions of the original 20D9 antibody, whereas the VH1-VH3 and VK1-VK3 were generated by CDR grafting, while VH4 and VK4 used the 3D modeling approach. Since each mutation introduces a potential liability and could alter the binding characteristics of the antibody, multiple sequences with increasing degrees of humanization have been generated based on which up to 16 new antibodies can be expressed (table 1). The germinality index (GI) is a measure of humanization and is defined by the fraction of identical amino acids in the framework regions between a given antibody and the closest human germline antibody sequence[272,273]. A GI of 100% therefore represents an antibody that contains a purely human framework. In our case, the number of mutated amino acids for humanized 20D9 (hum20D9) ranges from 6 (VH1) to 16 (VH3) for the VH domain and from 5 (VK1) to 13 (VK3) for the VK domain, respectively. These mutations lead to an increase of the GI value from 85,4% (rat 20D9 VH) and 84% (rat 20D9 VL), respectively, to a fully

humanized framework region with a GI of 100% for both chains. Since VH4 and VK4 were humanized based on their 3D structure instead of CDR grafting, their GI was lower than for the fully humanized VH3 and VK3 with 98,9% and 96,4%, respectively. Nevertheless, the mutational pattern of VH4 and VK4 is highly similar to VH3 and VK3, respectively.

5.2.2.2 Expression and Purification of Humanized 20D9 Antibody Candidates

A “mix and match” combination of the four humanized heavy and four humanized light chain variants leads to a total of 16 novel antibodies with varying degrees of humanization (that will be enumerated from #1-#16 herein). Achieving high yields is paramount for the development of a therapeutic in order to decrease productions costs. Therefore, we used the ExpiCHO expression system that is well established for antibody production both for laboratory as well as production scale with subsequent purification by FPLC using a Protein A column (Figure 14).

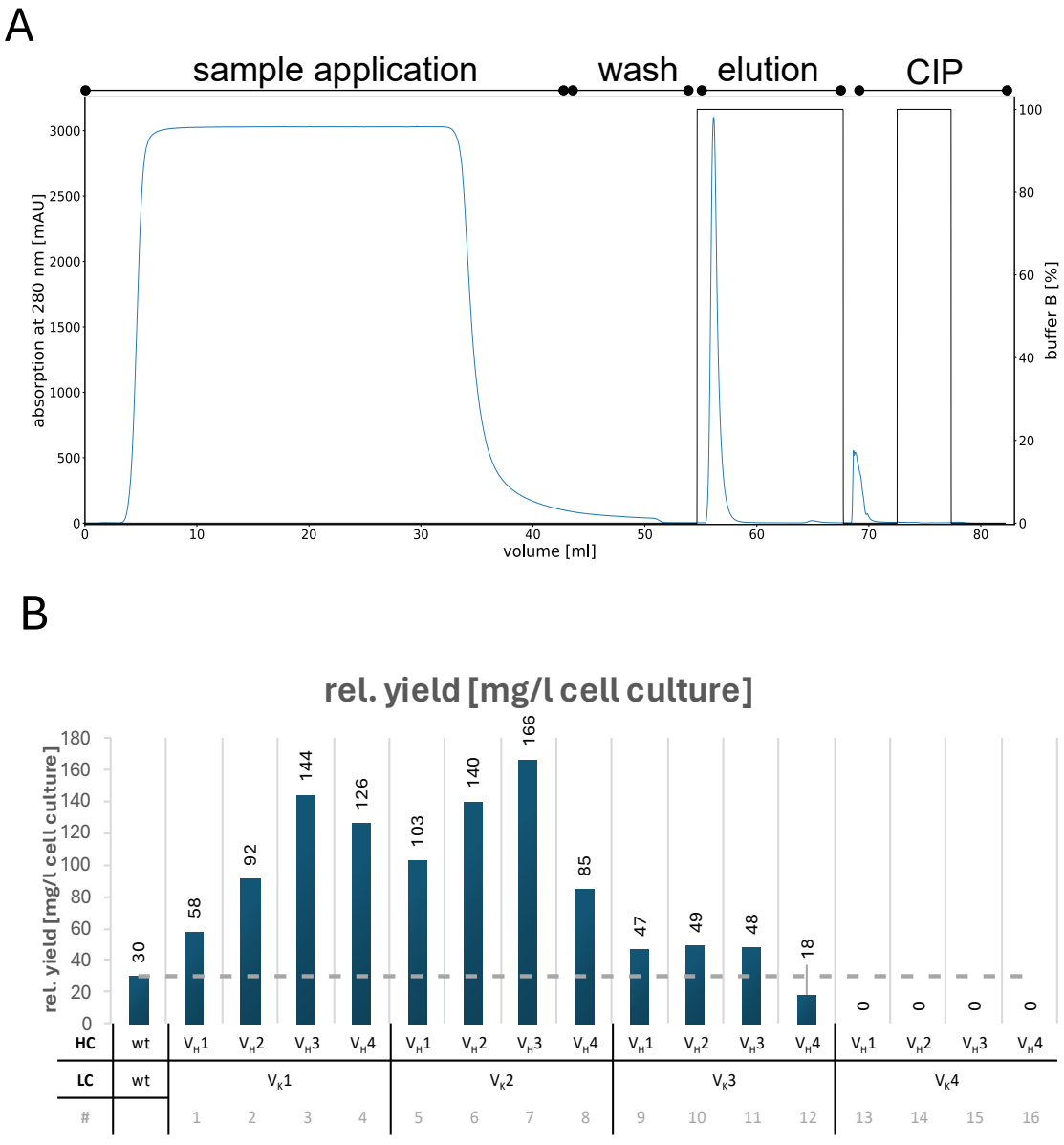

Figure 14: Expression and purification of 16 humanized variants of 20D9 aFlt3 antibody in ExpiCHO cells. (A) Typical chromatogram of a protein A based antibody purification on the example of antibody #7. The concentration of buffer B (elution buffer) is represented in grey. (B) Evaluation of expression yields. Cleared supernatant has been purified using Protein A FPLC after transient transfection of ExpiCHO cells and the relative yield calculated. Chimerized 20D9 (Figure 14 continued) antibody (wt) was used as control. No protein expression was observed for antibodies #13-16,

which all share the same light chain (VK4). Highest expression was observed for antibody #7 at 166 mg/L. With the exception of antibody #12, all humanized antibodies expressed at comparable or higher levels than the original chimeric 20D9.

We were able to successfully purify 12 out of 16 antibodies. Of the remaining 12 antibodies, only #12 expressed at lower levels than the rat control.

5.2.2.3 Selection of a Lead Candidate

A thorough characterization of therapeutic antibody candidates allows to select the antibody that is best suited for treatment. However, due to the high cost and time-intensive process of ADC development, fully characterizing every single candidate would be highly resource intensive. For this pragmatic reason, it is necessary to narrow down the antibody candidates as quickly as possible and focus on a lead candidate to proceed with further characterization. Thus, techniques that allow the measurement of multiple samples in parallel and automation of the sampling process enable us to quickly reduce the number of candidates to the most promising ones are usually the first step in antibody any development process. To this end, we used high-performance liquid chromatography (HPLC) to measure the stability of the antibody and ELISA to determine antigen specificity.

5.2.2.3.1 Accelerated Aging Experiment to determine Antibody Stability

A major factor in the safety of an antibody therapeutic is the propensity for aggregation that leads to adverse effects in the patients. Additionally, any vial of therapeutic antibody or ADC will be stored for an unknown duration between production and application in the patient. In this time frame, aggregates can form. A high propensity for aggregation therefore not only leads to adverse effects in therapy, but also a reduction in shelf-life and thereby an increase in costs.

To determine whether the generated antibodies are stable during storage, we performed an accelerated aging test (Figure 15)[274]. During this experiment, the antibody is subjected to thermal stress by storage at elevated temperatures and measurements are taken at defined intervals. We normalized the concentration of all antibody samples to 1 mg/ml in order to exclude a bias by different antibody concentrations. Samples were then stored at 4 °C (control), or room temperature and 37 °C, respectively, to induce thermal stress. We measured the aggregation at different time points for up to four weeks by HPLC-SEC to determine the amount of aggregate in the sample. In SEC, aggregates will elute faster than monomeric antibody due to their higher molecular weight.

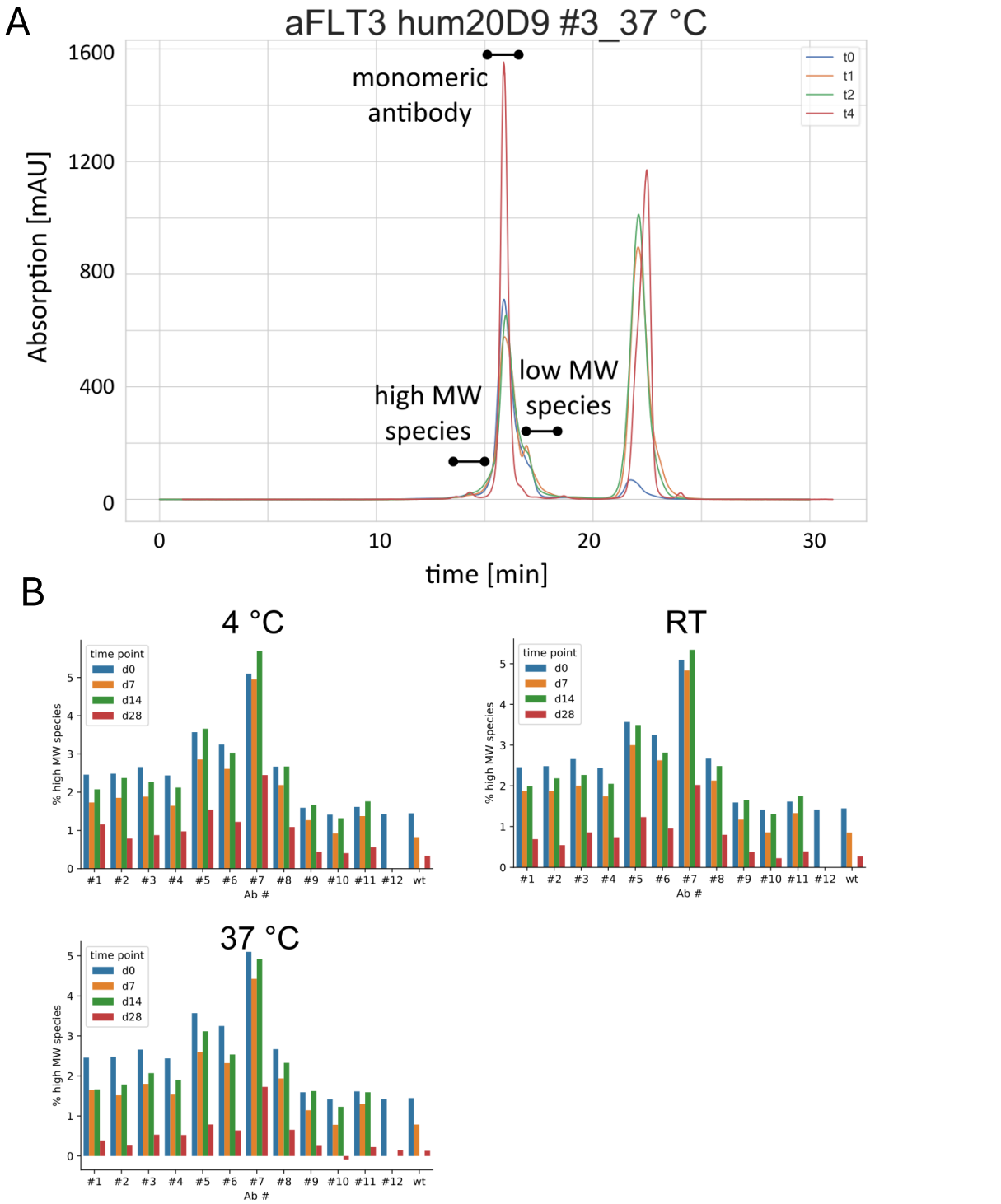

Figure 15: SEC-HPLC analysis in an accelerated aging experiment to determine stability of 12 antibody candidates. (A) Overlay of exemplary SEC chromatograms of antibody #3 stored at 37 °C for up to 28 days. To calculate the amount of aggregate in the sample, the area under the curve in the labeled high MW species range has been integrated and compared to the area under the curve of the monomeric antibody peak. The peaks at the 22 min mark represent buffer components. (B) Analysis of aggregates in all samples at 4 °C, room temperature and 37 °C.

We determined that the fraction of aggregates in the starting material ranged between 1,5% and 5%. While these measurements are not ideal, the initial aggregates can be removed by ion exchange chromatography to yield a purely monomeric antibody on a production scale.

For neither of the 12 antibody candidates, we were able to observe significant aggregation after 28 days. While the time window is relatively short, this data suggests that none of the studies antibodies shows major instability towards elevated temperatures. This observation is in line with published data from approved antibodies such as Rituximab, which exhibits little aggregation after one month in an accelerated aging setup[274]. However, it is important to note that the formulation of the storage buffer has a major influence on aggregation and is heavily optimized individually for therapeutic antibodies, whereas this study used a simple storage buffer consisting of PBS with 50 mM L-Arginine and 0,1 % sodium azide to prevent bacterial growth during the experiment.

5.2.2.3.2 Assessment of Binding Properties and Antigen-dependent Internalization

To narrow down the field of potential candidates, the binding characteristics of all 12 antibodies were assessed by ELISA on purified, recombinantly expressed Flt3 protein as well as by flow cytometry on Flt3-expressing Ba/F3. These assays provide different environments to determine the binding between the antigen and the antibody.

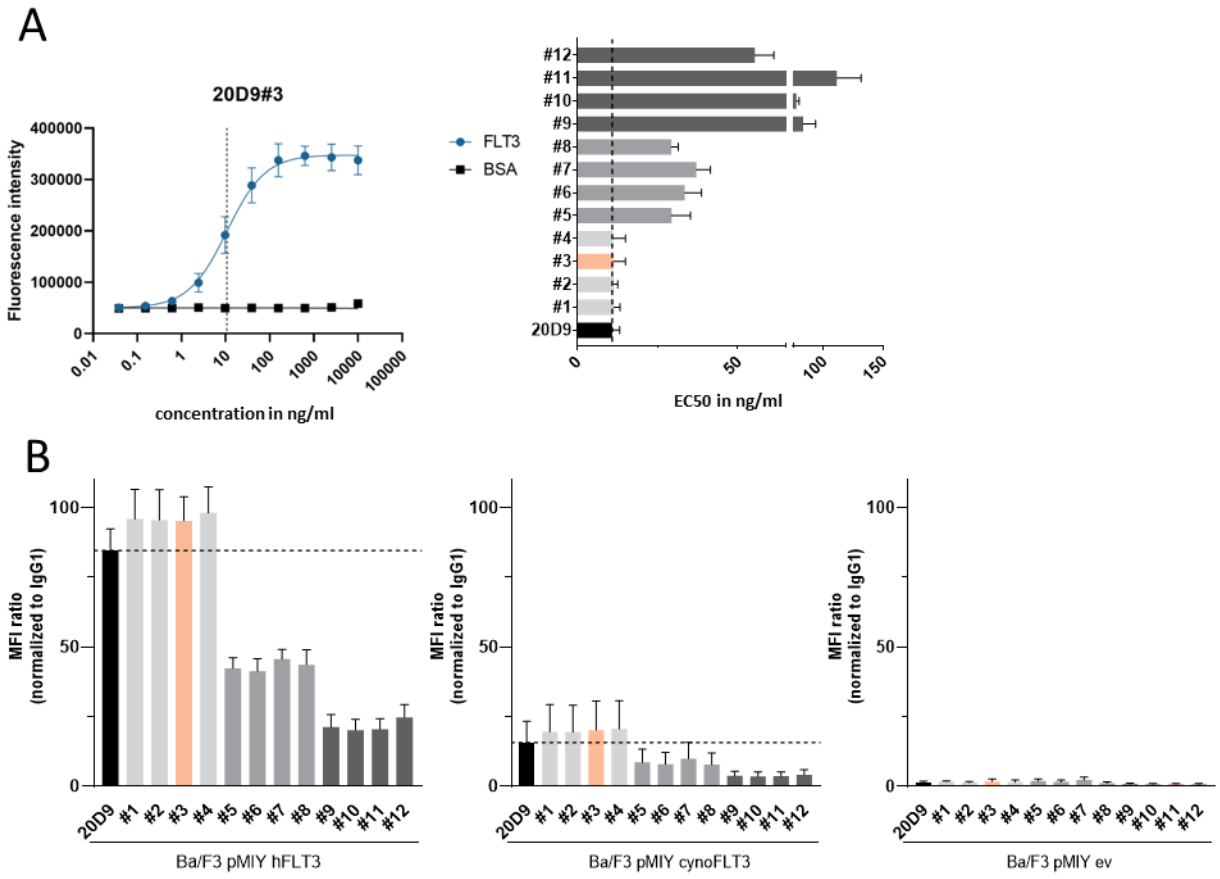

Figure 16: Binding of humanized aFlt3 antibody candidates to purified Flt3 antigen (A) and Flt3 presented on the cell surface of Flt3 expressing Ba/F3 cells. (A) ELISA using purified Flt3 protein. Exemplary ELISA profile of antibody #3 (left) and analysis after 4-paramatric fitting (right). (B) Binding to cell surface presented Flt3 antigen in saturating conditions in FACS. Left: Fluorescence intensity of Ba/F3 cells presenting human Flt3 on the surface. Middle: Fluorescence intensity of Ba/F3 cells presenting cyno Flt3 on the surface. Right: Fluorescence intensity of Ba/F3 cells presenting no antigen as a control. Samples were pre-gated on live, single cells. Experiment performed by Marina Able.

In ELISA, the antibodies showed significant differences regarding their binding strength to human Flt3 protein. The antibodies #1-#4 showed the highest affinity towards human Flt3 with values between 10,4 ng/ml and 11,4 ng/ml, which is comparable to the original chimeric 20D9 antibody of 10,6 ng/ml. Antibodies #5-#8 showed reduced affinity ranging from 28,7 ng/ml to 36,7 ng/ml. The last set, #9-#12, showed the lowest affinity with values from 54,7 ng/ml to 108,9 ng/ml. It is notable

that the antibodies fall into groups sharing the same light chain, whereas no such pattern was observed for the heavy chain. This data suggests that the light chain of this antibody is the major determinant for antigen binding and affinity, with the heavy chain playing a minor role (Figure 16 A).

Next, binding of the antibody to cell surface antigen was determined via FACS (Figure 16 B). In this assay, low affinity antibodies will show a reduced fluorescence intensity due to the molecules diffusing from the cell surface after staining, thereby reducing the overall fluorescence of the cell. Here, we observed a similar pattern compared to ELISA. The antibodies #1-#4 showed the highest mean fluorescence intensity with a slightly increased signal compared to chimeric 20D9 antibody, with subsequent reductions in intensity for the groups #5-#8 exhibiting intermediate and #9-#12 low fluorescence intensity. This data confirms the initial findings from the ELISA assay, suggesting that the lead candidate should be selected from the first group of antibodies. Similarly, binding to the Flt3 orthologue of cynomolgus monkey yielded a similar pattern. It has to be noted that, although the measured fluorescence intensity in Ba/F3 cells presenting cyno Flt3 was lower compared to cells presenting human Flt3, this reduction in signal does not necessarily suggest a lower affinity compared due to potential differences in cell surface expression of the antigen. Ba/F3 cells transduced with control plasmid without surface-presented antigen were unable to bind significant amounts of any of the 12 antibodies, confirming that the measured signal on Flt3-presenting cell lines is specific.

In summary, the 12 antibodies that were tested for stability and antigen binding grouped into three groups of four antibodies each, with each group of antibodies sharing the same light chain. The antibodies #1-#4 exhibited the best binding characteristics to antigen in ELISA and FACS. Given that antibody #3 shares the overall higher humanization due to a higher humanization in the heavy chain (mean GI for #3: 94,7% compared to the mean GI for #4: 94,1%), we decided to select antibody #3 as a lead candidate to proceed with further studies.

Next, in experiments performed by Marina Able (LMU), specificity of antibody #3 to known orthologues, homologues and common human FcγRs was determined (Figure 17). Binding to the human Flt3 homologues vascular endothelial growth factor receptor (VEGFR), platelet-derived growth factor receptor (PDGFR), stem cell factor receptor (c-KIT) and colony stimulating factor 1 receptor (CSF-1R) were investigated (Figure 17 A). These proteins are tyrosine kinases and are commonly targeted by the same small molecule drugs that are used for the treatment of Flt3 positive AML[275]. In ELISA, antibody binding was detected only on cells presenting human Flt3, but not any of its homologues, confirming that the antibody specifically recognized Flt3, but not closely related proteins. Furthermore, saturation staining in FACS to cells presenting Flt3 orthologues of cynomolgus monkey, rat or mouse, respectively, was performed (Figure 17 B). Confirming the previous finding, antibody #3 exhibited the strongest signal to human Flt3, with cyno Flt3 being lower, but detectable. Binding of the antibody to Flt3 from rat and mouse could not be detected. This result confirms specific binding to Flt3 orthologues that share high sequence identity with human Flt3. The ability to bind cyno Flt3 shows that the antibody is unable to clearly distinguish between the human and cynomolgus orthologue, this can proof advantageous in potential pre-clinical animal studies in cynomolgus monkeys.

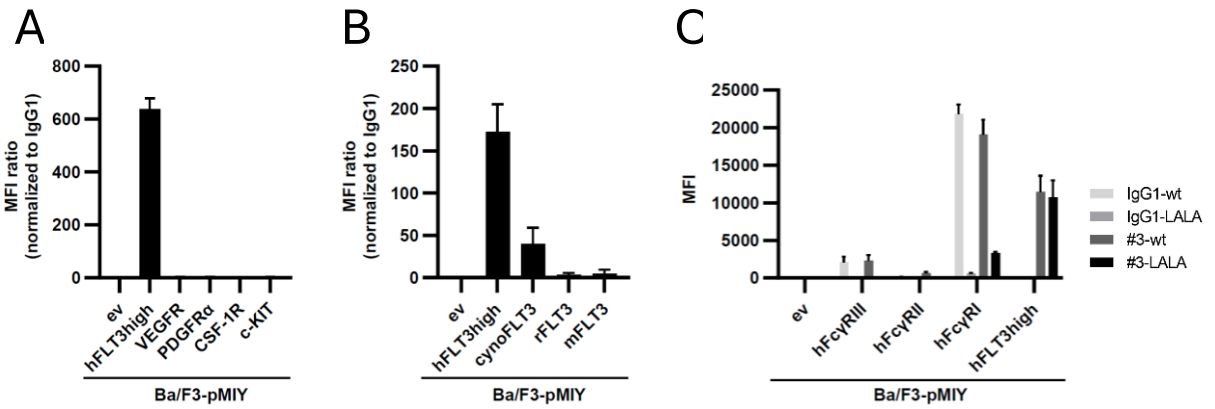

Figure 17: Binding of lead candidate antibody #3 to Flt3 orthologues (A), homologues (B) and human FcγRs (C) in FACS. (A) Humanized 20D9 #3 antibody showed strong binding towards human Flt3, but no binding was detectable to any of the tested homologues. (B) Confirming previous results, binding was detectable to human FLt3 and cynomolgus Flt3 orthologue, but not to Flt3 from rat or mouse. (C) Binding to FcγRI (CD64), FcγRII (CD32) or FcγRIII (CD16) was detected at similar levels to control IgG1 antibody. The introduction of a LALA double mutation completely inhibited binding to FcγRs on the Palivizumab IgG1 control antibody, whereas residual signal for the #3-LALA variant on FcγRI-expressing Ba/F3 cells was detected. Experiment performed by Marina Able.

Our assays so far indicated that the antibody was highly specific and adverse off-target effects on closely related proteins were not to be expected. However, undesired toxicities due to unspecific uptake by cells of the immune system via FcγRs are common in patients after ADC treatment. One way to inhibit the interaction between FcγRs and the antibody is the introduction of the so-called "LALA" mutant. Here, two leucines at positions 234 and 235 are mutated to alanines. This double mutation is situated at the beginning of the CH2 domain and inhibits the interaction between FcγRs and the antibody[276]. To determine the effect of the LALA mutation on our antibody, FcγR-mediated binding of antibody #3 (#3-wt) and the LALA-variant (#3-LALA) against Ba/F3 cells presenting either FcγRI (CD64), FcγRII (CD32) or FcγRIII (CD16) was assessed (Figure 17 C). #3-wt and IgG1-wt control antibody exhibited the strongest binding to FcγRI. For both antibodies, binding was lowered when the LALA-mutant was used, although #3-LALA exhibited a stronger signal than the IgG1-LALA control. Furthermore, binding of both wt antibodies to FcγRIII was observed at a low level which could be completely abolished by the introduction of LALA mutation. Lastly, no binding was detected to FcγRII-presenting cells regardless if wt antibody or the LALA mutant was used. These results suggest antibody #3 is able to be recognized by FcγRs and is therefore likely to invoke secondary effector functions via ADCC, ADCP and CDC. Additionally, Marina Able could show that the LALA mutant is a viable way to reduce unspecific uptake via FcγRs in case adverse events occur in the patient. However, it has to be noted that antibodies carrying the LALA mutation also exhibit less secondary effector functions. Since these effector functions have proven to be an important pillar for the effective killing of target cells, the introduction of the LALA mutant for therapeutic antibodies and ADCs is a double-edged sword. To date, most therapeutic ADCs do not utilize the LALA mutant or other means to reduce binding to FcγRs. Therefore, further experiments were conducted using antibody #3 without the LALA mutation.

We then proceeded to test the internalization of the antibody. For ADCs, internalization is a crucial step for the subsequent degradation of the construct in the lysosome and release of the toxin. To this end, we complexed aFlt3 antibody #3 with a secondary antibody that is conjugated to a pHrodo deep red dye. This dye is non-fluorescent in neutral conditions but becomes fluorescent in acidic conditions such as the environment of the late endosome and lysosome. We stained Ba/F3 cells presenting human Flt3 protein on the cell surface with the complex and assessed internalization both via confocal microscopy as well as flow cytometry (Figure 18).

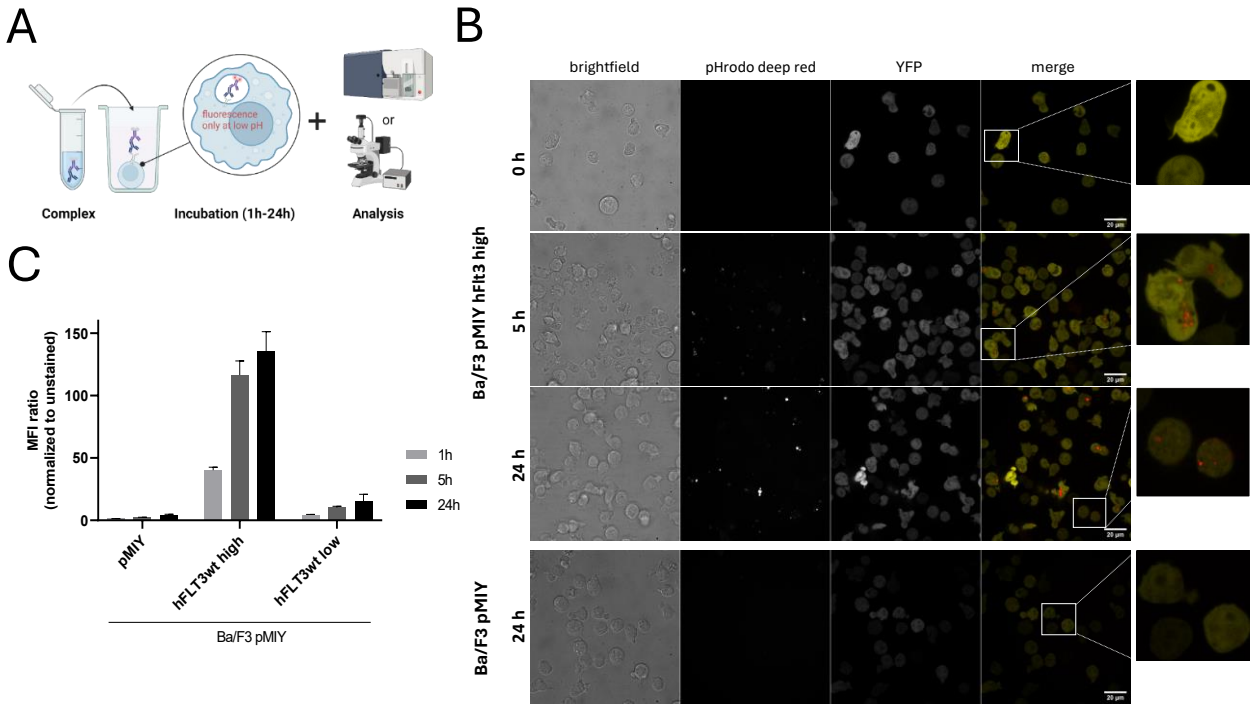

Figure 18: Internalization of humanized aFlt3 antibody #3. (A) Schematic overview over the experimental setup. Humanized aFlt3 antibody #3 was complexed with secondary antibody carrying a fluorophore that becomes fluorescent only in acidic conditions such as the lysosome. Flt3 expressing Ba/F3 cells were stained and analyzed either via confocal microscopy or FACS. (B) Internalization experiment as assessed by confocal fluorescence microscopy. Ba/F3 cells transduced with either Flt3 antigen (Ba/F3 pMIY hFlt3 high) or empty control vector (Ba/F3 pMIY) were incubated with a pre-formed complex of αFlt3 antibody #3 and anti-human secondary antibody with the secondary antibody being conjugated to pHrodo deep red fluorescent dye. pHrodo deep red is non-fluorescent in neutral conditions but becomes fluorescent in acidic conditions such as the endosomes and lysosomes and therefore acts as a marker for antibody uptake into these compartments. Internalization was detectable on Flt3 expressing cells 5 h and 24 h after incubation. On the Flt3 negative control cell line, only weak signal could be detected even after 24 h. Scale bars represent 20 µm. Red overlay = pHrodo deep red. Yellow overlay = YFP. (C) Quantification of internalization in flow cytometry. Internalization of the complex could be detected in Flt3 expressing cell lines depending on the surface expression level of Flt3. The Flt3 negative cell line showed minor unspecific uptake after 24 h. Fluorometric experiment performed by Marina Able.

In confocal microscopy, we were able to confirm internalization both after 5 h and 24 h (Figure 17 B). Signal appeared only within the circumference of the Flt3-expressing Ba/F3 cell line and not at the cell surface, confirming that the dye is in acidic conditions. The engineered Ba/F3 cell expresses both the Flt3 antigen as well as cytosolic eYFP from the same mRNA with both coding sequences separated by an internal ribosomal entry site. eYFP therefore acts as a marker for the cytosol and is excluded from internal vesicles such as lysosomes. In accordance with this design, we could detect pHrodo deep red signal only in areas of the cell with low eYFP signal. This residual eYFP signal most likely stems from background bleed through from layers beneath and above the vesicle. Additionally, only weak signal could be detected in the Flt3-negative Ba/F3 pMIY control cell line after 24 h of incubation, only low unspecific uptake of the antibody complex even after prolonged exposure.

Besides confocal microscopy, we observed internalization of humanized 20D9 #3 antibody in flow cytometry that allows for easier quantification and comparison of measured signal (Figure 18 C). Flt3-expressing cell lines showed internalization of the antibody complex in an expression-dependent manner, with $Flt3^{high}$ cells internalizing more antibody in comparison to $Flt3^{low}$ cells. Flt3-negative cells showed minor internalization with longer incubation times with the signal overall

being less intense than on the Flt3^{low} cell line, suggesting minor unspecific uptake during prolonged exposure to the complex.

In summary, four out of 12 different candidates exhibited favorable binding characteristics on recombinantly expressed protein as presented in ELISA, as well as binding to cell-surface presented Flt3 protein. Of these four, we selected antibody #3 as the lead candidate on the basis of the highest GI score, suggesting least immunogenicity. We were then able to show specific binding to human and cynomolgus Flt3, but not to Flt3 derived from rat or mouse. No binding was detected to human Flt3 homologues. We further confirmed interaction with FcγRs that can be vastly reduced with the introduction of the LALA mutation, suggesting that the selected lead antibody is likely to exhibit secondary effector functions. Furthermore, we could prove efficient internalization of the lead antibody by confocal microscopy and spectrometric measurements.

5.2.2.4 Assessment of ADC Efficacy

A long-term aim of this project is the generation of an ADC that is capable to target resting cells such as cancer stem cells (Figure 19). Those cells have a higher chance of surviving the initial treatment and induce relapse in patients. Commonly used toxins like the auristatins MMAE and MMAF inhibit tubulin polymerization and target primarily quickly dividing cells. Other toxin classes use different mechanisms of action that are thought to target resting cells more reliably. These classes include DNA damaging agents such as duocarmycin (DUBA) and the camptothecin derivative exatecan and have become more popular in ADC development over the past decade. To develop an ADC capable of targeting resting cells, cytotoxicity experiments were carried out to select a potent antibody drug conjugate based on efficacy towards AML and PDX model cell lines. In-depth information regarding this part of the project can be found in the dissertation of Marina Able (LMU) and key findings are communicated here only in brief.

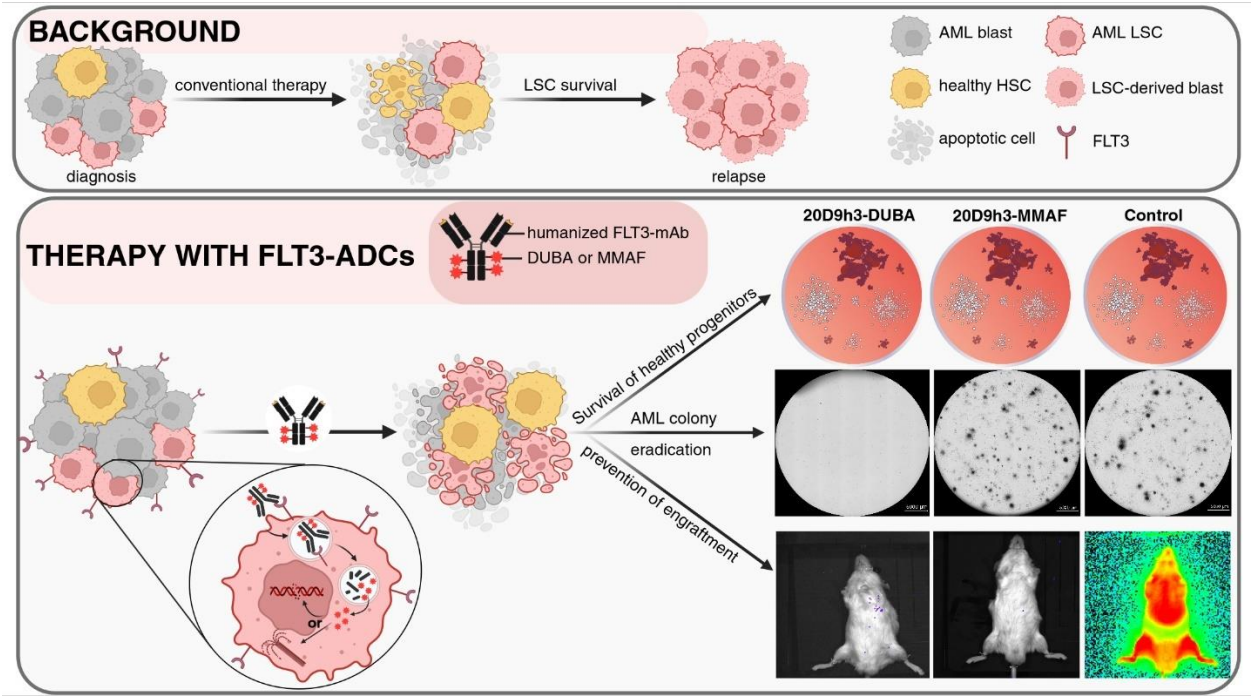

Figure 19: Graphical overview of the targeting of AML cancer stem cells using an ADC based on humanized 20D9 #3 and DUBA using long-term culture-initiating cell (LTC-IC) and colony forming unit (CFU) assays and PDX samples. These experiments assay for the long-term capability of cells to proliferate and regrow with is measured either by the number of colonies formed or the growth of tumor after re-engraftment into mice. In these experiments, both ADCs were able to reduce the number of progenitor cells. However, DUBA-based ADCs were generally more potent compared to MMAF-based ADCs.

Based on previously published studies and confirmed by experiments on resting cells, DUBA was selected as a suitable toxin for the targeting of resting and slowly dividing cells. Both the ADC based on DUBA as well as the ADC based on MMAF were effective in the killing of Flt3-expressing Ba/F3 cells as well as AML cell lines. In experiments utilizing long-term culture-initiating cell (LTC-IC) assays to determine whether the ADC is able to eradicate cancer stem cells in the PDX samples, cells are transferred to a feeder co-culture for 6 weeks to allow for differentiation, after which a CFU assay is performed. In these assays, both ADCs were able to reduce the number of colony forming cells with DUBA-ADC treatment usually leading to a stronger reduction in colonies compared to MMAF-ADC. Notably, strong differences were observed between PDX samples. While AML-388 proved highly susceptible even at low doses, colonies were detectable for AML-393 after treatment. When PDX cells were treated with ADC ex vivo before engraftment into mice, AML-388 was unable to engraft in any condition, while tumor growth was detected for AML-393 after treatment with MMAF-ADC, but not DUBA-ADC.

6 Discussion

6.1 Isolation of Antibodies for Treatment of Pediatric T-ALL

ALL is a disease that typically occurs at a young age. When identified in time, children have a high chance of cure and long-term survival. However, roughly 20% of patients will experience a relapse of the disease[277]. If ALL occurs at later stages in life such as adolescence, the overall survival rate decreases[278]. While overall only comprising 10-15% of all ALL cases, children diagnosed with T-ALL have generally a worse prognosis than children diagnosed with B-ALL[279]. Inotuzumab ozogamicin is a therapeutic ADC for the treatment of refractory B-ALL and has achieved great improvements for patient survival. However, patients with T-ALL currently lack the option of therapeutic ADCs and solely rely on chemotherapy and radiation therapy. Especially relapsed T-ALL patients have poor prognosis due to acquired resistance against the initial therapy[280]. Since the generation of hybridoma is a time-intensive experiment, our aim in this study was to implement a workflow that selects hybridoma-derived monoclonal antibodies for cell surface binding from the very start. This will reduce the time and resources wasted on the establishment of hybridoma cell lines with little therapeutic prospective and instead pre-select antibodies for the generation of ADCs. We chose the T-ALL targets CD2, CD5, CD7 and CD28 due to their reported overexpression in T-ALL, but also some B-ALL subsets.

The isolation and characterization of antibodies represents the early phase of ADC development and is usually composed of antigen expression, immunization, antibody isolation and characterization.

To this end, we expressed and purified all recombinant antigens as Fc-fusion proteins. Furthermore, we engineered Ba/F3 cells to present each antigen on the cell surface to allow for screening of hybridoma supernatants. In some immunization experiments, we tried to utilize the engineered Ba/F3 cell line as a “living antigen” instead of purified protein, a method which is regularly practiced to generate antibodies. In theory, the murine origin of the cell line should lead to an only minor immune response in mice against natural targets on the Ba/F3 cell surface, whereas the engineered antigen should be recognized as foreign. However, we were unable to identify any antigen-specific antibody when immunizing with engineered Ba/F3 cells (data not shown). While the exact reason is unknown, it is possible that the cell line responds to cytokines and other signaling molecules, leading to alterations in protein-surface expression and downregulation of the antigen. Nevertheless, immunization with recombinant protein reliably led to immune responses.

We were able to isolate antibodies against all four antigens. We were able to show internalization of purified antibody, which is a major requirement for its successful development into an ADC as well as the possibility of engineering by chimerization without loss of antigen binding capability in flow cytometry. However, to date some of the isolated antibodies still require further characterization. The therapeutic potential of these antibodies remains to be evaluated. All four antigens are expressed on the majority of T cells. Although the targeting of common T cell antigens is likely to cause severe side effects by forcing healthy T cells into apoptosis, it could provide an effective, albeit radical, approach to ensure complete eradication of cancer cells prior to hematopoietic stem cell transplantation. This could not only provide a last chance for relapsed patients with poor prognosis to survive the disease, but also pose a potential therapeutic strategy for patients with initial diagnosis and prospect of hematopoietic stem cell transplantation to achieve a deep remission before transplantation and thereby reduce the chance of relapsing in the first place.

With the availability of antibodies against multiple targets and the aim to achieve complete remission in patients, combinatorial co-treatment with two ADCs at the same time could provide

an interesting prospect T-ALL therapy. This approach would minimize immune evasion as it is typically seen in ADC therapy upon downregulation the antigen, since the cancer cell would need to downregulate both antigens simultaneously. Additionally, this system would provide an interesting platform to study potential synergistic effects of co-targeting certain combinations of antigens, as well as an opportunity to evaluate synergistic effects of different toxin payloads in a T-ALL setting.

Since the antibodies generated in this work have been fully sequenced, it is possible to further engineer the antibodies, e.g. for the generation of bispecific antibodies that require recombinant expression to guide correct pairing of heavy and light chains. Lastly, the binder sequences in this work can be used to generate chimeric antigen receptors (CAR), which are currently under investigation for the treatment of ALL. Similarly, it is also possible to develop a combinatorial therapy by utilizing both CARs and ADCs for the treatment of the patient. In current research and therapy, CARs and ADCs are almost seen as two exclusive alternatives. However, the different modes of action employed by these vastly different therapeutic approaches have potential to compensate for the disadvantages of monotherapy when used in conjunction. One such disadvantage of CARs would be the lack of control after administration to the patient. Patients with high tumor burden can experience cytokine storm due to the high activation status of CAR T cells[281,282]. ADC therapy on the other hand is transient and additional doses need to be frequently administered to keep titers high. In combination, patients with high tumor burden could benefit from initial ADC treatment to allow for reduction in tumor burden prior to CAR T cell administration. On the other hand, the sustained mode of action of CAR T cells does not require continued dosing as it is the case for ADCs and ensures deep remission in the patient before receiving a hematopoietic stem cell transplant.

6.2 Advantages and Pitfalls of Different Antibody-Oligonucleotide-Conjugate Generation Strategies

The use of AOCs is a rather new and yet mostly unexplored field of research. AOCs combine two major biological moieties with very different building blocks into a single molecule: Proteins made from the 20 canonical amino acids with their high chemical diversity and oligonucleotides with their comparatively limited amount of building blocks but ability to hybridize and the possibility to be easily altered. While direct conjugation to surface-presented amino acids such as lysine and cysteine have become the primary strategy for generation of small molecule toxin ADCs, the conjugation strategies of AOCs are much more diverse. One such approach relies on ionic interactions between the negatively charged DNA and a positively charged carrier molecule such as proteamine[89,283] or poly-arginine[249]. This makes “attaching” the oligonucleotides by incubation very easy. However, the ionic binding is reversible, rendering these conjugates unsuitable for some applications such as DNA-PAINT in microscopy and raising doubts about the efficacy and safety as therapeutics. Notably though, Bäumer et al. reported *in vivo* efficacy using this approach in mice[89], suggesting that these concerns might be unfounded. However, current *in* vivo data is rather scarce compared to traditional toxin-based ADCs and it remains to be seen if studies can reliably replicate efficacy *in vivo* after AOC treatment when using different oligonucleotides, target antigens and cancer settings. Instead of ionic interactions, some groups utilize the affinity between biotin and avidin to form stable complexes[284]. Nevertheless, this method usually requires chemical modification of the antibody and oligonucleotide with avidin and biotin, leading to a hybrid method between direct conjugation and affinity interaction. Direct conjugation to surface-exposed amino acids such as lysine[246,285] and cysteine[248] provides a straight-forward way for AOC generation similar to small molecule toxin ADCs and requires chemically modified oligonucleotides that can be attached via bi-functional linkers. Conjugation via lysine is very reliable and can be applied to

almost any protein, but, as discussed previously, it is impossible to control how many oligonucleotides will be attached and where the sites of attachment will be, leading to problems akin to small molecule toxin ADCs. Similarly, cysteine-based conjugation strategies lead to a more defined product due to the reduction of potential attachment sites.

Lastly, enzyme-catalyzed conjugation via Sortase A has been reported for the generation of AOCs[286]. Sortase A conjugation involves the introduction of small amino acid sequences both on the oligonucleotide and the antibody in order for the Sortase A enzyme to recognize and ligate both molecules together. A major advantage is the high specificity and knowledge about the exact positioning of the oligonucleotide within the conjugate. However, Sortase A-catalyzed reactions are easily reversible and require high excess of one reaction partner for efficient conjugation. Additionally, the strategy as used by Harmand et al. necessitates the modification of the oligonucleotide with amino acids, which for many research laboratories is much more difficult to obtain than oligonucleotides modified with chemical groups. Taken together, this makes Sortase A-based conjugation much more costly due to higher usage of reactants.

Our group has previously shown that Tub-tag-based conjugation can be used to efficiently generate small molecule toxin ADCs. Although this conjugation limits the conjugation site to the C-terminus of a protein, the combination with strain-promoted azide-alkyne click chemistry (SpAAC) yields very stable conjugates, unlike for example cysteine-maleimide-based ADCs that are prone to transfer the toxin to blood proteins such as albumin, and effective in mice. To date, this technology has not been used to generate AOCs. Given previous successes for ADC generation, we hypothesized that Tub-tag-mediated conjugation is a promising tool for efficient generation of AOCs as well. Additionally, PNAs have become a promising tool with their main advantage being the lack of a highly charged backbone leading to stronger binding to other PNA and DNA strands and reduction of unspecific interactions with positively charged molecules. These characteristics render PNAs an interesting molecule class for applications in complex environments such as the cytosol and nucleus of the cell. However, the high cost of synthesis necessitates an efficient conjugation strategy, which we wanted to provide with Tub-tag-mediated conjugation.

6.2.1 Chemo-enzymatic functionalization of Tub-tagged Proteins with Oligonucleotides

Similarly to Sortase-A mediated ligation, Tub-tag-based conjugation requires a C-terminal recognition tag, which has the disadvantage of requiring genetic engineering of the protein beforehand but grants precise control over the point of attachment of the conjugation partner. An advantage over Sortase A mediated conjugation is the usage of a low-cost derivative of tyrosine that can be used in large excess for efficient conjugation, reducing the need for a high excess of more expensive compounds such as functionalized oligonucleotides.

In this work, we aimed to introduce Tub-tag-based conjugation as a strategy for AOC generation. Our conjugation strategy involves a two-step process: First, the TTL enzyme ligates an alkyne-containing derivative of tyrosine, O-propargyl-L-tyrosine, to the C-terminus of the Tub-tagged nanobody. Due to its cheap cost and low molecular weight, it can be used in large excess during the ligation step and easily removed by size-exclusion chromatography or desalting before conjugation of the oligonucleotide. Second, using CuAAC, we conjugated azide-containing DNA and PNA of 15 bp length with the modified nanobody.

Using SDS-PAGE and AEX, we could show efficient conjugation of both azide-DNA and azide-PNA to the nanobody. In AEX, we observed binding of the alkynyl-functionalized nanobody to the column matrix due to the negative charges introduced by the glutamic acid of the Tub-tag. For DNA

conjugates, it was possible to remove unconjugated nanobody. Although we saw two distinct peaks during the purification representing the final conjugate product and unconjugated azide-DNA, we were unable to fully remove unconjugated DNA by AEX. This is likely due to the DNA carrying a strong negative charge, largely overshadowing the charge of the Tub-tag and nanobody itself. Interaction with the column matrix is therefore largely mediated by the DNA so that conjugate and free DNA are mostly indistinguishable under the chosen purification conditions. On the other hand, PNA-conjugates could be separated from azide-PNA which eluted during the sample application and column wash steps due to the lack of negative charge, but not from alkynyl-nanobody. We observed a minor shift between alkynyl-nanobody and PNA-conjugate likely due to a shielding effect of the PNA towards the negative charges of the Tub-tag.

Our DNA and PNA oligonucleotides were designed to have a length of only 15 bp so that the melting temperatures in hybridized strands are low. This allows reversible hybridization without applying heat or other harsh stripping conditions to the sample. Our functional assays included a binding/hybridization assay in a 96-well format and staining of fixed and permeabilized cells in confocal microscopy. We observed fluorescence in the binding assay on GFP-coated plates after incubation with the GBP-binding nanobody conjugated to either DNA or PNA and hybridization of a complementary imager strand. Similarly, fluorescence was not observed when hybridizing with a non-complementary probe or when the GFP antigen was not presented on the plate surface as recombinant protein or in the form of GFP-expressing cells. This confirmed that both the nanobody and oligonucleotide were still intact. This finding is important since Cu[I]-ions can form reactive oxygen species that in turn either degrade proteins or modify amino acid side chains such as histidine, cysteine, methionine, tryptophan, and tyrosine[268,287]. While we used THPTA as a copper ligand to reduce the potential damage, the chance to damage crucial functional regions such as the CDRs is especially high in small binding molecules such as nanobodies, because they do not provide as many surface groups that can be altered and do not contribute to the binding of the antigen. Similarly, reactive oxygen species might react with the oligonucleotide and lead to chemically altered bases that could abolish binding of the imager strand. While the majority of our conjugate appeared to be functional, damage might still occur. We did not determine to which extend damage might have occurred in the final product. To circumvent Cu[I]-catalyzed damage, switching to a copper-free SPAAG conjugation strategy is beneficial. Since no tyrosine derivative has been reported that includes a strained-alkyne moiety such as DIBO or DBCO and can be ligated by the TTL enzyme, this would require a switch in of functional groups between the Tub-tag-tyrosine derivative and oligonucleotide compared to our strategy. Azido-tyrosine has already been readily used for Tub-tag-mediated protein functionalization[175] so that the oligonucleotide needs to carry the alkyne group. This approach might need further optimization regarding reaction conditions, since the efficiency of SpAAC is generally considered to be lower and slower than CuAAC, which would result in lower yields.

In our final microscopy experiment, we could show that the binding of the hybridized imager strand to DNA-conjugate could be reversed by washing with a 50% formamide solution and the sample re-stained using the same imager sequence, but a different fluorophore. Since we did not observe significant residual signal from the first round of imaging, we conclude that our stripping method was very efficient, thereby freeing up the channel and allowing for re-using the same or a similar fluorophore for visualizing other targets.

6.2.2 Use of Antibody-Oligonucleotide-Conjugates within and beyond Microscopy

This sequential imaging protocol with alternating rounds of stripping and annealing of imager strands is a common technique to visualize a multitude of cellular structures and targets within the same sample[270,288-290]. While our approach is not equivalent to these studies, our data provides

proof of concept that nanobody-oligonucleotide conjugates generated by TTL-technology allow for reversible staining and theoretically for multiple rounds of imaging. Additionally, current publications often use full-length antibodies for AOC generation due to the fact that most staining reagents rely on antibodies to confer specificity and are therefore often the only source of reagent available. As shown with the generation of ADCs, Tub-tag technology can likely be extended to generate oligonucleotide conjugates based on full-length antibodies and other smaller formats such as Fabs and scFvs. The technique might be suitable for screenings using AOCs e.g. in the context of cancer diagnostics and antigen detection, where many samples are screened with a standardized set of antibodies that can be sequences and generated in larger quantities. One major downside of the technique is that the antibody sequence must be known in order to genetically attach the Tub-tag to the C-terminus. This is impossible for most commercially available antibodies used in microscopy because their amino acid sequence is not publicly available, therefore limiting its usage for research groups that typically use only small quantities but a high variety of different antibodies. Although we used microscopy as a read-out to confirm the functionality of our conjugate, Tub-tag technology might be best employed for other areas of AOC research.

A major field of application for AOCs are therapeutic AOCs that leverage the main strength of oligonucleotides: Oligonucleotides can be readily customized, synthesized and chemical handles attached at the ends or via modified bases even within the sequence, allowing for the availability of virtually any sequence to be conjugated with a variety of chemical handles. While traditional ADCs using small molecule toxins have a highly limited set of commercially purchasable payloads with even fewer targets within the cell, the variability of oligonucleotides opens up the possibility of directly targeting RNA and DNA within the cell. As previously described, the usage of AOCs for siRNA delivery is an upcoming field of research. Tub-tag technology might provide a promising avenue to generate therapeutic AOCs with defined stoichiometry. In the case of full-length antibodies, the expected product would either be a DAR2 (if the Tub-tag is attached to either the light chain or the heavy chain) or a DAR4 (when attached to both). We can hypothesize that the fixed stoichiometry and site of attachment lead to similar benefits for the product as they do for small molecule ADCs: They provide a highly defined product with all antibodies having similar drug load and positioning. This prevents differential clearance of conjugates with different DARs and exposure of the oligonucleotide. Therefore, the behaviour of the product in mice or finally the patient is better predictable, leading to an overall safer use and improved therapeutic potential.

6.3 Pre-Clinical Evaluation of an αFlt3 ADC for the Treatment of AML

The development of therapeutic antibodies and ADCs has opened new avenues for patients in their combat with cancer. However, the highly intertwined role of antibodies in the immune system and the utilization of highly potent toxins pose – especially in combination – a major risk for the patient receiving the therapeutic drug. Any misdirection e.g. by off-target binding or early and unspecific release of the toxin can cause severe toxicities. Besides the strict requirements for safety, the development of an ADC also comes with high financial cost. Although more than two decades have passed since the first approval of an ADC, relatively few products have made it to the market to date, leaving many types of cancer without an ADC-treatment option. Thorough pre-clinical characterization is therefore of the utmost importance for increasing both the safety of the therapeutic and the chance of it passing clinical trials. The development process is therefore a highly collaborative one involving the expertise of people from multiple scientific fields, e.g. molecular biology for protein engineering, organic chemistry and biochemistry for conjugation methods and cellular biology and medicine for testing and evaluation.

In the case of AML, multiple antigens have either been identified as candidates or are used as targets for ADC therapy. These include the CD33[291] (the targeting of which has already been approved by the FDA and EMA with the therapeutic Gemtuzumab-ozagamycin), CLL-1[292] and CD123[293]. However, some of these targets, including CD33, are also expressed on healthy hematopoietic stem cells. Although Flt3 expression has been described in healthy cells as well, the expression on healthy cells is generally low and Flt3 is generally expressed in a wide variety of AML cells including cancer stem cells[294], rendering it an interesting target for therapy.

Thus, our aim was to use the Flt3-directed antibody 20D9 that has been investigated in a previous study as a chimeric rat/human ADC based on MMAF with promising results[295] and to develop a further humanized ADC for pre-clinical studies. As mentioned previously, this project involved the work and scientific input of multiple people across different scientific fields.

6.3.1 Physico-Chemical Evaluation of αFlt3 Antibody Candidates for Lead Selection

First, we set out for in-silico humanization of 20D9. Of the resulting humanized sequences, we succeeded in expressing and purifying a total of 12 out of 16 possible antibodies. Interestingly, the four antibodies that did not express all shared the same light chain with VK4, suggesting that the F84A mutation that occurs between VK3 and VK4 was not well tolerated. In addition, both chains also differ on position 2 with either having an isoleucine (VK3) or valine (VK4). However, the valine is also present in the rat 20D9 framework that was successfully expressed as a control, suggesting that the mutation at position 2 is not responsible for the failed expression. All humanized antibodies showed satisfactory expression levels with some even exceeding the expression yield of the original chimeric 20D9 antibody, suggesting that the humanization of the sequence provides an improved framework for expression in CHO cells. This finding is in line with previously reported results[296].

To select a lead candidate, the remaining 12 antibodies have been characterized by HPLC after induced thermal stress. To that end, we performed an accelerated aging assay by incubating protein aliquots for up to four weeks at 4 °C to 37 °C and analyzed the samples by SEC-HPLC. We did not observe an increase in aggregation by analyzing high molecular weight species even after four weeks of incubation at 37 °C. We therefore conclude that the antibody is stable for processing steps such as conjugation and storage at 4 °C, a trait which is necessary for therapeutic antibodies that need stability in storage from production to final application at the patient. While the environmental conditions in the body are vastly different from the storage conditions we have chosen, observing no aggregation at 37 °C – which corresponds to the normal core body temperature of humans – suggests that aggregation in the body is unlikely to be observed. While impractical for selection of a lead candidate due to the long delay, further studies should evaluate the extended shelf life of the antibody by extending storage conditions to multiple months, since slow degradation and aggregation kinetics cannot be excluded with our data.

Initial testing on recombinant human Flt3 protein and Ba/F3 Flt3-presenting cell lines revealed a clear grouping of all antibodies according to their light chain, suggesting that either for 20D9 the light chain plays a dominant role in antigen recognition, or that the mutations introduced in the VH domain in the humanization procedure do not alter its the binding properties. Based on these results, we selected antibody #3 as the lead candidate for further studies.

6.3.2 In-vitro Characterization of the αFlt3 ADC Lead Candidate

Off-target specificity would pose a knock-out criterion for ADC development. Binding to homologues not only poses the risk of adverse side effects in non-targeted cells but can also lead to faster depletion due to an overall higher uptake and increased availability of binding partners.

Fortunately, we did not observe any binding to cell-surface-presented homologues of Flt3. On the other side, binding to orthologues is a double-edged sword. While binding to an orthologue could indicate potential target promiscuity, these tested targets are not present in the human body and will not lead directly to unspecific uptake. In our case, we observed binding mainly to human Flt3 and – to a minor extend – also cynomolgus Flt3. Since those two species share about 97% sequence identity of the Flt3 protein, recognition of both proteins can be expected. Furthermore, recognition of cynomolgus Flt3 enables the possibility of performing pre-clinical studies in cynomolgus monkeys to assess potential adverse toxicities before initiating human trials. One important finding is that murine Flt3 was not recognized, enabling tumor clearance studies in mice without expectancy of major side effects. Additionally, we were able to show that antibody #3 bind via the constant domains to FcγRs on Ba/F3 cells, which has improved efficacy of the original chimeric ADC over sole targeting via Flt3[295]. Using flow cytometry and confocal microscopy, we could confirm that the antibody is internalized depending on the Flt3-expression level of the cells, which is a prerequisite for ADC development. Since we observed internalization after as little as one hour, the Flt3-antibody complex seems to have a high turnover despite the overall low expression level of Flt3, suggesting that the ADC can be quickly and efficiently internalized.

Since our aim was to develop an ADC capable of targeting cancer stem cells in order to prevent relapse, we aimed to select a toxin capable of targeting resting cells. Although some patients do not relapse after treatment with ADCs based on the commonly used microtubule inhibitors MMAE and MMAF, it is commonly thought that these toxins are overall less potent in resting cells. The reasoning behind this assumption is the critical role of the microtubule network during cell division, rendering dividing cells more susceptible to treatment than resting or slowly dividing cells. Other toxins such as the DNA alkylator duocarmycin are thought to be less biased towards dividing cells by introducing random DNA damage and thereby forcing even resting cells into apoptosis[297].

Thus, both toxins were used for the generation of ADCs and further characterized in comparison. In in-vitro assays, both ADCs were able to target Flt3 expressing cancer cell lines efficiently and specifically and induce apoptosis on Ba/F3 cells depending on the expression level of Flt3. This result suggests a high specificity and no significant uptake of ADC in Flt3-negative cell lines.

While established cancer cell lines provide an easy first read-out regarding the specificity and cytotoxic capacity of an ADC, many of these cell lines have been established decades ago and cannot represent the diversity of a tumor as found in a patient. PDX samples mimic the diversity of cancer cells much more closely and additionally contain slowly dividing progenitor cells that are phenotypically close to cancer stem cells. Therefore, we assessed the effectiveness of our ADCs in PDX samples. Using long-term culture-initiating cell and colony-forming unit assays, Marina Able determined the capacity of each ADC to kill cancer stem on PDX samples. In these experiments, strong differences between PDX samples were observed, confirming both that the ADC treatment is generally effective, but also that patient-specific characteristics of the cancer heavily influence the efficacy of the treatment.

Taken together, we were able to generate a humanized aFlt3 antibody with high stability and good expression yields, which are imperative for therapeutic and commercial development. We aimed to utilize this antibody as a platform for ADC development to target resting cells. We were able to show cytotoxicity in AML cell lines and PDX samples. Our results suggest that DUBA as an ADC payload is an overall superior choice for targeting cancer stem cells compared to commonly used MMAF. However, contrary to the common belief in the ADC field, MMAF was not generally ineffective for stem cell targeting. Treatment with MMAF-ADC also led to a decrease in progenitor cells, albeit usually at higher dosage, suggesting that MMAF can act against stem cells and treatment lead to sustained tumor suppression in the patient.

6.4 Outlook - Open Questions and Future Experiments

In this work, data covering different aspects of antibody and ADC development have been presented. We were able to establish a screening pipeline based on hybridoma technology and identify binders recognizing cell surface-presented antigen. The antibodies generated in this part of this work are of murine origin and have been partially chimerized. To determine whether these antibodies are suitable for therapeutic use, similar experiments must be performed as have been done on the αFlt3 antibody that was described in the latter part of this work. On the antibody itself, this includes improving the expression yield by sequence optimization on the DNA level as well as the expression system. While the expression yield does not influence the quality of the antibody or antibody derivative itself, a high yield ensures the economic viability of the product. Another important factor is the determination of antibody stability in solution. Chromatographic methods such as HPLC-SEC offer a convenient and mostly automated solution for determining protein aggregation. However, other methods such as dynamic light scattering, laser diffraction or fluorescence spectroscopy using dyes that bind to hydrophobic, hence unfolded patches of the protein could be utilized as well. There is currently no gold standard for determining protein aggregation and each method comes with its own set of limitations and strengths regarding sensitivity, the size of particles that can be measured or the complexity of data analysis. Regardless of the method used, a stable antibody with long shelf life will lead to a reduction in wasted product due to reaching the expiration date. On top of that, high stability and low aggregation lead to a safer product for the patient. Since ADCs rely on efficient internalization of the conjugate, internalization kinetics have to be assessed which can be done by microscopy, flow cytometry or experiments in plate-reader format when using pH-sensitive dyes. Lastly, lead candidates have to be selected for each antigen and used for generation of ADCs that can be tested *in vitro* and *in vivo* for cytotoxic activity. If an ADC shows promising results for further therapeutic development, the immunogenicity can be reduced by humanization. These changes in antibody sequence will need re-evaluation of the antibody to ensure no major alterations or unspecific binding has been introduced which in turn represented the starting point for the development of the humanized αFlt3 antibody 20D9 in the latter parts of this work.

The conjugation technique to generate AOCs described in this work has been shown to efficiently generate AOCs using fluorescence microscopy as a proof-of-concept. As discussed earlier, fluorescence microscopy provides a valuable readout to prove functionality of the conjugate, but our conjugation strategy is less suitable for smaller research laboratories that rely on commercially available antibodies and typically do not know the antibody sequence. However, the technique might be used for generation of therapeutic AOCs. Currently, most therapeutic AOCs are based on full-length antibodies. The higher molecular weight and slower reaction kinetics compared to nanobodies as well as the double stranded nature of siRNA would likely require optimization of the reaction conditions. Stability of AOCs can be determined in a similar fashion to classic ADCs e.g. chromatography or spectrometric methods. *In vitro* read-outs should include the determination of mRNA levels of at least the targeted transcript e.g. by real time PCR in addition to viability measurements, with special consideration to related mRNAs that might share similar sequences. A common obstacle AOCs are facing is the inefficient release of the large oligonucleotide from the lysosome into the cytosol. Co-treatment with inhibitors of lysosomal acidification such as chloroquine can improve lysosomal escape while also being already approved for other diseases and might be factually mandatory for efficient treatment with AOCs, especially in *in vivo* settings.

Lastly, we were able to develop a humanized ADC that is able to target slowly dividing cells, some open questions remain. Firstly, the DUBA-ADC showed poor stability in mouse plasma (private communication Marina Able, LMU and Marc-André Kasper, Tubulis GmbH), a finding which has already been reported by other groups[298]. Although this problem is specific to mouse and does not occur in human plasma, suggesting no concerns towards overall stability and safety of the ADC in humans, instability in mice complicates and adds artifacts to pre-clinical mouse studies. It has been shown that the site of attachment has a strong influence over the stability of the ADC[299], suggesting that a more stable variant of our DUBA-ADC can be generated by finding a more protected conjugation site, a requirement that is likely to be applied to all ADCs based on the duocarmycin payload class. Furthermore, we have shown that the antibody is capable of binding to FcγRs, suggesting a general ability of the ADC to act via secondary cytotoxic pathways such as ADCC, ADCP and CPC. However, to which extend these effects contribute to the overall cytotoxicity and which activation paths are primarily used in the case of 20D9#3 has not been studied in detail. These effects can be determined *in vitro* in co-cultivation assays using not only the antibody or ADC on Flt3-positive cells but adding effector cells such as natural killer cells or macrophages to determine improved cytotoxic effects. Additionally, the application of secondary pathways could be fine-tuned e.g. by afucosylation by genetic engineering of the antibody which has been shown to increase ADCC[300]. This would allow to a decrease in the DAR without sacrificing efficacy of the ADC, leading to further improvement in stability and pharmacokinetics. If these problems can be solved, *in vivo* studies in mice are necessary to evaluate the efficacy of the ADC in a living organism, which is a major milestone before starting official clinical trials.

While ADCs have come a long way from their inception to by today having established themselves as effective treatments for a variety of cancer types, patients still suffer from frequent relapse suggesting an incomplete clearance of the tumor in the initial treatment, bearing not only physical damage for patients that actually relapse, but also mental strain for patients in remission due to the possibility that a relapse might occur. It has become clear that sustained tumor suppression requires eradication of all tumor cells, especially tumor stem cells, regardless of their cellular state and characteristics. Our work here aimed to provide one more piece to the puzzle, how we can effectively generate ADCs to target cancer stem cells and ultimately enable treatments allowing for a cancer-free life after treatment.

7 Literature References

1 Bray, F., Laversanne, M., Weiderpass, E. & Soerjomataram, I. The ever-increasing importance of cancer as a leading cause of premature death worldwide. *Cancer* **127**, 3029-3030 (2021).
2 Heron, M. Deaths: Leading Causes for 2016. *National Vital Statistics Report* **67**, 1-77 (2018).
3 Bray, F. *et al.* Global cancer statistics 2018: GLOBOCAN estimates of incidence and mortality worldwide for 36 cancers in 185 countries. *CA: A Cancer Journal for Clinicians* **68**, 394-424 (2018).
4 Soerjomataram, I. & Bray, F. Planning for tomorrow: global cancer incidence and the role of prevention 2020–2070. *Nature Reviews Clinical Oncology* **18**, 663-672 (2021).
5 Sleeman, K. E. *et al.* The escalating global burden of serious health-related suffering: projections to 2060 by world regions, age groups, and health conditions. *The Lancet Global Health* **7**, e883-e892 (2019).
6 Cao, W., Chen, H.-D., Yu, Y.-W., Li, N. & Chen, W.-Q. Changing profiles of cancer burden worldwide and in China: a secondary analysis of the global cancer statistics 2020. *Chinese Medical Journal* **134**, 783-791 (2021).
7 Danaei, G., Vander Hoorn, S., Lopez, A. D., Murray, C. J. & Ezzati, M. Causes of cancer in the world: comparative risk assessment of nine behavioural and environmental risk factors. *The Lancet* **366**, 1784-1793 (2005).
8 Boffetta, P. *et al.* The causes of cancer in France. *Annals of Oncology* **20**, 550-555 (2009).
9 Blackadar, C. B. Historical review of the causes of cancer. *World Journal of Clinical Oncology* **7**, 54 (2016).
10 Singh, N. *et al.* Inflammation and cancer. *Annals of African Medicine* **18**, 121 (2019).
11 Moore, P. S. & Chang, Y. Why do viruses cause cancer? Highlights of the first century of human tumour virology. *Nature Reviews Cancer* **10**, 878-889 (2010).
12 Sun, Y. S. *et al.* Risk Factors and Preventions of Breast Cancer. *International Journal of Biological Sciences* **13**, 1387-1397 (2017).
13 Basu, A. K. DNA damage, mutagenesis and cancer. *International Journal of Molecular Sciences* **19**, 970 (2018).
14 Hanahan, D. & Weinberg, R. A. The Hallmarks of Cancer. *Cell* **100**, 57-70 (2000).
15 Hanahan, D. & Weinberg, Robert A. Hallmarks of Cancer: The Next Generation. *Cell* **144**, 646-674 (2011).
16 Hanahan, D. Hallmarks of Cancer: New Dimensions. *Cancer Discovery* **12**, 31 (2022).
17 Yates, L. R. & Campbell, P. J. Evolution of the cancer genome. *Nature Reviews Genetics* **13**, 795-806 (2012).
18 Black, J. R. & McGranahan, N. Genetic and non-genetic clonal diversity in cancer evolution. *Nature Reviews Cancer* **21**, 379-392 (2021).
19 DeVita Jr, V. T. & Chu, E. A history of cancer chemotherapy. *Cancer Research* **68**, 8643-8653 (2008).
20 Sudhakar, A. History of cancer, ancient and modern treatment methods. *Journal of Cancer Science & Therapy* **1**, 1 (2009).
21 Arruebo, M. *et al.* Assessment of the evolution of cancer treatment therapies. *Cancers* **3**, 3279-3330 (2011).
22 Marijnen, C. *et al.* Acute side effects and complications after short-term preoperative radiotherapy combined with total mesorectal excision in primary rectal cancer: report of a multicenter randomized trial. *Journal of Clinical Oncology* **20**, 817-825 (2002).
23 Berkey, F. J. Managing the adverse effects of radiation therapy. *American Family Physician* **82**, 381-388 (2010).
24 van den Boogaard, W. M., Komninos, D. S. & Vermeij, W. P. Chemotherapy side-effects: not all DNA damage is equal. *Cancers* **14**, 627 (2022).
25 Dua, P., Dua, V. & Pistikopoulos, E. N. Optimal delivery of chemotherapeutic agents in cancer. *Computers & Chemical Engineering* **32**, 99-107 (2008).

26 Miranda-Filho, A. *et al*. Epidemiological patterns of leukaemia in 184 countries: a population-based study. *The Lancet Haematology* **5**, e14-e24 (2018).
27 Paul, S., Kantarjian, H. & Jabbour, E. J. in *Mayo Clinic Proceedings*. 1645-1666 (Elsevier).
28 Jabbour, E., O'Brien, S., Konopleva, M. & Kantarjian, H. New insights into the pathophysiology and therapy of adult acute lymphoblastic leukemia. *Cancer* **121**, 2517-2528 (2015).
29 Arber, D. A. *et al*. The 2016 revision to the World Health Organization classification of myeloid neoplasms and acute leukemia. *Blood* **127**, 2391-2405 (2016).
30 Rowe, J. M. *et al*. Induction therapy for adults with acute lymphoblastic leukemia: results of more than 1500 patients from the international ALL trial: MRC UKALL XII/ECOG E2993. *Blood* **106**, 3760-3767 (2005).
31 Andersson, A. K. *et al*. The landscape of somatic mutations in infant MLL-rearranged acute lymphoblastic leukemias. *Nature Genetics* **47**, 330-337 (2015).
32 Meyer, C. *et al*. The MLL recombinome of acute leukemias in 2013. *Leukemia* **27**, 2165-2176 (2013).
33 Iacobucci, I. & Mullighan, C. G. Genetic basis of acute lymphoblastic leukemia. *Journal of Clinical Oncology* **35**, 975 (2017).
34 Brady, S. W. *et al*. The genomic landscape of pediatric acute lymphoblastic leukemia. *Nature Genetics* **54**, 1376-1389 (2022).
35 Narayanan, S. & Shami, P. J. Treatment of acute lymphoblastic leukemia in adults. *Critical Reviews in Oncology/Hematology* **81**, 94-102 (2012).
36 Terwilliger, T. & Abdul-Hay, M. Acute lymphoblastic leukemia: a comprehensive review and 2017 update. *Blood Cancer Journal* **7**, e577-e577 (2017).
37 Faderl, S. *et al*. Augmented hyper-CVAD based on dose-intensified vincristine, dexamethasone, and asparaginase in adult acute lymphoblastic leukemia salvage therapy. *Clinical Lymphoma Myeloma and Leukemia* **11**, 54-59 (2011).
38 Queudeville, M. & Ebinger, M. Blinatumomab in Pediatric Acute Lymphoblastic Leukemia—From Salvage to First Line Therapy (A Systematic Review). *Journal of Clinical Medicine* **10**, 2544 (2021).
39 Al-Salama, Z. T. Inotuzumab ozogamicin: a review in relapsed/refractory B-cell acute lymphoblastic leukaemia. *Targeted Oncology* **13**, 525-532 (2018).
40 Hwang, S. M. Classification of acute myeloid leukemia. *Blood Research* **55**, S1-S4 (2020).
41 Heath, E. *et al*. Biological and clinical consequences of NPM1 mutations in AML. *Leukemia* **31**, 798-807 (2017).
42 Rakheja, D., Konoplev, S., Medeiros, L. J. & Chen, W. IDH mutations in acute myeloid leukemia. *Human Pathology* **43**, 1541-1551 (2012).
43 Montalban-Bravo, G. & DiNardo, C. D. The role of IDH mutations in acute myeloid leukemia. *Future Oncology* **14**, 979-993 (2018).
44 Sandoval, J. E., Huang, Y.-H., Muise, A., Goodell, M. A. & Reich, N. O. Mutations in the DNMT3A DNA methyltransferase in acute myeloid leukemia patients cause both loss and gain of function and differential regulation by protein partners. *Journal of Biological Chemistry* **294**, 4898-4910 (2019).
45 Wong, K. K., Lawrie, C. H. & Green, T. M. Oncogenic roles and inhibitors of DNMT1, DNMT3A, and DNMT3B in acute myeloid leukaemia. *Biomarker Insights* **14** (2019).
46 Chiba, S. Dysregulation of TET2 in hematologic malignancies. *International Journal of Hematology* **105**, 17-22 (2017).
47 Bowman, R. L. & Levine, R. L. TET2 in normal and malignant hematopoiesis. *Cold Spring Harbor Perspectives in Medicine* **7** (2017).
48 Daver, N., Schlenk, R. F., Russell, N. H. & Levis, M. J. Targeting FLT3 mutations in AML: review of current knowledge and evidence. *Leukemia* **33**, 299-312 (2019).
49 Kikushige, Y. *et al*. Human Flt3 is expressed at the hematopoietic stem cell and the granulocyte/macrophage progenitor stages to maintain cell survival. *The Journal of Immunology* **180**, 7358-7367 (2008).

50 Griffith, J. *et al*. The structural basis for autoinhibition of FLT3 by the juxtamembrane domain. *Molecular Cell* **13**, 169-178 (2004).
51 Tse, K. F., Mukherjee, G. & Small, D. Constitutive activation of FLT3 stimulates multiple intracellular signal transducers and results in transformation. *Leukemia* **14**, 1766-1776 (2000).
52 Scholl, C., Gilliland, D. G. & Fröhling, S. Deregulation of signaling pathways in acute myeloid leukemia. *Semin Oncol* **35**, 336-345 (2008).
53 Breitenbuecher, F. *et al*. Identification of a novel type of ITD mutations located in nonjuxtamembrane domains of the FLT3 tyrosine kinase receptor. *Blood* **113**, 4074-4077 (2009).
54 Chung, K. Y. *et al*. Enforced expression of an Flt3 internal tandem duplication in human CD34+ cells confers properties of self-renewal and enhanced erythropoiesis. *Blood* **105**, 77-84 (2005).
55 Stubbins, R. J., Francis, A., Kuchenbauer, F. & Sanford, D. Management of acute myeloid leukemia: A review for general practitioners in oncology. *Current Oncology* **29**, 6245-6259 (2022).
56 Gardin, C. & Dombret, H. Hypomethylating agents as a therapy for AML. *Current Hematologic Malignancy Reports* **12**, 1-10 (2017).
57 Cruijsen, M., Lübbert, M., Wijermans, P. & Huls, G. Clinical results of hypomethylating agents in AML treatment. *Journal of Clinical Medicine* **4**, 1-17 (2014).
58 Grafone, T., Palmisano, M., Nicci, C. & Storti, S. An overview on the role of FLT3-tyrosine kinase receptor in acute myeloid leukemia: biology and treatment. *Oncology Reviews* **6**, e8 (2012).
59 Badar, T. *et al*. Improvement in clinical outcome of FLT3 ITD mutated acute myeloid leukemia patients over the last one and a half decade. *American Journal of Hematology* **90**, 1065-1070 (2015).
60 Oliva, E. N. *et al*. The real-world incidence of relapse in acute myeloid leukemia (AML): a systematic literature review (SLR). *Blood* **132**, 5188 (2018).
61 Thol, F. & Ganser, A. Treatment of relapsed acute myeloid leukemia. *Current Treatment Options in Oncology* **21**, 1-11 (2020).
62 Ding, L. *et al*. Clonal evolution in relapsed acute myeloid leukaemia revealed by whole-genome sequencing. *Nature* **481**, 506-510 (2012).
63 Strebhardt, K. & Ullrich, A. Paul Ehrlich's magic bullet concept: 100 years of progress. *Nature Reviews Cancer* **8**, 473-480 (2008).
64 Gronski, P., Seiler, F. & Schwick, H. Discovery of antitoxins and development of antibody preparations for clinical uses from 1890 to 1990. *Molecular Immunology* **28**, 1321-1332 (1991).
65 Yu, J., Song, Y. & Tian, W. How to select IgG subclasses in developing anti-tumor therapeutic antibodies. *J Hematol Oncol* **13**, 1-10 (2020).
66 Schroeder Jr, H. W. & Cavacini, L. Structure and function of immunoglobulins. *Journal of Allergy and Clinical Immunology* **125**, S41-S52 (2010).
67 Saito, S., Namisaki, H., Hiraishi, K., Takahashi, N. & Iida, S. A stable engineered human IgG3 antibody with decreased aggregation during antibody expression and low pH stress. *Protein Science* **28**, 900-909 (2019).
68 Bindon, C. I., Hale, G., Brüggemann, M. & Waldmann, H. Human monoclonal IgG isotypes differ in complement activating function at the level of C4 as well as C1q. *The Journal of Experimental Medicine* **168**, 127-142 (1988).
69 Stewart, R., Hammond, S. A., Oberst, M. & Wilkinson, R. W. The role of Fc gamma receptors in the activity of immunomodulatory antibodies for cancer. *J Immunother Cancer* **2**, 1-10 (2014).
70 De Taeye, S. W. *et al*. FcγR binding and ADCC activity of human IgG allotypes. *Frontiers in Immunology* **11**, 740 (2020).

71 Andersen, J. T. *et al.* Extending serum half-life of albumin by engineering neonatal Fc receptor (FcRn) binding. *Journal of Biological Chemistry* **289**, 13492-13502 (2014).
72 Stapleton, N. M. *et al.* Competition for FcRn-mediated transport gives rise to short half-life of human IgG3 and offers therapeutic potential. *Nature Communications* **2**, 599 (2011).
73 Köhler, G. & Milstein, C. Continuous cultures of fused cells secreting antibody of predefined specificity. *Nature* **256**, 495-497 (1975).
74 Zahavi, D. & Weiner, L. Monoclonal Antibodies in Cancer Therapy. *Antibodies* **9**, 34 (2020).
75 Patel, D. *et al.* Anti-epidermal growth factor receptor monoclonal antibody cetuximab inhibits EGFR/HER-2 heterodimerization and activation. *International Journal of Oncology* **34**, 25-32 (2009).
76 Cosimi, A. B. *et al.* Treatment of acute renal allograft rejection with OKT3 monoclonal antibody. *Transplantation* **32**, 535-539 (1981).
77 Sgro, C. Side-effects of a monoclonal antibody, muromonab CD3/orthoclone OKT3: bibliographic review. *Toxicology* **105**, 23-29 (1995).
78 Goldstein, G. *et al.* OKT3 monoclonal antibody plasma levels during therapy and the subsequent development of host antibodies to OKT3. *Transplantation* **42**, 507-510 (1986).
79 Khazaeli, M., Conry, R. M. & LoBuglio, A. F. Human immune response to monoclonal antibodies. *Journal of Immunotherapy* **15**, 42-52 (1994).
80 Badger, C. C., Anasetti, C., Davis, J. & Bernstein, I. D. Treatment of malignancy with unmodified antibody. *Survey and Synthesis of Pathology Research* **6**, 419-434 (1987).
81 Presta, L. G. Engineering of therapeutic antibodies to minimize immunogenicity and optimize function. *Advanced Drug Delivery Reviews* **58**, 640-656 (2006).
82 Jones, P. T., Dear, P. H., Foote, J., Neuberger, M. S. & Winter, G. Replacing the complementarity-determining regions in a human antibody with those from a mouse. *Nature* **321**, 522-525 (1986).
83 Liang, S. & Zhang, C. Prediction of immunogenicity for humanized and full human therapeutic antibodies. *PLoS One* **15**, e0238150 (2020).
84 Davis, T. A. *et al.* Rituximab anti-CD20 monoclonal antibody therapy in non-Hodgkin's lymphoma: safety and efficacy of re-treatment. *Journal of Clinical Oncology* **18**, 3135-3143 (2000).
85 Cruz, E. & Kayser, V. Monoclonal antibody therapy of solid tumors: clinical limitations and novel strategies to enhance treatment efficacy. *Biologics: Targets and Therapy*, 33-51 (2019).
86 Peterson, G. M. *et al.* Monoclonal antibody therapy in cancer: When two is better (and considerably more expensive) than one. *Journal of Clinical Pharmacy and Therapeutics* **43**, 925-930 (2018).
87 Marusyk, A. & Polyak, K. Tumor heterogeneity: causes and consequences. *Biochimica et Biophysica Acta (BBA)-Reviews on Cancer* **1805**, 105-117 (2010).
88 Loganzo, F., Sung, M. & Gerber, H.-P. Mechanisms of Resistance to Antibody–Drug Conjugates. *Molecular Cancer Therapeutics* **15**, 2825-2834 (2016).
89 Bäumer, S. *et al.* Antibody-Mediated Delivery of Anti–KRAS-siRNA In Vivo Overcomes Therapy Resistance in Colon Cancer. *Clinical Cancer Research* **21**, 1383-1394 (2015).
90 Collins, D. M., Bossenmaier, B., Kollmorgen, G. & Niederfellner, G. Acquired Resistance to Antibody-Drug Conjugates. *Cancers* **11**, 394 (2019).
91 Glassman, P. M., Abuqayyas, L. & Balthasar, J. P. Assessments of antibody biodistribution. *The Journal of Clinical Pharmacology* **55**, S29-S38 (2015).
92 Kholodenko, R. V., Kalinovsky, D. V., Doronin, I. I., Ponomarev, E. D. & Kholodenko, I. V. Antibody fragments as potential biopharmaceuticals for cancer therapy: success and limitations. *Current Medicinal Chemistry* **26**, 396-426 (2019).
93 Brinkmann, U. & Kontermann, R. E. The making of bispecific antibodies. *mAbs* **9**, 182-212 (2017).
94 Kontermann, R. E. & Brinkmann, U. Bispecific antibodies. *Drug Discovery Today* **20**, 838-847 (2015).

95 Stengl, A. *et al*. TuPPL: Tub-tag mediated C-terminal protein–protein-ligation using complementary click-chemistry handles. *Organic & Biomolecular Chemistry* **17**, 4964-4969 (2019).
96 Zhu, Z., Presta, L. G., Zapata, G. & Carter, P. Remodeling domain interfaces to enhance heterodimer formation. *Protein Science* **6**, 781-788 (1997).
97 Giese, G., Williams, A., Rodriguez, M. & Persson, J. Bispecific antibody process development: Assembly and purification of knob and hole bispecific antibodies. *Biotechnology Progress* **34**, 397-404 (2018).
98 Zeidler, R. *et al*. Simultaneous activation of T cells and accessory cells by a new class of intact bispecific antibody results in efficient tumor cell killing. *The Journal of Immunology* **163**, 1246-1252 (1999).
99 Krishnamurthy, A. & Jimeno, A. Bispecific antibodies for cancer therapy: A review. *Pharmacology & Therapeutics* **185**, 122-134 (2018).
100 Bazin-Redureau, M. I., Renard, C. B. & Scherrmann, J.-M. G. Pharmacokinetics of heterologous and homologous immunoglobulin G, F (ab ') 2 and Fab after intravenous administration in the rat. *Journal of Pharmacy and Pharmacology* **49**, 277-281 (1997).
101 Wahab, A. *et al*. Ocular toxicity of belantamab mafodotin, an oncological perspective of management in relapsed and refractory multiple myeloma. *Frontiers in Oncology*, 1690 (2021).
102 Kumagai, K. *et al*. Interstitial pneumonitis related to trastuzumab deruxtecan, a human epidermal growth factor receptor 2-targeting Ab–drug conjugate, in monkeys. *Cancer Science* **111**, 4636-4645 (2020).
103 Röthlisberger, D., Honegger, A. & Plückthun, A. Domain interactions in the Fab fragment: a comparative evaluation of the single-chain Fv and Fab format engineered with variable domains of different stability. *Journal of Molecular Biology* **347**, 773-789 (2005).
104 Muller, D. *et al*. Improved pharmacokinetics of recombinant bispecific antibody molecules by fusion to human serum albumin. *Journal of Biological Chemistry* **282**, 12650-12660 (2007).
105 Schreiber, S. Certolizumab pegol for the treatment of Crohn's disease. *Therapeutic Advances in Gastroenterology* **4**, 375-389 (2011).
106 Usta, C., Turgut, N. T. & Bedel, A. How abciximab might be clinically useful. *International Journal of Cardiology* **222**, 1074-1078 (2016).
107 Chong, V. Ranibizumab for the treatment of wet AMD: a summary of real-world studies. *Eye* **30**, 270-286 (2016).
108 Melmed, G. Y., Targan, S. R., Yasothan, U., Hanicq, D. & Kirkpatrick, P. Certolizumab pegol. *Nature Reviews Drug Discovery* **7** (2008).
109 Burness, C. B. Idarucizumab: first global approval. *Drugs* **75**, 2155-2161 (2015).
110 Chauhan, S. C. *et al*. Pharmacokinetics and biodistribution of 177 Lu-labeled multivalent single-chain Fv construct of the pancarcinoma monoclonal antibody CC49. *European Journal of Nuclear Medicine and Molecular Imaging* **32**, 264-273 (2005).
111 Jee, P. F. *et al*. Insertion of single-chain variable fragment (scFv) peptide linker improves surface display of influenza hemagglutinin (HA1) on non-recombinant Lactococcus lactis. *Biotechnology Progress* **33**, 154-162 (2017).
112 Wen, D., Foley, S. F., Hronowski, X. L., Gu, S. & Meier, W. Discovery and investigation of O-xylosylation in engineered proteins containing a (GGGGS) n linker. *Anal Chem* **85**, 4805-4812 (2013).
113 Kortt, A. A., Dolezal, O., Power, B. E. & Hudson, P. J. Dimeric and trimeric antibodies: high avidity scFvs for cancer targeting. *Biomolecular Engineering* **18**, 95-108 (2001).
114 Le Gall, F., Reusch, U., Little, M. & Kipriyanov, S. M. Effect of linker sequences between the antibody variable domains on the formation, stability and biological activity of a bispecific tandem diabody. *Protein Engineering Design and Selection* **17**, 357-366 (2004).
115 Muñoz-López, P. *et al*. Single-chain fragment variable: recent Progress in cancer diagnosis and therapy. *Cancers* **14**, 4206 (2022).

116 Wu, Y., Jiang, S. & Ying, T. From therapeutic antibodies to chimeric antigen receptors (CARs): making better CARs based on antigen-binding domain. *Expert Opinion on Biological Therapy* **16**, 1469-1478 (2016).
117 Zhao, J., Song, Y. & Liu, D. Recent advances on blinatumomab for acute lymphoblastic leukemia. *Experimental Hematology & Oncology* **8**, 1-8 (2019).
118 Damato, B. E., Dukes, J., Goodall, H. & Carvajal, R. D. Tebentafusp: T cell redirection for the treatment of metastatic uveal melanoma. *Cancers* **11**, 971 (2019).
119 Hamers-Casterman, C. *et al*. Naturally occurring antibodies devoid of light chains. *Nature* **363**, 446-448 (1993).
120 Muyldermans, S. Nanobodies: natural single-domain antibodies. *Annual Review of Biochemistry* **82**, 775-797 (2013).
121 Ackaert, C. *et al*. Immunogenicity risk profile of nanobodies. *Frontiers in Immunology* **12**, 578 (2021).
122 Ramon, A. *et al*. Assessing antibody and nanobody nativeness for hit selection and humanization with AbNatiV. *Nature Machine Intelligence* **6**, 74-91 (2024).
123 Könning, D. *et al*. Camelid and shark single domain antibodies: structural features and therapeutic potential. *Current Opinion in Structural Biology* **45**, 10-16 (2017).
124 Zavrtanik, U., Lukan, J., Loris, R., Lah, J. & Hadži, S. Structural basis of epitope recognition by heavy-chain camelid antibodies. *Journal of Molecular Biology* **430**, 4369-4386 (2018).
125 Tanaka, Y. Ozoralizumab: First nanobody® therapeutic for rheumatoid arthritis. *Expert Opinion on Biological Therapy* **23**, 579-587 (2023).
126 Zhang, F. *et al*. Structural basis of a novel PD-L1 nanobody for immune checkpoint blockade. *Cell Discovery* **3**, 1-12 (2017).
127 Homayouni, V. *et al*. Preparation and characterization of a novel nanobody against T-cell immunoglobulin and mucin-3 (TIM-3). *Iranian Journal of Basic Medical Sciences* **19**, 1201 (2016).
128 Harwood, S. L. *et al*. ATTACK, a novel bispecific T cell-recruiting antibody with trivalent EGFR binding and monovalent CD3 binding for cancer immunotherapy. *Oncoimmunology* **7**, e1377874 (2018).
129 Mølgaard, K. *et al*. Bispecific light T-cell engagers for gene-based immunotherapy of epidermal growth factor receptor (EGFR)-positive malignancies. *Cancer Immunology, Immunotherapy* **67**, 1251-1260 (2018).
130 Matsuda, Y. & Mendelsohn, B. A. Recent Advances in Drug–Antibody Ratio Determination of Antibody–Drug Conjugates. *Chemical and Pharmaceutical Bulletin* **69**, 976-983 (2021).
131 Wagh, A., Song, H., Zeng, M., Tao, L. & Das, T. K. Challenges and new frontiers in analytical characterization of antibody-drug conjugates. *mAbs* **10**, 222-243 (2018).
132 Strop, P. *et al*. Site-specific conjugation improves therapeutic index of antibody drug conjugates with high drug loading. *Nature Biotechnology* **33**, 694-696 (2015).
133 Strop, P. *et al*. Location Matters: Site of Conjugation Modulates Stability and Pharmacokinetics of Antibody Drug Conjugates. *Chemistry & Biology* **20**, 161-167 (2013).
134 Hermanson, G. T. *Bioconjugate Techniques*. 3. ed. edn, (Acad. Press, 2013).
135 Anderson, G. W., Zimmerman, J. E. & Callahan, F. M. The use of esters of N-hydroxysuccinimide in peptide synthesis. *J Am Chem Soc* **86**, 1839-1842 (1964).
136 Tantipanjaporn, A. & Wong, M. K. Development and Recent Advances in Lysine and N-Terminal Bioconjugation for Peptides and Proteins. *Molecules* **28** (2023).
137 Apel, C., Kasper, M.-A., Stieger, C. E., Hackenberger, C. P. & Christmann, M. Protein modification of lysine with 2-(2-styrylcyclopropyl) ethanal. *Organic Letters* **21**, 10043-10047 (2019).
138 Yi, S., Wei, S., Wu, Q., Wang, H. & Yao, Z. J. Azaphilones as Activation-Free Primary-Amine-Specific Bioconjugation Reagents for Peptides, Proteins and Lipids. *Angewandte Chemie International Edition* **61**, e202111783 (2022).
139 Diethelm, S., Schafroth, M. A. & Carreira, E. M. Amine-selective bioconjugation using arene diazonium salts. *Organic Letters* **16**, 3908-3911 (2014).

140 Ravasco, J. M., Faustino, H., Trindade, A. & Gois, P. M. Bioconjugation with maleimides: a useful tool for chemical biology. *Chemistry–A European Journal* **25**, 43-59 (2019).
141 Alley, S. C. *et al*. Contribution of linker stability to the activities of anticancer immunoconjugates. *Bioconjugate Chemistry* **19**, 759-765 (2008).
142 Fontaine, S. D., Reid, R., Robinson, L., Ashley, G. W. & Santi, D. V. Long-term stabilization of maleimide–thiol conjugates. *Bioconjugate Chemistry* **26**, 145-152 (2015).
143 Baldwin, A. D. & Kiick, K. L. Tunable Degradation of Maleimide–Thiol Adducts in Reducing Environments. *Bioconjugate Chemistry* **22**, 1946-1953 (2011).
144 Kasper, M.-A. *et al*. Ethynylphosphonamidates for the Rapid and Cysteine-Selective Generation of Efficacious Antibody–Drug Conjugates. *Angewandte Chemie International Edition* **58**, 11631-11636 (2019).
145 Christie, R. J. *et al*. Stabilization of cysteine-linked antibody drug conjugates with N-aryl maleimides. *Journal of Controlled Release* **220**, 660-670 (2015).
146 Christie, R. J. *et al*. Pyrrolobenzodiazepine Antibody-Drug Conjugates Designed for Stable Thiol Conjugation. *Antibodies* **6**, 20 (2017).
147 Kasper, M.-A. *et al*. Cysteine-Selective Phosphonamidate Electrophiles for Modular Protein Bioconjugations. *Angewandte Chemie International Edition* **58**, 11625-11630 (2019).
148 Ochtrop, P. & Hackenberger, C. P. R. Recent advances of thiol-selective bioconjugation reactions. *Current Opinion in Chemical Biology* **58**, 28-36 (2020).
149 Huang, R. *et al*. N-Methyl-N-phenylvinylsulfonamides for Cysteine-Selective Conjugation. *Organic Letters* **20**, 6526-6529 (2018).
150 Junutula, J. R. *et al*. Site-specific conjugation of a cytotoxic drug to an antibody improves the therapeutic index. *Nature Biotechnology* **26**, 925-932 (2008).
151 Tumey, L. N. *et al*. Site Selection: a Case Study in the Identification of Optimal Cysteine Engineered Antibody Drug Conjugates. *The AAPS Journal* **19**, 1123-1135 (2017).
152 Shinmi, D. *et al*. One-Step Conjugation Method for Site-Specific Antibody–Drug Conjugates through Reactive Cysteine-Engineered Antibodies. *Bioconjugate Chemistry* **27**, 1324-1331 (2016).
153 Patterson, J. T., Asano, S., Li, X., Rader, C. & Barbas III, C. F. Improving the serum stability of site-specific antibody conjugates with sulfone linkers. *Bioconjugate Chemistry* **25**, 1402-1407 (2014).
154 Bhakta, S., Raab, H. & Junutula, J. R. Engineering THIOMABs for site-specific conjugation of thiol-reactive linkers. *Antibody-Drug Conjugates*, 189-203 (2013).
155 Vollmar, B. S. *et al*. Attachment site cysteine thiol p K a is a key driver for site-dependent stability of THIOMAB antibody–drug conjugates. *Bioconjugate Chemistry* **28**, 2538-2548 (2017).
156 Bruins, J. J. *et al*. Non-Genetic Generation of Antibody Conjugates Based on Chemoenzymatic Tyrosine Click Chemistry. *Bioconjugate Chemistry* **32**, 2167-2172 (2021).
157 Bruins, J. J. *et al*. Inducible, Site-Specific Protein Labeling by Tyrosine Oxidation-Strain-Promoted (4 + 2) Cycloaddition. *Bioconjugate Chemistry* **28**, 1189-1193 (2017).
158 Chapman-Smith, A. & Cronan, J. E. The enzymatic biotinylation of proteins: a post-translational modification of exceptional specificity. *Trends in Biochemical Sciences* **24**, 359-363 (1999).
159 Kay, B. K., Thai, S. & Volgina, V. V. High-throughput biotinylation of proteins. *High Throughput Protein Expression and Purification: Methods and Protocols*, 185-198 (2009).
160 Samavarchi-Tehrani, P., Samson, R. & Gingras, A.-C. Proximity dependent biotinylation: key enzymes and adaptation to proteomics approaches. *Molecular & Cellular Proteomics* **19**, 757-773 (2020).
161 Altman, J. D. & Davis, M. M. MHC-peptide tetramers to visualize antigen-specific T cells. *Current Protocols in Immunology* **115**, 17.13. 11-17.13. 44 (2016).

162 Dickgiesser, S., Deweid, L., Kellner, R., Kolmar, H. & Rasche, N. Site-Specific Antibody-Drug Conjugation Using Microbial Transglutaminase. *Methods in Molecular Biology* **2012**, 135-149 (2019).

163 Jeger, S. *et al.* Site-Specific and Stoichiometric Modification of Antibodies by Bacterial Transglutaminase. *Angewandte Chemie International Edition* **49**, 9995-9997 (2010).

164 Dennler, P. *et al.* Transglutaminase-Based Chemo-Enzymatic Conjugation Approach Yields Homogeneous Antibody–Drug Conjugates. *Bioconjugate Chemistry* **25**, 569-578 (2014).

165 Mao, H., Hart, S. A., Schink, A. & Pollok, B. A. Sortase-mediated protein ligation: a new method for protein engineering. *J Am Chem Soc* **126**, 2670-2671 (2004).

166 Stefan, N. *et al.* Highly Potent, Anthracycline-based Antibody–Drug Conjugates Generated by Enzymatic, Site-specific Conjugation. *Molecular Cancer Therapeutics* **16**, 879-892 (2017).

167 Beerli, R. R., Hell, T., Merkel, A. S. & Grawunder, U. Sortase Enzyme-Mediated Generation of Site-Specifically Conjugated Antibody Drug Conjugates with High In Vitro and In Vivo Potency. *PLOS ONE* **10**, e0131177 (2015).

168 Gébleux, R., Briendl, M., Grawunder, U. & Beerli, R. R. Sortase A Enzyme-Mediated Generation of Site-Specifically Conjugated Antibody-Drug Conjugates. *Methods in Molecular Biology* **2012**, 1-13 (2019).

169 Pan, L. *et al.* Sortase A-Generated Highly Potent Anti-CD20-MMAE Conjugates for Efficient Elimination of B-Lineage Lymphomas. *Small* **13**, 1602267 (2017).

170 Ou, C. *et al.* One-Pot Conversion of Free Sialoglycans to Functionalized Glycan Oxazolines and Efficient Synthesis of Homogeneous Antibody–Drug Conjugates through Site-Specific Chemoenzymatic Glycan Remodeling. *Bioconjugate Chemistry* **32**, 1888-1897 (2021).

171 Zhu, Z. *et al.* Site-specific antibody-drug conjugation through an engineered glycotransferase and a chemically reactive sugar. *mAbs* **6**, 1190-1200 (2014).

172 van Geel, R. *et al.* Chemoenzymatic Conjugation of Toxic Payloads to the Globally Conserved N-Glycan of Native mAbs Provides Homogeneous and Highly Efficacious Antibody–Drug Conjugates. *Bioconjugate Chemistry* **26**, 2233-2242 (2015).

173 Wolf, B. *et al.* Therapeutic antibody glycosylation impacts antigen recognition and immunogenicity. *Immunology* **166**, 380-407 (2022).

174 Zhou, Q. & Qiu, H. The mechanistic impact of N-glycosylation on stability, pharmacokinetics, and immunogenicity of therapeutic proteins. *Journal of Pharmaceutical Sciences* **108**, 1366-1377 (2019).

175 Schumacher, D. *et al.* Versatile and efficient site-specific protein functionalization by tubulin tyrosine ligase. *Angewandte Chemie International Edition* **54**, 13787-13791 (2015).

176 Schumacher, D., Hackenberger, C. P., Leonhardt, H. & Helma, J. Current Status: Site-Specific Antibody Drug Conjugates. *Journal of Clinical Immunology* **36 Suppl 1**, 100-107 (2016).

177 Schwach, J. *et al.* Site-Specific Antibody Fragment Conjugates for Reversible Staining in Fluorescence Microscopy. *ChemBioChem* **22**, 1205-1209 (2021).

178 Schumacher, D. *et al.* Broad substrate tolerance of tubulin tyrosine ligase enables one-step site-specific enzymatic protein labeling. *Chemical Science* **8**, 3471-3478 (2017).

179 Schwach, J., Abdellatif, M. & Stengl, A. More than Toxins—Current Prospects in Designing the Next Generation of Antibody Drug Conjugates. *Frontiers in Bioscience-Landmark* **27**, 240 (2022).

180 Erickson, H. K. *et al.* Antibody-Maytansinoid Conjugates Are Activated in Targeted Cancer Cells by Lysosomal Degradation and Linker-Dependent Intracellular Processing. *Cancer Research* **66**, 4426-4433 (2006).

181 Lu, J., Jiang, F., Lu, A. & Zhang, G. Linkers Having a Crucial Role in Antibody–Drug Conjugates. *International Journal of Molecular Sciences* **17**, 561 (2016).

182 Naito, K. *et al*. Calicheamicin-conjugated humanized anti-CD33 monoclonal antibody (gemtuzumab zogamicin, CMA-676) shows cytocidal effect on CD33-positive leukemia cell lines, but is inactive on P-glycoprotein-expressing sublines. *Leukemia* **14**, 1436-1443 (2000).
183 DiJoseph, J. F. *et al*. Antibody-targeted chemotherapy with CMC-544: a CD22-targeted immunoconjugate of calicheamicin for the treatment of B-lymphoid malignancies. *Blood* **103**, 1807-1814 (2004).
184 Jain, N., Smith, S. W., Ghone, S. & Tomczuk, B. Current ADC linker chemistry. *Pharmaceutical Research* **32**, 3526-3540 (2015).
185 Bhattacharyya, B. & Wolff, J. Maytansine binding to the vinblastine sites of tubulin. *FEBS Letters* **75**, 159-162 (1977).
186 Sasse, F., Sieinmetz, H., Heil, J., Hoefle, G. & Reichenbach, H. Tubulysins, new cytostatic peptides from myxobacteria acting on microtubuli production, isolation, physico-chemical and biological properties. *The Journal of Antibiotics* **53**, 879-885 (2000).
187 Akhmanova, A. & Steinmetz, M. O. Control of microtubule organization and dynamics: two ends in the limelight. *Nature Reviews Molecular Cell Biology* **16**, 711-726 (2015).
188 Marcucci, F., Caserta, C. A., Romeo, E. & Rumio, C. Antibody-Drug Conjugates (ADC) Against Cancer Stem-Like Cells (CSC)—Is There Still Room for Optimism? *Frontiers in Oncology* **9** (2019).
189 Jiang, Y.-P. *et al*. CLT030, a leukemic stem cell–targeting CLL1 antibody-drug conjugate for treatment of acute myeloid leukemia. *Blood Advances* **2**, 1738-1749 (2018).
190 Garber, K. Cancer stem cell pipeline flounders. *Nature Reviews Drug Discovery* **17**, 771-773 (2018).
191 Masuda, S., Miyagawa, S., Sougawa, N. & Sawa, Y. CD30-targeting immunoconjugates and bystander effects. *Nature Reviews Clinical Oncology* **12**, 245-245 (2015).
192 Khera, E. & Thurber, G. M. Pharmacokinetic and Immunological Considerations for Expanding the Therapeutic Window of Next-Generation Antibody–Drug Conjugates. *BioDrugs* **32**, 465-480 (2018).
193 Ogitani, Y., Hagihara, K., Oitate, M., Naito, H. & Agatsuma, T. Bystander killing effect of DS-8201a, a novel anti-human epidermal growth factor receptor 2 antibody–drug conjugate, in tumors with human epidermal growth factor receptor 2 heterogeneity. *Cancer Science* **107**, 1039-1046 (2016).
194 Jaffry, M., Choudhry, H., Aftab, O. M. & Dastjerdi, M. H. Antibody-Drug Conjugates and Ocular Toxicity. *Journal of Ocular Pharmacology and Therapeutics* **39**, 675-691 (2023).
195 Domínguez-Llamas, S. *et al*. Adverse events of antibody–drug conjugates on the ocular surface in cancer therapy. *Clinical and Translational Oncology* **25**, 3086-3100 (2023).
196 Hamblett, K. J. *et al*. Effects of Drug Loading on the Antitumor Activity of a Monoclonal Antibody Drug Conjugate. *Clinical Cancer Research* **10**, 7063-7070 (2004).
197 Sun, X. *et al*. Effects of Drug–Antibody Ratio on Pharmacokinetics, Biodistribution, Efficacy, and Tolerability of Antibody–Maytansinoid Conjugates. *Bioconjugate Chemistry* **28**, 1371-1381 (2017).
198 Lin, A. Y. & Dinner, S. N. Moxetumomab pasudotox for hairy cell leukemia: preclinical development to FDA approval. *Blood Advances* **3**, 2905-2910 (2019).
199 Gholami, A., Minai-Tehrani, D., Mahdizadeh, S. J., Saenz-Mendez, P. & Eriksson, L. A. Structural Insights into Pseudomonas aeruginosa Exotoxin A–Elongation Factor 2 Interactions: A Molecular Dynamics Study. *Journal of Chemical Information and Modeling* **63**, 1578-1591 (2023).
200 Shapira, A. & Benhar, I. Toxin-based Therapeutic Approaches. *Toxins* **2**, 2519-2583 (2010).
201 Hansen, J. K. *et al*. A recombinant immunotoxin targeting CD22 with low immunogenicity, low nonspecific toxicity, and high antitumor activity in mice. *Journal of Immunotherapy* **33**, 297 (2010).
202 Mazor, R. & Pastan, I. Immunogenicity of Immunotoxins Containing Pseudomonas Exotoxin A: Causes, Consequences, and Mitigation. *Frontiers in Immunology* **11** (2020).

203 Di Paolo, C. *et al.* A recombinant immunotoxin derived from a humanized epithelial cell adhesion molecule-specific single-chain antibody fragment has potent and selective antitumor activity. *Clinical Cancer Research* **9**, 2837-2848 (2003).
204 O'Donnell, M. *et al.* MP16-03 phase 3 study of vicineum in Bgc-Unresponsive Non-Muscle invasive bladder cancer: 24-Month results. *Journal of Urology* **206**, e296-e297 (2021).
205 Vallera, D. A. *et al.* A Bispecific Recombinant Immunotoxin, DT2219, Targeting Human CD19 and CD22 Receptors in a Mouse Xenograft Model of B-Cell Leukemia/Lymphoma. *Clinical Cancer Research* **11**, 3879-3888 (2005).
206 Bachanova, V. *et al.* Phase I study of a bispecific ligand-directed toxin targeting CD22 and CD19 (DT2219) for refractory B-cell malignancies. *Clinical Cancer Research* **21**, 1267-1272 (2015).
207 Stish, B. J., Chen, H., Shu, Y., Panoskaltsis-Mortari, A. & Vallera, D. A. Increasing anticarcinoma activity of an anti-erbB2 recombinant immunotoxin by the addition of an anti-EpCAM sFv. *Clinical Cancer Research* **13**, 3058-3067 (2007).
208 Zhang, F. *et al.* An anti-PSMA bivalent immunotoxin exhibits specificity and efficacy for prostate cancer imaging and therapy. *Advanced Healthcare Materials* **2**, 736-744 (2013).
209 Meng, J. *et al.* A bivalent recombinant immunotoxin with high potency against tumors with EGFR and EGFRvIII expression. *Cancer Biology & Therapy* **16**, 1764-1774 (2015).
210 Yokoo, H., Naito, M. & Demizu, Y. Investigating the cell permeability of proteolysis-targeting chimeras (PROTACs). *Expert Opinion on Drug Discovery* **18**, 357-361 (2023).
211 Benowitz, A. B., Scott-Stevens, P. T. & Harling, J. D. Challenges and opportunities for in vivo PROTAC delivery. *Future Medicinal Chemistry* **14**, 119-121 (2022).
212 Satija, Y. K., Bhardwaj, A. & Das, S. A portrayal of E3 ubiquitin ligases and deubiquitylases in cancer. *International Journal of Cancer* **133**, 2759-2768 (2013).
213 Liu, J. *et al.* E3 ubiquitin ligase TRIM32 negatively regulates tumor suppressor p53 to promote tumorigenesis. *Cell Death & Differentiation* **21**, 1792-1804 (2014).
214 Rodriguez-Gonzalez, A. *et al.* Targeting steroid hormone receptors for ubiquitination and degradation in breast and prostate cancer. *Oncogene* **27**, 7201-7211 (2008).
215 Han, X. *et al.* Discovery of Highly Potent and Efficient PROTAC Degraders of Androgen Receptor (AR) by Employing Weak Binding Affinity VHL E3 Ligase Ligands. *Journal of Medicinal Chemistry* **62**, 11218-11231 (2019).
216 Bond, M. J., Chu, L., Nalawansha, D. A., Li, K. & Crews, C. M. Targeted Degradation of Oncogenic KRASG12C by VHL-Recruiting PROTACs. *ACS Central Science* **6**, 1367-1375 (2020).
217 Bai, N. *et al.* Modeling the CRL4A ligase complex to predict target protein ubiquitination induced by cereblon-recruiting PROTACs. *Journal of Biological Chemistry*, 101653 (2022).
218 Gasic, I. *et al.* Tubulin resists degradation by cereblon-recruiting PROTACs. *Cells* **9**, 1083 (2020).
219 Maneiro, M. a. *et al.* Antibody–PROTAC Conjugates Enable HER2-Dependent Targeted Protein Degradation of BRD4. *ACS Chemical Biology* **15**, 1306-1312 (2020).
220 Chan, K. *et al.* Antibody-proteolysis targeting chimera conjugate enables selective degradation of receptor-interacting serine/threonine-protein kinase 2 in HER2+ cell lines. *Bioconjugate Chemistry* **34**, 2049-2054 (2023).
221 Dragovich, P. S. *et al.* Antibody-Mediated Delivery of Chimeric BRD4 Degraders. Part 1: Exploration of Antibody Linker, Payload Loading, and Payload Molecular Properties. *Journal of Medicinal Chemistry* **64**, 2534-2575 (2021).
222 Dragovich, P. S. *et al.* Antibody-Mediated Delivery of Chimeric BRD4 Degraders. Part 2: Improvement of In Vitro Antiproliferation Activity and In Vivo Antitumor Efficacy. *Journal of Medicinal Chemistry* **64**, 2576-2607 (2021).
223 Dragovich, P. S. *et al.* Antibody-mediated delivery of chimeric protein degraders which target estrogen receptor alpha (ERα). *Bioorg Med Chem Lett* **30**, 126907 (2020).
224 Conlon, K. C., Miljkovic, M. D. & Waldmann, T. A. Cytokines in the treatment of cancer. *Journal of Interferon & Cytokine Research* **39**, 6-21 (2019).

225 Sleijfer, S., Bannink, M., Van Gool, A. R., Kruit, W. H. & Stoter, G. Side effects of interferon-α therapy. *Pharmacy World and Science* **27**, 423-431 (2005).
226 Lee, S. & Margolin, K. Cytokines in cancer immunotherapy. *Cancers* **3**, 3856-3893 (2011).
227 Fercher, C., Keshvari, S., McGuckin, M. A. & Barnard, R. T. Evolution of the magic bullet: Single chain antibody fragments for the targeted delivery of immunomodulatory proteins. *Experimental Biology and Medicine* **243**, 166-183 (2018).
228 Suzuki, K. *et al.* Adenovirus-mediated gene transfer of interferon α improves dimethylnitrosamine-induced liver cirrhosis in rat model. *Gene Therapy* **10**, 765-773 (2003).
229 He, Y. *et al.* Tumor-associated extracellular matrix: how to be a potential aide to anti-tumor immunotherapy? *Frontiers in Cell and Developmental Biology* **9**, 739161 (2021).
230 Huang, J. *et al.* Extracellular matrix and its therapeutic potential for cancer treatment. *Signal Transduction and Targeted Therapy* **6**, 153 (2021).
231 Gillies, S. D. *et al.* A low-toxicity IL-2–based immunocytokine retains antitumor activity despite its high degree of IL-2 receptor selectivity. *Clinical Cancer Research* **17**, 3673-3685 (2011).
232 Gillies, S. D. *et al.* An anti-CD20–IL-2 immunocytokine is highly efficacious in a SCID mouse model of established human B lymphoma. *Blood* **105**, 3972-3978 (2005).
233 Connor, J. P. *et al.* A phase 1b study of humanized KS-interleukin-2 (huKS-IL2) immunocytokine with cyclophosphamide in patients with EpCAM-positive advanced solid tumors. *BMC Cancer* **13**, 20-20 (2013).
234 Halin, C. *et al.* Synergistic therapeutic effects of a tumor targeting antibody fragment, fused to interleukin 12 and to tumor necrosis factor α. *Cancer Research* **63**, 3202-3210 (2003).
235 Gafner, V., Trachsel, E. & Neri, D. An engineered antibody–interleukin-12 fusion protein with enhanced tumor vascular targeting properties. *International Journal of Cancer* **119**, 2205-2212 (2006).
236 Kaspar, M., Trachsel, E. & Neri, D. The antibody-mediated targeted delivery of interleukin-15 and GM-CSF to the tumor neovasculature inhibits tumor growth and metastasis. *Cancer Research* **67**, 4940-4948 (2007).
237 Ebbinghaus, C. *et al.* Engineered vascular-targeting antibody-interferon-γ fusion protein for cancer therapy. *International Journal of Cancer* **116**, 304-313 (2005).
238 Roberts, T. C., Langer, R. & Wood, M. J. Advances in oligonucleotide drug delivery. *Nature Reviews Drug Discovery* **19**, 673-694 (2020).
239 Mullard, A. Antibody-oligonucleotide conjugates enter the clinic. *Nature Reviews Drug Discovery* **21**, 6-8 (2022).
240 Geary, R. S., Norris, D., Yu, R. & Bennett, C. F. Pharmacokinetics, biodistribution and cell uptake of antisense oligonucleotides. *Advanced Drug Delivery Reviews* **87**, 46-51 (2015).
241 Park, J., Park, J., Pei, Y., Xu, J. & Yeo, Y. Pharmacokinetics and biodistribution of recently-developed siRNA nanomedicines. *Advanced Drug Delivery Reviews* **104**, 93-109 (2016).
242 Nakase, I., Kobayashi, S. & Futaki, S. Endosome-disruptive peptides for improving cytosolic delivery of bioactive macromolecules. *Peptide Science* **94**, 763-770 (2010).
243 Ye, J. *et al.* High-Yield Synthesis of Monomeric LMWP(CPP)-siRNA Covalent Conjugate for Effective Cytosolic Delivery of siRNA. *Theranostics* **7**, 2495-2508 (2017).
244 Smith, S. A., Selby, L. I., Johnston, A. P. R. & Such, G. K. The Endosomal Escape of Nanoparticles: Toward More Efficient Cellular Delivery. *Bioconjugate Chemistry* **30**, 263-272 (2019).
245 Varkouhi, A. K., Scholte, M., Storm, G. & Haisma, H. J. Endosomal escape pathways for delivery of biologicals. *Journal of Controlled Release* **151**, 220-228 (2011).
246 Gong, H. *et al.* Simple Method To Prepare Oligonucleotide-Conjugated Antibodies and Its Application in Multiplex Protein Detection in Single Cells. *Bioconjugate Chemistry* **27**, 217-225 (2016).

247 Satake, N. *et al.* Novel Targeted Therapy for Precursor B-Cell Acute Lymphoblastic Leukemia: Anti-CD22 Antibody-MXD3 Antisense Oligonucleotide Conjugate. *Molecular Medicine* **22**, 632-642 (2016).
248 Cuellar, T. L. *et al.* Systematic evaluation of antibody-mediated siRNA delivery using an industrial platform of THIOMAB–siRNA conjugates. *Nucleic Acids Res* **43**, 1189-1203 (2015).
249 Lu, H. *et al.* Site-specific antibody-polymer conjugates for siRNA delivery. *J Am Chem Soc* **135**, 13885-13891 (2013).
250 Ma, Y. *et al.* Humanized Lewis-Y specific antibody based delivery of STAT3 siRNA. *ACS Chemical Biology* **6**, 962-970 (2011).
251 Meyer, L. *et al.* A simplified workflow for monoclonal antibody sequencing. *PloS One* **14**, e0218717 (2019).
252 Dunphy, C. H. & Chu, J. Y. Aberrant CD2 expression in precursor-B acute lymphoblastic leukemia of childhood. *American Journal of Hematology* **52**, 224-226 (1996).
253 Rozenova, K. A. *et al.* CD2 and CD7 are sensitive flow cytometry screening markers for T-lineage acute leukemia (s): A study of 465 acute leukemia cases. *Human Pathology* **114**, 66-73 (2021).
254 Jaseb, K. *et al.* Prognostic significance of aberrant CD5 expression in B-cell leukemia. *Oncology Reviews* **13** (2019).
255 Feng, J. *et al.* Treatment of aggressive T cell lymphoblastic lymphoma/leukemia using anti-CD5 CAR T cells. *Stem Cell Reviews and Reports* **17**, 652-661 (2021).
256 Wang, S., Zhang, R., Zhong, K., Guo, W. & Tong, A. An Anti-CD7 Antibody–Drug Conjugate Target Showing Potent Antitumor Activity for T-Lymphoblastic Leukemia (T-ALL). *Biomolecules* **14**, 106 (2024).
257 Teachey, D. T. & Hunger, S. P. Anti-CD7 CAR T cells for T-ALL: impressive early-stage efficacy. *Nature Reviews Clinical Oncology* **18**, 677-678 (2021).
258 Sakamoto, Y. *et al.* Clinicopathological significance of CD28 overexpression in adult T-cell leukemia/lymphoma. *Cancer Science* **113**, 349-361 (2022).
259 Dumont, J. A., Low, S. C., Peters, R. T. & Bitonti, A. J. Monomeric Fc fusions: impact on pharmacokinetic and biological activity of protein therapeutics. *BioDrugs* **20**, 151-160 (2006).
260 Zaharatos, G. J. *et al.* HIV-1 and influenza antigens synthetically linked to IgG2a Fc elicit superior humoral responses compared to unmodified antigens in mice. *Vaccine* **30**, 42-50 (2011).
261 Zhao, Z. *et al.* Nanocaged enzymes with enhanced catalytic activity and increased stability against protease digestion. *Nature Communications* **7**, 10619 (2016).
262 Xiang, Y. & Lu, Y. Using personal glucose meters and functional DNA sensors to quantify a variety of analytical targets. *Nature Chemistry* **3**, 697-703 (2011).
263 van Buggenum, J. A. G. L. *et al.* A covalent and cleavable antibody-DNA conjugation strategy for sensitive protein detection via immuno-PCR. *Scientific Reports* **6**, 22675 (2016).
264 Wiener, J., Kokotek, D., Rosowski, S., Lickert, H. & Meier, M. Preparation of single- and double-oligonucleotide antibody conjugates and their application for protein analytics. *Scientific Reports* **10**, 1457-1457 (2020).
265 Hou, C. *et al.* Supramolecular Protein Assemblies Based on DNA Templates. *The Journal of Physical Chemistry Letters* **8**, 3970-3979 (2017).
266 McMillan, J. R. & Mirkin, C. A. DNA-Functionalized, Bivalent Proteins. *J Am Chem Soc* **140**, 6776-6779 (2018).
267 Gogolin, L. *et al.* Protein–DNA Arrays as Tools for Detection of Protein–Protein Interactions by Mass Spectrometry. *ChemBioChem* **14**, 92-99 (2013).
268 Li, S. *et al.* Extent of the oxidative side reactions to peptides and proteins during the CuAAC reaction. *Bioconjugate Chemistry* **27**, 2315-2322 (2016).

269 Chakrabarti, M. C. & Schwarz, F. P. Thermal stability of PNA/DNA and DNA/DNA duplexes by differential scanning calorimetry. *Nucleic Acids Res* **27**, 4801-4806 (1999).
270 Jungmann, R. *et al.* Multiplexed 3D cellular super-resolution imaging with DNA-PAINT and Exchange-PAINT. *Nature Methods* **11**, 313 (2014).
271 Jungmann, R. *et al.* Single-Molecule Kinetics and Super-Resolution Microscopy by Fluorescence Imaging of Transient Binding on DNA Origami. *Nano Letters* **10**, 4756-4761 (2010).
272 Pelat, T. *et al.* Germline humanization of a non-human primate antibody that neutralizes the anthrax toxin, by in vitro and in silico engineering. *Journal of Molecular Biology* **384**, 1400-1407 (2008).
273 Gao, S. H., Huang, K., Tu, H. & Adler, A. S. Monoclonal antibody humanness score and its applications. *BMC Biotechnology* **13**, 1-12 (2013).
274 Kuzman, D. *et al.* Long-term stability predictions of therapeutic monoclonal antibodies in solution using Arrhenius-based kinetics. *Scientific Reports* **11**, 20534 (2021).
275 El Fakih, R., Rasheed, W., Hawsawi, Y., Alsermani, M. & Hassanein, M. Targeting FLT3 mutations in acute myeloid leukemia. *Cells* **7**, 4 (2018).
276 Tamm, A. & Schmidt, R. E. IgG binding sites on human Fc gamma receptors. *International Reviews of Immunology* **16**, 57-85 (1997).
277 Roberts, K. G. Genetics and prognosis of ALL in children vs adults. *Hematology, American Society of Hematology Education Program 2018* **2018**, 137-145 (2018).
278 Vrooman, L. M. & Silverman, L. B. Treatment of childhood acute lymphoblastic leukemia: prognostic factors and clinical advances. *Current Hematologic Malignancy Reports* **11**, 385-394 (2016).
279 Hunger, S. P. *et al.* Improved survival for children and adolescents with acute lymphoblastic leukemia between 1990 and 2005: a report from the children's oncology group. *Journal of Clinical Oncology* **30**, 1663 (2012).
280 McMahon, C. M. & Luger, S. M. Relapsed T cell ALL: current approaches and new directions. *Current Hematologic Malignancy Reports* **14**, 83-93 (2019).
281 Borrega, J. G. *et al.* In the eye of the storm: immune-mediated toxicities associated with CAR-T cell therapy. *Hemasphere* **3**, e191 (2019).
282 Hong, R. *et al.* Clinical characterization and risk factors associated with cytokine release syndrome induced by COVID-19 and chimeric antigen receptor T-cell therapy. *Bone Marrow Transplantation* **56**, 570-580 (2021).
283 Peer, D., Zhu, P., Carman Christopher, V., Lieberman, J. & Shimaoka, M. Selective gene silencing in activated leukocytes by targeting siRNAs to the integrin lymphocyte function-associated antigen-1. *Proceedings of the National Academy of Sciences* **104**, 4095-4100 (2007).
284 Xia, C.-F., Boado, R. J. & Pardridge, W. M. Antibody-mediated targeting of siRNA via the human insulin receptor using avidin– biotin technology. *Molecular Pharmaceutics* **6**, 747-751 (2009).
285 Li, G. & Moellering, R. E. A Concise, Modular Antibody–Oligonucleotide Conjugation Strategy Based on Disuccinimidyl Ester Activation Chemistry. *ChemBioChem* **20**, 1599-1605 (2019).
286 Harmand, T. J. *et al.* One-pot dual labeling of IgG 1 and preparation of C-to-C fusion proteins through a combination of sortase A and butelase 1. *Bioconjugate Chemistry* **29**, 3245-3249 (2018).
287 Kennedy, D. C. *et al.* Cellular consequences of copper complexes used to catalyze bioorthogonal click reactions. *J Am Chem Soc* **133**, 17993-18001 (2011).
288 Black, S. *et al.* CODEX multiplexed tissue imaging with DNA-conjugated antibodies. *Nature Protocols* **16**, 3802-3835 (2021).
289 Pallikkuth, S. *et al.* Sequential super-resolution imaging using DNA strand displacement. *PloS One* **13**, e0203291 (2018).

290 Schueder, F. *et al.* Universal Super-Resolution Multiplexing by DNA Exchange. *Angewandte Chemie International Edition* **56**, 4052-4055 (2017).
291 Guo, Y., Deng, L., Qiao, Y. & Liu, B. Efficacy and safety of adding gemtuzumab ozogamicin to conventional chemotherapy for adult acute myeloid leukemia: a systematic review and meta-analysis. *Hematology* **27**, 53-64 (2022).
292 Zheng, B. *et al.* An anti–CLL-1 antibody–drug conjugate for the treatment of acute myeloid leukemia. *Clinical Cancer Research* **25**, 1358-1368 (2019).
293 Li, F. *et al.* Characterization of SGN-CD123A, A Potent CD123-Directed Antibody–Drug Conjugate for Acute Myeloid Leukemia. *Molecular Cancer Therapeutics* **17**, 554-564 (2018).
294 Yoshimoto, G. *et al.* FLT3-ITD up-regulates MCL-1 to promote survival of stem cells in acute myeloid leukemia via FLT3-ITD–specific STAT5 activation. *Blood* **114**, 5034-5043 (2009).
295 Roas, M. *et al.* Targeting FLT3 with a new-generation antibody-drug conjugate in combination with kinase inhibitors for treatment of AML. *Blood* (2022).
296 Lazar, G. A., Desjarlais, J. R., Jacinto, J., Karki, S. & Hammond, P. W. A molecular immunology approach to antibody humanization and functional optimization. *Molecular Immunology* **44**, 1986-1998 (2007).
297 Yao, H.-P., Zhao, H., Hudson, R., Tong, X.-M. & Wang, M.-H. Duocarmycin-based antibody–drug conjugates as an emerging biotherapeutic entity for targeted cancer therapy: pharmaceutical strategy and clinical progress. *Drug Discovery Today* **26**, 1857-1874 (2021).
298 Dokter, W. *et al.* Preclinical profile of the HER2-targeting ADC SYD983/SYD985: introduction of a new duocarmycin-based linker-drug platform. *Molecular Cancer Therapeutics* **13**, 2618-2629 (2014).
299 Kaempffe, A. *et al.* Effect of conjugation site and technique on the stability and pharmacokinetics of antibody-drug conjugates. *Journal of Pharmaceutical Sciences* **110**, 3776-3785 (2021).
300 Golay, J., Andrea, A. E. & Cattaneo, I. Role of Fc core fucosylation in the effector function of IgG1 antibodies. *Frontiers in Immunology* **13**, 929895 (2022).

8 Appendix

8.1 Figure Overview

8.2 Abbreviations

ADC	antibody drug conjugate
ADCC	antibody-dependent cytotoxicity
ADCP	antibody-dependent cellular phagocytosis
AEX	anion exchange chromatography
ALL	acute lymphoblastic leukemia
AML	acute myeloid leukemia
AOC	antibody oligonucleotide conjugate
ATP	adenosine triphosphate
BCR	B cell receptor
bsAb	bispecific antibody
CDC	complement-dependent cytotoxicity
CDR	complementary determining region
CH	constant heavy
CL	constant light
CuAAC	copper(I)-catalyzed azide-alkyne cycloaddition
DAR	drug-to-antibody ratio
DBCO	dibenzocyclooctyne
DNA	desoxyribonucleic acid
DNMT3	DNA methyltransferase 3
DUBA	duocarmycin
ELISA	enzyme-linked immunosorbent assay
EpCAM	epithelial cell adhesion molecule
Fab	antigen binding fragment
FACS	fluorescence-activated cell sorting
Fc	fragment crystallizable
FcR	Fc receptor
FcγR	Fc-gamma receptor
Flt3	FMS-like tyrosine kinase
HAMA	human anti-mouse antibody
HcAb	heavy chain-only antibody
HPLC	high performance liquid chromatography
HSCT	hematopoietic stem cell transplantation
HSCT	hematopoietic stem cell transplantation
IDH	isocitrate dehydrogenase
ITD	internal tandem duplication
KMT2A	histone-lysine N-methyltransferase 2A
mAb	monoclonal antibody
MET	mesenchymal-epithelial-transition
MMAE	monomethyl auristatin E
MMAF	monomethyl auristatin F
NDC	nanobody drug conjugate
NHS	N-hydroxysuccinimide
NPM1	nucleophosmin
ON	oligonucleotide
PCR	polymerase chain reaction
PE	*Pseudomonas* exotoxin A
PEG	polyethylene glycol
PEI	polyethylenimin
PRLR	prolactin receptor
PROTAC	protein targeting chimera
PSMA	prostate-specific membrane antigen

RNA	ribonucleic acid
scFv	single-chain variable fragment
sdAb	single domain antibody
SDS-PAGE	sodium dodecyl sulfate polyacrylamide gel electrophoresis
SEC	size exclusion chromatography
SpAAC	strain-promoted azide-alkyne click chemistry
TAA	tumor-associated antigens
TET2	Tet methylcytosine dioxygenase 2
TTL	tubulin tyrosine ligase
VH	variable heavy
VHH	single variable heavy domain
VL	variable light

8.3 Acknowledgements

After a years-long thesis with luckily many collaborations and great scientists that I could meet, share ideas and discuss with on one hand, and all the things necessary outside of science that are needed to make a thesis happen, the question is always where to start.

First, I want to thank Prof. Dr. Heinrich Leonhardt his supervision of my thesis, guidance when it was necessary, the freedom to develop my ideas on my own, the knowledge when it was best to do so and the trust in my work.

I would like to extend my thanks to many collaboration partners that I could work with together during this thesis and made many parts of the projects happen: Marina and Karsten with whom it was a pleasure to work with, the people from Tubulis, in particular Marc, Marcus, Phil, Philipp and Saskia for a ton of expertise regarding antibodies and a lot of troubleshooting, and Binje and Prof. Dr. Irmela Jeremias and Prof. Dr. Christian Hackenberger for so many insights into their fields of research.

Furthermore, I am grateful for the members of my TAC committee, Prof. Dr. Dirk Busch, Prof. Dr. Julian Stingele and Dr. Jonas Helma-Smets for their discussions and scientific input, as well as the coordination office of IMPRS-LS for providing excellent support throughout my thesis, be it through courses or extra-curricular activities that both helped me grow as a scientist.

My final scientific thanks go to many members of the lab: Andreas, both for excellent discussions and guidance and for always being positive and supportive and with whom I ended up writing almost all of my papers with. Heinrich Flaswinkel and Elisabeth Kremmer for generation of the hybridoma lines and antibodies. My former master's student-turned colleague Mustafa with whom it was and is a pleasure to collaborate, as well as the many other students that I could supervise and also learn from during my thesis: Pablo, Flo, Nina, Denise and Raphael.

All the members of the Leonhardt lab – former and present – have a special place in this thesis too for making the time in the lab so much more enjoyable and work through many frustrations. Enes for so many light-hearted moments and showing a true passion for science. Weihua for countless jokes and managing to get me thinking about HP1 and epigenetics more than I planned to in hours of discussions. Clemens for a lot of fun and sincere moments and talks. And, of course, to the "antibuddies", even though some will be mentioned twice: Andreas, Mustafa, Marlene and Joey, for providing not only help in many situations, but a truly enjoyable place to work and be at.

Last but not least, I want to thank my family and friends for their continued support throughout the years during not only my thesis but university and way beyond. Without my parents and my brother David, none of this would have been possible. Thank you for helping me grow at every step up to here. And to Aleksandra, who I was lucky to meet and for going so much of this journey together.